Hermes Manuel Medina Morais

Licenciado em Biologia

Development of secretome-based therapy by motor neuron modulation of miRNA-124 in ALS mouse models

Dissertação para obtenção do Grau de Mestre em
Genética Molecular e Biomedicina

Orientadora: Dora Maria Tuna de Oliveira Brites
Investigadora Coordenadora
Faculdade de Farmácia da Universidade de Lisboa

Co-orientadoras: Ana Rita Mendonça Vaz Botelho
Professora Auxiliar
Faculdade de Farmácia da Universidade de Lisboa

Margarida Casal Ribeiro Castro Caldas Braga
Professora Auxiliar
Faculdade de Ciências e Tecnologia da Universidade NOVA de Lisboa

Júri:

Presidente:	Professora Doutora Maria Alexandra Fernandes
Arguente:	Professora Doutora Sandra Vaz
Vogal:	Professora Doutora Dora Brites

FACULDADE DE CIÊNCIAS E TECNOLOGIA
UNIVERSIDADE NOVA DE LISBOA

Dezembro, 2020

Hermes Manuel Medina Morais
Licenciado em Biologia

Development of secretome-based therapy by motor neuron modulation of miRNA-124 in ALS mouse models

Dissertação para obtenção do Grau de Mestre em
Genética Molecular e Biomedicina

Orientadora: Dora Maria Tuna de Oliveira Brites
Investigadora Coordenadora
Faculdade de Farmácia da Universidade de Lisboa

Co-orientadoras: Ana Rita Mendonça Vaz Botelho
Professora Auxiliar
Faculdade de Farmácia da Universidade de Lisboa

Margarida Casal Ribeiro Castro Caldas Braga
Professora Auxiliar
Faculdade de Ciências e Tecnologia da Universidade NOVA de Lisboa

Júri:

Presidente:	Professora Doutora Maria Alexandra Fernandes
Arguente:	Professora Doutora Sandra Vaz
Vogal:	Professora Doutora Dora Brites

FACULDADE DE CIÊNCIAS E TECNOLOGIA
UNIVERSIDADE NOVA DE LISBOA

Dezembro, 2020

Development of secretome-based therapy by motor neuron modulation of miRNA-124 in ALS mouse models

This work was funded by Santa Casa da Misericórdia de Lisboa (SCML), project ref. ALS-Research Grant ELA-2015-002, and by Fundação para a Ciência e a Tecnologia (FCT), project PTDC/MED-NEU/31395/2017 and LISBOA-01-0145-FEDER-031395 to Dora Brites, and by FCT: UIDB/04138/2020 and UIDP/04138/2020, to iMed.ULisboa.

Para os meus pais e
para os meus irmãos.

AGRADECIMENTOS

Em primeiro, quero agradecer à **Professora Doutora Dora Brites** com a qual dei os meus primeiros verdadeiros passos no mundo da investigação. Considero a Professora um modelo de frontalidade, determinação, perseverança e de sabedoria, uma autêntica força da natureza! Obrigado pelo apoio e pelos ensinamentos que forneceu durante este ano. Obrigado por me ter ajudado a construir este grande trabalho que considero a minha tese. Um trabalho que puxou tanto por mim, mas donde tantos frutos podem ser colhidos. Obrigado por me ter ensinado que é a olhar para a frente que se faz ciência!

À **Rita** que tanto me acolheu e me ensinou neste ano. Obrigado por seres uma pessoa tão amável e atenciosa. Uma pessoa que está sempre lá quando mais precisamos. Obrigado por conseguires arranjar uma 25ª hora no teu dia para socorrer os teus educandos. Simples palavras não fazem jus à grande Rita que conheço, Muito obrigado!

À **Professora Margarida Castro Caldas** que me despertou ainda mais o interesse pela Neurobiologia. Obrigado pela simpatia e pelo conhecimento transmitido!

À **Adelaide**, **Andreia**, ao **Professor Doutor Rui Silva** e à **Professora Doutora Alexandra Brito** agradeço pela simpatia e entreajuda!

À **Geci** não só por me ter ensinado a dar os primeiros passos naquele fluxo como também por me ter demonstrado tanto carinho ao longo deste ano. Obrigado por teres sido um poço de alegria nos momentos mais difíceis!

Obrigado à **Catarina Sequeira**, **Catarina Barros**, **Maria**, **Rita**, **João**, **Gonçalo** e à **Helena** por estarem sempre disponíveis para ajudar e por trazerem um ambiente de camaradagem ao grupo. Também agradeço a vocês **Colaço** e **Marta** pela ajuda e paciência durante este ano. À **Nísia** que ainda ontem chegou mais que me ajudou e que demonstrou ser uma pessoa muito querida.

Um agradecimento muito especial aos pupilos pois com vocês este ano foi incrível! Obrigado pelas conversas e pelos momentos vividos. Um Obrigado a vocês todos à **Laura**, **Isabel**, **Daniela** e **Alexandre** pois cada um à sua maneira fez com que mesmo os momentos mais difíceis valessem a pena. Um grande obrigado ao meu amigalhaço **Paulo**. Não me podia ter calhado melhor companheiro de bancada, sempre a fundo o Paulo faz as suas coisas! Obrigado pelos desabafos, gargalhadas e pelo "fritanço" ao longo deste ano. Contigo o espírito de camaradagem foi tão grande que aprendemos a puxar um pelo outro e a não desistir nos momentos difíceis. Um amigo que vou levar para a vida!

Um grande obrigado ao "**quarteto" fantástico** com vocês a vida é um mar de rosas. Vamos continuar a partilhar experiência a desabafar, a combinar piqueniques porque já não vos largo, do sexto ano à vida! Aos **animalubus** pelos jantares, jogos e momentos vividos. À **minha baby dama** que é uma pessoa incrível. Obrigado pelos que partilhamos momentos desde a licenciatura. Ao **Fernando**, o meu amigo dos memes, obrigado pela coleção par, pelos gins, pelos momentos partilhados até às 6h. És uma pessoa adorável. Muito obrigado ao meu polaco, **Kamil**, revelaste ser uma pessoa incrível. Sempre com ideias que não cabem na cabeça de ninguém, mas que tornam a vida tão bela. Ao **Luís** a quem considero um grande amigo. Obrigado por tudo! Ao **Miguel** e ao **Guilherme** que com quem tive a sorte de conhecer metade da europa. Desde aí tornamos grandes amigos e ainda grandes momentos nos esperam! Ao **engenheiro** que está sempre lá para ajudar e que considero um grande amigo.

Um obrigado muito especial ao **Agustín** pois foste o meu ponto alto neste ano tão catastrófico! És um amor de pessoa e sinto-me afortunado por me ter calhado este guapo na rifa. Muito obrigado pela culinária, conforto e pela paciência que tiveste comigo.

Um obrigado muito especial à minha família por me ter transmitido tanta força não só neste ano, mas durante a vida toda. Um obrigado ao **Danilson** pelos vídeos mais à toa no WhatsApp, pela bordearem e por me teres mostrado ser tão compreensível. Um agradecimento muito especial à minha irmã **Eva**, pois és para mim um modelo de esforço e dedicação. Ao meu irmão

Stalino uma pessoa sempre alegre que põe a casa às gargalhadas com as suas palhaçadas. À minha irmã **Cleida** por mostrar sempre o lado doce mesmo quando a vida lhe foi mais dura. És um amor de pessoa que admiro muito. Ao meu mais novo, **Leo**, que tão diferente, mas ao mesmo tempo tão igual a mim. És o meu modelo de descontração na vida e contigo vou aprendendo que tudo leva o seu tempo, mas que a vida é o presente! À minha chatinha mais nova, **Eliane**, obrigado pelas mil conversas repetidas e sem sentido à hora do jantar, mas que me deram tanta alegria!

Por último, e mais importante **os meus pais**, que me ensinaram tanto e a quem devo tanto nesta vida. Muito obrigado por cada ensinamento que me transmitiram. São o meu modelo de luta constante na vida. Espero no dia de amanhã proporcionar-vos um mundo mais cor de rosa! Obrigado do fundo do coração por tudo!

RESUMO

A Esclerose Lateral Amiotrófica (ELA) é uma doença fatal caracterizada pela degeneração de neurónios motores (NMs) superiores (corticais) e inferiores (medula espinhal, ME). Os nossos resultados indicam que os níveis aumentados do miRNA-124 se encontrem associados às características patológicas dos NMs, astrócitos e microglia na ELA.

Tivemos como objetivo validar se a regulação do miR-124 encontrado elevado em NMs hSOD1^{G93A} (mSOD1) prevenia a neurodegeneração, o perfil aberrante de astrócitos e a ativação da microglia em ratinhos mSOD1 no início da doença (10-12 semanas). Para tal usámos dois modelos de ELA: a linha de NMs NSC-34 expressando mSOD1 (transgénicos, TG) ou não (selvagem, WT); e as culturas organotípicas (COs) da ME de ratinhos WT e TG. Investigámos diferenças patológicas entre COs de ratinhos TG e WT. Relativamente aos modelos de NMs, utilizou-se a modulação com pré-miR-124 (apenas nos WT) e anti-miR-124 (apenas nos TG). Os secretomas foram isolados e incubados em COs de ratinhos WT e TG para avaliar efeitos adversos e/ou neuroprotetores. Em COs de TG observámos (i) aumento da morte celular por necrose; (ii) desregulação de miRNAs inflamatórios (aumento de miR-21/miR-146a); (iii) alteração de genes neuronais e gliais (aumento de CX3CR1, IL-1β, IL-10, SYP, DRP1, GLT-1 e redução de iNOS, HMGB1, Dlg4, CX3CL1 e GFAP). O secretoma de NMs WT preveniu os marcadores patológicos em COs de ratinhos TG. Em contraste, o secretoma de NMs TG foi deletério em COs de ratinhos WT. O secretoma de NMs WT enriquecidos com miR-124 incubado na CO WT provocou um perfil de miRNAs e genes codificadores de proteínas semelhante ao causado pelo secretoma de NMs TG. Pelo contrário, o secretoma dos NMs TG depletados em miR-124 amorteceu o perfil patológico obtido na CO do TG.

O nosso estudo valida a sobre-expressão do miR-124 em NMs TG como tendo um papel chave nos processos patológicos da ELA.

Palavras-chave: Esclerose lateral amiotrófica; Neurónio motor, Glia; Modulação do miR-124; Secretoma; Culturas organotípicas da medula espinhal

ABSTRACT

Amyotrophic Lateral Sclerosis (ALS) is a fatal disease characterized by the degeneration of upper (cortical) and lower (spinal cord, SC) motor neurons (MNs) and aberrancy of glial cells. Results from our group point to a close connection between increased levels of miRNA-124 and the acquisition of pathological characteristics in MNs, astrocytes and microglia in ALS.

Our main aim was to validate if the downregulation of the elevated levels of miR-124 in hSOD1^{G93A} (mSOD1) MNs toward normal levels was preventive over neurodegeneration, astrocyte aberrancies and microglia activation in the mSOD1 mice at the early onset of the disease (10-12 weeks). Two ALS models were used: the NSC-34 MN-like cell line expressing mSOD1 (transgenic, TG) or not (wild-type, WT); and the SC organotypic cultures (OCs) from WT and TG mice. Pathological differences between TG and WT SCOCs were investigated. Relatively to the MN models, we used the modulation with pre-miR-124 (only in WT) and that of anti-miR-124 (only in the TG). The isolated secretomes were incubated in WT and TG SCOCs to assess harmful and/or neuroprotective properties.

In TG SCOCs we observed: (i) increased necrotic cell death; (ii) disturbed inflammatory-associated miRNAs (increase in miR-21/miR-146a); (iii) and dysregulated neuronal and glial genes (increased CX3CR1, IL-1β, IL-10, SYP, DRP1, GLT-1 and downregulation of iNOS, HMGB1, Dlg4, CX3CL1 and GFAP). WT-MN secretome counteracted pathological markers in TG SCOCs. In contrast, TG MN secretome induced deleterious effects in WT SCOCs. Secretome from miR-124-enriched WT MNs incubated in WT SCOCs led to a profile of miRNAs and protein-coding genes similar to that caused by the TG MN secretome. On the contrary, the secretome from TG MNs depleted in miR-124 restored a deactivated profile in TG SCOCs.

Our data reveals MN upregulation of miR-124 as a key player in ALS pathological processes.

Keywords: Amyotrophic lateral sclerosis; Motor neuron, Glial cells; miR-124 modulation; Secretome; Spinal cord organotypic cultures

TABLE OF CONTENTS

FIGURE INDEX

I. INTRODUCTION

III. MATERIALS AND METHODS

IV. RESULTS

V. DISCUSSION

TABLE INDEX

III. MATERIALS AND METHODS

ABBREVIATIONS

Aldh1l1	Aldehyde dehydrogenase 1 family, member L1
ALS	Amyotrophic lateral sclerosis
AMPA	α-amino-3-hydroxy-5-methyl-4-isoxazolepropionic acid
ApoBDs	Apoptotic bodies
AST	Astrocyte
BBB	Blood-brain barrier
C9ORF72	Chromosome 9 open reading frame 72
CSF	Cerebrospinal fluid
EEAT2	Excitatory amino acid transporter 2
fALS	Familial amyotrophic lateral sclerosis
FUS	Fused in sarcoma
GFAP	Glial fibrillary acidic protein
GLAST	Glutamate aspartate transporter
GLT-1	Glutamate transporter solute carrier family 1
HDL	High-density lipoproteins
Iba1	Ionized calcium-binding adaptor molecule 1
lEVS	Large extracellular vesicles
LMN	Lower motor neuron(s)
MHC-II	Major histocompatibility complex class II
MN	Motor neuron(s)
MND	Motor neuron disease
mSOD1	Mutant superoxide dismutase 1
MUNIX	Motor unit number index
MUTE	Motor unit number estimation
NF-κB	Nuclear factor kappa B
OC	Organotypic cultures
$p75^{ECD}$	p75 extracellular domain
ROS	Reactive oxygen species
s100B	S100 calcium-binding protein B
sALS	Sporadic amyotrophic lateral sclerosis
SC	Spinal cord
SCOCs	Spinal cord organotypic cultures

sEVs	Small extracellular vesicles
snoRNA	Small nucleolar RNAs
SOD1	Superoxide dismutase 1
TARDBP	TAR DNA-binding protein 43
TG	Transgenic
TMS	Transcranial magnetic stimulation
tRNA	Transfer RNA
UMN	Upper motor neuron(s)
WT	Wild type

I. INTRODUCTION

1. Amyotrophic lateral sclerosis (ALS): current knowledge on its pathogenesis, biomarkers, and therapeutic strategies

Amyotrophic lateral sclerosis (ALS) is a fatal neurodegenerative disease whose main feature is the degeneration of both upper and lower motor neurons (UMN/ LMN). The loss of the above-mentioned MN leads to neuromuscular denervation that consequently culminates in muscular weakness, spasticity, fasciculations and atrophy (Hardiman et al. 2017; Brown & Al-Chalabi, 2017) (**Figure I.1**). The average onset age is in the middle-to-late 50 years. If the onset occurs in the late teens or early adult years, it can be an indicator of familial ALS (fALS). Equally to the time of onset the region where ALS can occur differ between patients, with some of them presenting spinal-onset disease whereas others show a bulbar-onset disease. It is the third most common neurodegenerative disease with an estimated worldwide mortality of 30,000 patients per year. Typically, the patients die after 2 to 5 years because of respiratory paralysis (Brown & Al-Chalabi, 2017; Hardiman et al., 2017; Mathis et al., 2019). Earlier age of onset, longer duration of disease and beginning of symptoms in the lower limbs are some of the specificities found in patients with SOD1-related ALS (Pansarasa et al., 2018; Mathis et al., 2019).

In Europe and the United States, there are 1-2 new cases of ALS per year per 100,000 individuals. Regarding the prevalence, studies point to 3 to 5 total cases per 100,000 individuals. According to Conde and his colleagues in Portugal, the estimated number of ALS/motor neuron disease (MND) patients is 10.32 per 100,000 inhabitants. There is a lack of ALS epidemiological studies outside the above-mentioned regions and the few existent studies made point to a heterogeneous incidence and prevalence of ALS cases worldwide, thus more studies are required to acquire a better estimative of ALS epidemiology (Brown & Al-Chalabi, 2017, Conde et al., 2019).

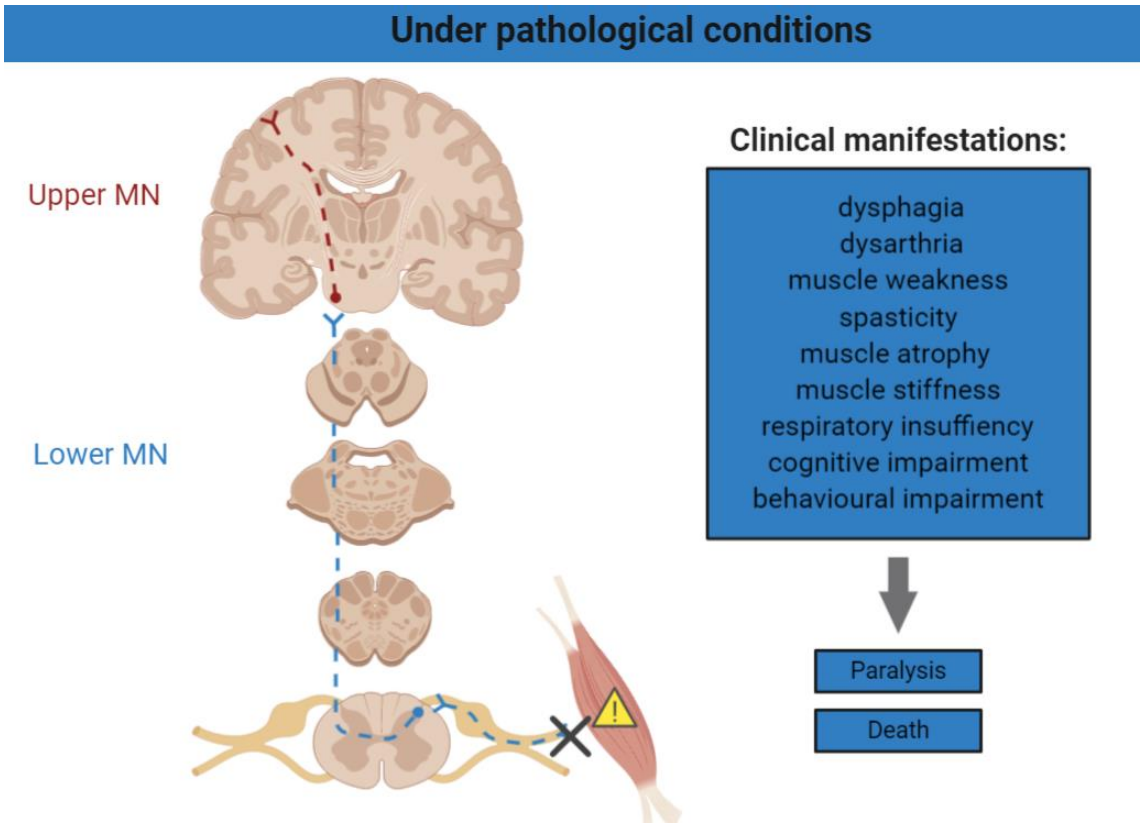

Figure I.1 - Amyotrophic lateral sclerosis is a progressive neurodegenerative disease with a complex genetic basis and pathophysiology that affects motor neurons (MN). Both upper (from motor cortex and brainstem) and lower MN (from spinal cord) are affected, with consequent neuromuscular denervation (dashed lines represent degenerating MN). As a result, a wide range of clinical manifestations can be observed. Typically, the patient dies by respiratory paralysis. (Created with BioRender.com)

1.1. ALS risk factors: particular emphasis on the genetic basis

It is believed that this multifactorial disease results from interactions between genetic predisposing factors and environmental risk factors. Regarding the environmental factors, their role in ALS is not yet defined. Some studies show a slight or null effect of these factors whereas others show a controversial performance. Among the wide list of external factors are heavy metals, pesticides, smoking, electromagnetic factors, and even physical exercise, reason of the increase incidence of ALS among football players (Bozzoni et al., 2016). Because this is an intriguing research field and since genetic research on ALS is discovering a quite number of genes involved in fALS and sALS cases, a possible hypothesis to clarify the influence of environmental factors in ALS is the combination of some relevant ALS genes with xenobiotics. From this kind of study, we expect a better understanding of the relationship between susceptible/ causative factors of ALS and so a greater knowledge on the pathological basis of the disease.

Considering the presence of genetics or not, there are two groups of ALS, familial ALS (fALS) that accounts for 5 to 10% of ALS cases and sporadic ALS (sALS) that accounts for the remaining 90%, respectively. Despite genetic differences, these groups share similar clinical presentations. The involvement of genetics in ALS can occur at different levels. There are susceptible genes,

which increase the vulnerability to develop sALS, whereas on the other hand there are the causative genes that usually have an autosomal dominant pattern of inheritance. Most of these genes are involved in precise cellular functions, such as autophagy, vesicle transport, oxidative stress, RNA processing and metabolism (Ghasemi & Brown, 2018; Mathis et al., 2019). The first gene linked to fALS was Superoxide dismutase 1 (*SOD1*) in 1993 (Rosen et al., 1993). Currently, there are more than 30 genes linked to fALS and other more to sALS cases. Chromosome 9 open reading frame 72 (*C9ORF72*), *SOD1*, TAR DNA-binding protein 43 (*TARDBP*) and Fused in Sarcoma (*FUS*) are the most frequently mutated genes in ALS and they show a different repartition, which depends on the ancestral origin. According to former studies, in Europe *C90RF72* (33,7 % of fALS cases) is the most mutated gene followed by *SOD1* (14,8%) whereas in Asia the most mutated gene is *SOD1* (30%) and *C9ORF72* only appears to be the third most mutated one (2.3%). This finding is quite interesting once they suggest that exist population-specific genetic risk factors (Mathis et al., 2019).

SOD1 is a 9307 bp gene that encodes for a 32 KDa homodimeric metalloprotein. This protein is mainly distributed in the cytosol but can also be found in different parts of human cells, such as nucleus, lysosomes, and mitochondria. Protecting cells from reactive oxygen species (ROS) and reducing the steady-state amount of superoxide, by converting it into oxygen and hydrogen peroxide, are the functions of this enzyme (Pansarasa et al., 2018; Mathis et al., 2019). As a result of mutations in *SOD1*, oxidative stress and iron metabolism dysregulations have been observed, but details from which of these mutations lead to neurotoxicity are still not fully known. Despite this, there is a hallmark of SOD1-associated ALS that is generally accepted by the community, which is the deposition of SOD1 into insoluble aggregates in MNs. It is believed that this hallmark is a consequence of structural destabilization and/ or oxidative stress induced by several kinds of mutations. As a result, SOD1 neurotoxic species (aggregates, dimers destabilized and/ or SOD1 oligomers) are generated (Pansarasa et al., 2018; Mathis et al., 2019). It is important to mention that SOD1 aggregates have been found in glial cells from ALS patients as well (Forsberg et al., 2011). Moreover, former studies (Chia et al., 2010; Münch et al., 2011) suggest that cell-to-cell transmission of mutant SOD1 (mSOD1) aggregates as prion-like propagation is involved in ALS progression. Presently, more than 180 different mutations have been described in the five existing exons of the *SOD1* gene. Of these different types of mutations, the most common ones are the D90A (aspartic acid at codon 90 changed to alanine), the A4V (alanine at codon 4 changed to valine) and the G93A (glycine at codon 93 changed to alanine). The G93A mutation carries an identical Wild Type (WT) SOD1 biological activity and although it is a relatively rare mutation it has been extensively investigated. It was the first mutation to be studied in a transgenic mouse model where it was possible to achieve MN degeneration syndrome (Valentine & Hart, 2003).

The development of several SOD1 models, such as transgenic mice and rats, has allowed a better understanding of the implication of SOD1 in ALS. However, critical issues must be better explained. Some of them are the mechanisms responsible for the up-regulation of *SOD1* gene, the fact that SOD1 not only can give rise to neurotoxic species, but also can have protective

functions (when it re-localizes in the nucleus acquires a new protective function against DNA damage) (Pansarasa et al., 2018), and not less important the understanding of the prion-like protein misfolding mechanism and the disease pathology dissemination. These issues are essential for the understanding of the etiology of ALS and the development of powerful therapeutics.

1.2. ALS current biomarkers and treatments

There is no definitive test for the diagnosis of ALS. Current diagnosis is based on the history of progressive weakness spreading within a region or to other regions, evidence of the involvement of UMN and LMN and other tests that exclude similar diseases (Brown & Al-Chalabi, 2017; Hardiman et al., 2017; Mathis et al., 2019). ALS shows a complex heterogeneity between patients and so this gives restriction for using single reliable biomarkers.

Some of the techniques being used give rise to a set of novel neurophysiological biomarkers that can be useful to effectively evaluate UMN and LMN dysfunction, as well as for the characterization of their changes during disease progression. Therefore, these techniques may be able to improve ALS diagnosis. Transcranial magnetic stimulation (TMS) is a non-invasive technique that utilizes a transient magnetic field to stimulate nerve cells in the cortical region. It provides valuable comprehension of the functional integrity of brain pathways. Focal cortical change and hyperexcitability were established as a specific feature of ALS using TMS. Moreover, this technique allows to distinguish between ALS and other neurological mimic conditions and so it can be used as a useful biomarker of UMN dysfunction in ALS (Huynh et al., 2019). Regarding LMNs, motor unit number estimation (MUTE) and motor unit number index (MUNIX) seem to be potential biomarkers of degeneration of these group of neurons. MUNE is a technique that uses electromyography to estimate the number of motor units in a muscle. It also determines the countervailing collateral reinnervation. A decline in MUNE counts during ALS progression has been detected in several studies (Gooch & Shefnet et al., 2004; Jacobsen et al., 2019). MUNIX assess the number and size of motor units by using surface electromyographic interference pattern and compound muscle action potential. LMN loss before clinical weakness was detected using MUNIX technique (Neuwirth et al., 2017). In conclusion, TMS, MUNE and MUNIX seem to be a set of promising biomarkers.

Imaging evaluations are also essential to discriminate ALS from neurological mimic syndromes. Knowing that disease metabolic alterations have been observed at the systemic and cellular level, metabolic biomarkers in addition to other current biomarkers (neurophysiological and imaging techniques) are probably the best tool for an appropriate diagnosis, categorization and tracking of the disease. Some relevant metabolic biomarkers are the following: glucose with decreased levels across cerebrum and increased use by LMN, cortisol showing increased levels in saliva, pyruvate dehydrogenase lipoamide kinase isozyme 4 (PDK4) with increased levels in

muscle mitochondrial and p75 extracellular domain ($p75^{ECD}$) that increase in urine. Additionally, glucose, structural lipids, metabolites, and modulators of metabolism were found altered in the cerebrospinal fluid (CSF) of ALS patients (Kirk et al., 2019).

Regarding therapy, there is no cure for ALS and the present treatment only provides a limited improvement in survival. Clinical care is mostly based on symptom management. During disease progression, a set of several physical and physiological problems can be developed (**Figure I.1**). According to that, a multidisciplinary approach seems to be supportive to diminish the above-mentioned problems. Gastrostomy, assisted ventilation, mobility equipment, alternative communication devices and counselling to patient and relatives are some of the strategies to increase the life quality of the patients (Hogden et al., 2017). Although several drugs have been studied for the treatment of ALS only two are approved by the Food and Drug Administration, i.e. Riluzole, a blocker of persistent sodium channels, and Edaravone, both being free radical scavengers. The first has an anti-glutamatergic action, suppressing excessive MN firing, whereas the second one acts by suppressing oxidative stress (Brown & Al-Chalabi, 2017; Hardiman et al. 2017; Mathis et al. 2019).

1.3. Neuroanatomic propagation in ALS

Most ALS motor phenotypes display a set of common clinical observations. In the beginning, initial symptoms emerge focally in random regions of the body. These symptoms can appear in limb, bulbar, axial, or respiratory muscles. If ALS begins in limbs the deficits that occur are usually unilateral (Grad et al., 2017).

First, abnormalities start in MNs. At this point, the abnormality remain local and clinical presentations are not detected. Later, early symptoms appear because of subsequent neuronal degeneration and sequential spread of cellular dysfunction. The symptoms turn out to be gradually worse in the same region over time. Subsequently, neurotoxicity starts to spread to adjacent neurons and from region to region. Destroyed MNs are the outcome of this process. Ultimately systemic MN abnormalities are detected, which present as severe disease. Here, the degeneration proceeds independently in UMN and LMN (Grad et al., 2017). During disease development, progressive accumulation of specific misfolded proteins, as SOD1, may occur (Kanouchi et al. 2012).

It is important to mention that the focal body where early symptoms appear is the area where is possible to observe a maximum degeneration of both UMN and LMN, suggesting that at the onset of the disease the degeneration occurs in a dependent manner. Adding to this, studies have been proposing the multifocal onset in ALS (Kanouchi et al. 2012), which in fact can contribute to the heterogeneity observed in this disease. A topic that must be elucidated is whether progression is similar in UMN and LMN and if the overall progression is a result of the sum between these two groups of neurons.

Moreover, two types of pathological dissemination mechanisms have been detected in ALS. In the first one, contiguous spread, the pathological propagation occurs side-to-side and independently of synaptic connection (Ravits & La Spada 2009; Kanouchi et al. 2012). On the other hand, network spread is dependent on synaptic connectivity. The dissemination advances end-to-end in anatomically and functionally connected networks (Brooks 1991; Seeley et al. 2009). These two types of mechanisms can coexist with each other. Together with the combination of single or multiple hits a complex clinical picture can be obtained.

1.4. Pathophysiologic mechanisms involved in MN degeneration

To date, several pathophysiological mechanisms that contribute to MN degeneration in ALS are known (**Figure I.2**). Some of them will be explained in more detail hereafter. Several mechanisms, if not all, have been observed in SOD1 mutations (Hardiman et al. 2017).

Protein inclusions and misfolding are a pathological hallmark of diverse neurodegenerative disorders, such as ALS, in which protein inclusions are commonly found in MNs of the spinal cord (SC). SOD1 inclusions have been detected in MNs of sALS and fALS cases. The contribution of protein aggregates (not only SOD1) to MN degeneration is still unknown. There is some possible hypothesis. In the first one, protein aggregates can be inoffensive neurodegeneration-derived products. In the other, the formation of this aggregates may be responsible for the cellular toxicity and ALS pathogenesis observed. Lastly, they can represent a protective reaction of the cell to reduce the concentration of toxic proteins (Mancuso & Navarro, 2015).

Oxidative stress is a mechanism that is associated with mitochondria damages and it has been documented in cellular and rodent models of ALS (Barber & Shaw, 2010; Parakh et al., 2013). This stress is a result of the imbalance between the production of reactive species (ROS) and the capacity of the biological systems to remove ROS or repair the ROS-induced damage. It seems that one of its most important effects is the damage of RNA species (Mancuso & Navarro, 2015).

Several mitochondrial impairments have been observed in ALS models and patients. In NSC-34 cells (a MN-like cell line) expressing mSOD1, morphological and functional mitochondrial alterations have been observed (Menzies et al., 2012). Some possible explanation by which mSOD1 might disrupt mitochondrial functions includes the mSOD1 aggregates into the mitochondrial intermembrane space, which in turn leads to impairment in mitochondrial protein import. Another mitochondrial damage process that contributes to the toxicity of ALS is the oxidative damage of mitochondrial proteins that consequently leads to defects in respiratory chain function. Deficiency in ATP synthesis, dysregulation of apoptosis and impairment of calcium buffering are observed under these conditions (Mancuso & Navarro, 2015; Hardiman et al. 2017).

A mechanism that is thought to be present in all forms of ALS is the glutamate-induced excitotoxicity. Excitotoxicity can result from a deficiency in neurotransmitter clearance from the synaptic cleft, excessive activation of glutamate receptors, or elevated postsynaptic sensitivity to glutamate. A possible reason for the frequency of this mechanism in ALS could be the fact that ALS vulnerable MNs seems to display a lower calcium buffering capacity (Alexianu et al., 1994). Moreover, MNs has α-amino-3-hydroxy-5-methyl-4-isoxazolepropionic acid (AMPA) receptors that are more permeable to calcium in contrast with other neuronal subtypes (Hardiman et al. 2017). Besides, deficits in glutamate transporters, responsible for the clearance of the glutamate on the synaptic cleft, have been identified in ALS patients, especially in the astroglial Excitatory amino acid transporter 2 (EEAT2) (Bristol & Rothstein, 1996).

Axonal transport, with a key role in neuronal function, was also found dysregulated in ALS. Neurons are polarized cells that transmit signals across long distances, consequently, organelles and protein must travel further in comparison with other cells (Mancuso & Navarro, 2015). Hereupon, neuron transport machinery is more overloaded, which in turn enhance the susceptibility to deficits of this mechanism. Accumulation of neurofilaments and deficits in axonal transport were detected in $SOD1^{G93A}$ mice (Zhang et al., 1997). The molecular mechanism that may be responsible for the impaired axonal transport are the following: mitochondrial damage, decrease in microtubule stability and alterations in the phosphorylation of the motor proteins kinesin and dynein.

Neuroinflammation is a pathological event that results from harmful effects of diverse stimuli. It participates in the pathogenesis of brain and SC injury (SCI) and is commonly found in neurodegenerative disorders, where ALS is not an exception. In ALS, damages in MNs lead to the activation of microglia, astrocytes, and the complement system, which in turn will contribute to neurodegeneration (Mancuso & Navarro, 2015). Since Microglia compose the innate immune system of the Central Nervous System (CNS) it displays a key role in neuroinflammatory responses. Increased microglial activation, T cell infiltration and elevated concentration of proinflammatory mediators have been found in sALS and fALS patients (Henkel at al., 2004).

As formerly referred, MN degeneration is a process that is believed to be a consequence of a combination of several mechanisms rather than one. Whatever the mechanism involved, the outcome is the loss of capacity of MNs to preserve their axonal projections, which in turn cause axonal retraction and denervation of the target cell. If the cells involved are the LMNs there will be denervation of the muscle; on the other hand, if it is the UMN affected it will lose the capacity to control LMN (Hardiman et al. 2017).

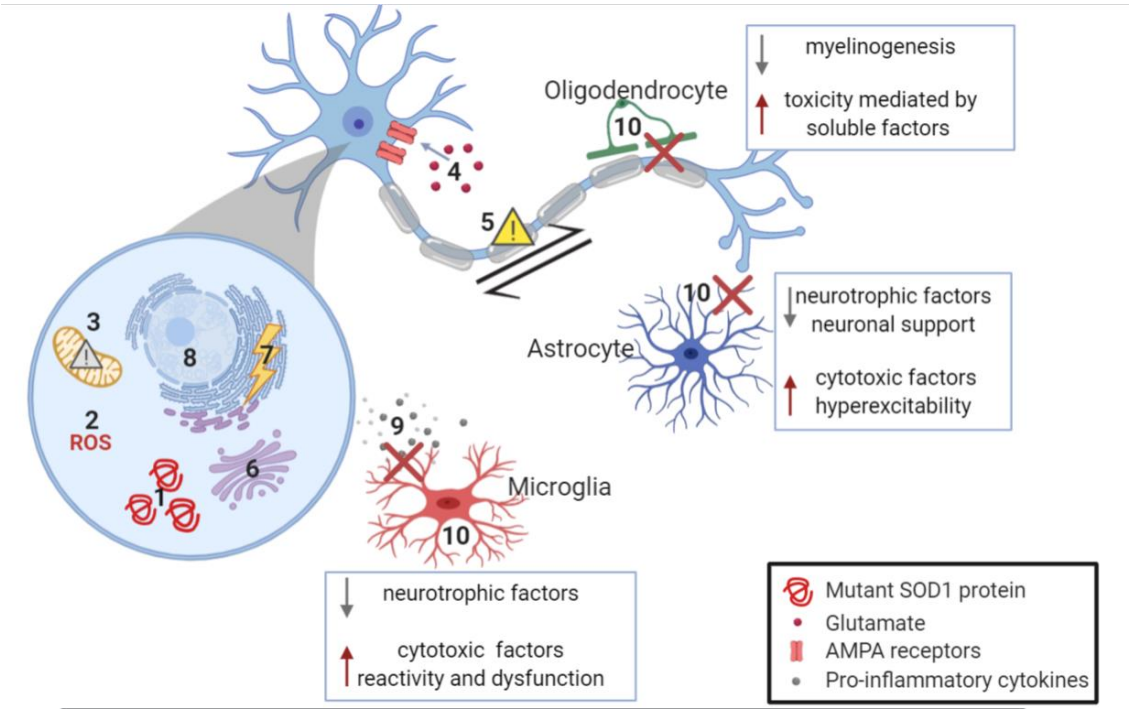

Figure I.2 - Main pathological mechanisms involved in motor neuron (MN) degeneration. Some of these mechanisms involve the MN itself, whereas others are more related with glial cells. Loss of physiologic role of glial cells and/or gain of toxic functions has harmful repercussion in MN homeostasis, contributing to disease evolution. Moreover, it is believed that the combination of the below mechanisms rather than a single one occurs in neurodegenerative diseases, namely in ALS. (1) Misfolding and aggregation of proteins, (2) Oxidative stress, (3) Mitochondrial dysfunction, (4) Excitoxicity, (5) Impaired axonal transport, (6) Golgi fragmentation, (7) Endoplasmic reticulum stress, (8) Abnormal RNA processing, (9) Neuroinflammation, and (10) Non-cell autonomous disease. **ROS**, reactive oxygen species; **SOD1**, superoxide dismutase 1; **AMPA**, α-Amino-3-hydroxy-5-methyl-4-isoxazolepropionic acid. (Created with BioRender.com)

1.5. The key role of glial cells in ALS

Several studies have shown that the neuronal homeostasis and survival, which are compromised in ALS, do not result only from MN biological aberrant processes. The pathogenesis observed in this neurodegenerative disease is mostly attributed to anomalous interactions of neurons and surrounding glial cells in the brain and SC. Herewith, ALS arises from a combination of mutant damages in MN and surrounding glial cells, the last one described as a non-cell-autonomous mechanism (Komine & Yamanaka, 2015).

Glial cells, glia or Neuroglial cells include microglia, astrocytes, oligodendrocytes and, Schwann cells which are quite different from nerve cells. Although they help in the preservation of neurons signaling abilities and define synaptic contacts they do not directly participate in synaptic interactions and electrical signaling. Glial cells are generally smaller than neurons and they lack dendrites and axons. First, glial cells were described as a connective tissue which binds the nervous elements together. Today it is known that these cells are important for the maintenance of the ionic milieu of nerve cells, modulation of the nerve signal propagation rate, modulation of synaptic action by supervising the uptake of neurotransmitters, giving assistance

or preventing recovery from neural injury and as a scaffold in some neural development processes (Purves et al., 2001).

Several studies have been pointing out that glial cells dysfunction in ALS contributes to MN degeneration. In the ’90s the first evidence of glial dysfunction in animal models, as well as in ALS patients, was observed. Those studies were made in astroglial glutamate transporters and they (Rothstein et al., 1992; Bruijn et al., 1997) provide evidence that reduced EAAT2/GLT-1 protein level, which is responsible for the clearance of the glutamate on the synaptic cleft, in the motor cortex and SC contributes to paralysis and MN degeneration. Further, in 2003 Clement and co-workers showed that the loss of MNs in chimeric mice for mSOD1 was more notorious when they were surrounded by glial cells expressing mSOD1 in comparison with WT glial cells (Clement et al., 2003). When compared with the ubiquitous expression of mSOD1, its expression in MN alone was not enough to cause full-blown MN disease, thus strongly suggesting that surrounding glial cells expressing mSOD1 influence the degeneration of MN. These and further studies, where mSOD1 was depleted in specific cells, suggest that selective deletion of mSOD1 from MN affects ALS onset, whereas deletion from glial cells affects the progression of this disease. However, Wang and his fellow workers noticed that deletion of mSOD1 G85R from astrocytes affected both disease onset and progression (Wang et al., 2011). This discrepancy may be due to the different nature of mutations. So, the attribution of changes in onset and progression cannot only be given to a particular cell type (Philips & Rothstein, 2014).

Unfortunately, to this day, the identification of glial mechanisms in the several existent ALS models has not led to the targeting of effective therapeutics. Thus, the major question remains unanswered*, i.e.,* is the contribution of glial to non-cell-autonomous mechanism because glial and neuronal cells need to communicate and/or they do truly contribute to the neurodegenerative process.

1.5.1. Microglia Phenotypes

It seems that microglia can switch phenotypes and therewith their responses depending on the regional, temporal, and immune environmental variation (**Figure I.3**). Upon different stimuli surveilling microglia can switch to an activated state and thus being able to acquire different phenotypes and to participate in cytotoxic response, immune regulation, and injury resolution (Brites & Vaz, 2014). When activated, microglia may be polarized to acquire a pro-inflammatory phenotype, or a reparative and anti-inflammatory subtype. Microglia activation states are heterogeneous and represent a continuum between these 2 phenotypes. Pro-inflammatory microglia are cytotoxic and are usually the first in line, promoting the destruction of pathogenic compounds and/or harmful stimuli. They are characterized by the release of proinflammatory cytokines. Interferon-gamma (IFN-γ) and Toll-like receptor 4 (TLR4), the receptor of lipopolysaccharide (LPS) are known inducers of this polarized state (Brites & Vaz, 2014).

Interestingly, the release of pro-inflammatory cytokines by such microglia has been proposed to promote the anti-inflammatory phenotype, known as a “destroy and clean up” cell hypothesis (David & Kroner, 2011). Anti-inflammatory microglia are recognized by their capacity to establish a more neuroprotective environment. Some known mediators of this phenotype are the cytokines interleukin (IL)-4, IL-10, and IL-13 (Brites & Vaz, 2014). Studies have shown that release of Insulin-like growth factor 1 (IGF-1) favor neuronal extension and support other glial cells (Isgaard et al., 2007), whereas IL-4 protects MN from injury produced by LPS-activated microglia (Zhao et al. 2006). Therefore, there is a temptation to think that anti-inflammatory microglia only act as a good kind. However, disproportionate anti-inflammatory polarization may become detrimental, once it might allow unwanted fibrotic responses and scars, not facilitating axonal growth (Brites & Vaz, 2014), being deleterious in disease, specifically in late stages.

Besides these phenotypes, senescent or dystrophic microglia can be noticed after a prolonged (toxic) stimulus. At this stage, microglia are morphologically characterized by the loss of thin branched cytoplasmic processes, spheroid formation and cytoplasmic disintegration. Cell fusion (multinucleated giant cells) can be formed as a severe abnormality. Functionally, they have restricted responsiveness, impaired phagocytosis, and a reduced capacity to produce neurotrophic factors. Adding to this, senescent microglia is not capable to switch to an anti-inflammatory/ reparative state which limits injury repair. These microglia are commonly related to neurodegenerative disorders mainly at the end stage where they display abnormal and dysregulated functions diminishing glial-mediated neuroprotection (Luo & Chen, 2012; Brites & Vaz, 2014). Moreover, studies suggest that senescent microglia maybe be responsible for the release of compounds that inhibit neuronal autophagy (Alirezaei et al., 2008) and neurogenesis (Wong, 2013).

As above mentioned, microglia can switch during ageing and in disease. They acquire different phenotypes and activate specific transcriptional programs leading to a homeostatic and/or disease-associated microglia. These two major functions (pro- vs anti-inflammatory) are based on microglia molecular signature, a signature that is not fully known (Butovsky & Weiner, 2018). Much work must be done to fully understand these microglia dynamics (switching from an activated type to another one) in inflammatory responses such as that happening on this aggressive MN disease. Regarding what has been described, microglia seem to be a crucial tool that can be used in therapeutics with the goal of preventing or rescuing ALS progression. Healthy microglia may be used to replace the senescent/irresponsive cell once microglia are important players in sustaining brain homeostasis. Additionally, modulation of dysfunctional microglia with a specific or a set of inflammatory miRNAs to obtain a less reactive cell upon chronic neuroinflammation, or rejuvenation of microglia to ameliorate their capacity to fight the insult and to improve disease outcomes (Brites & Vaz, 2014) appear to be promising approaches.

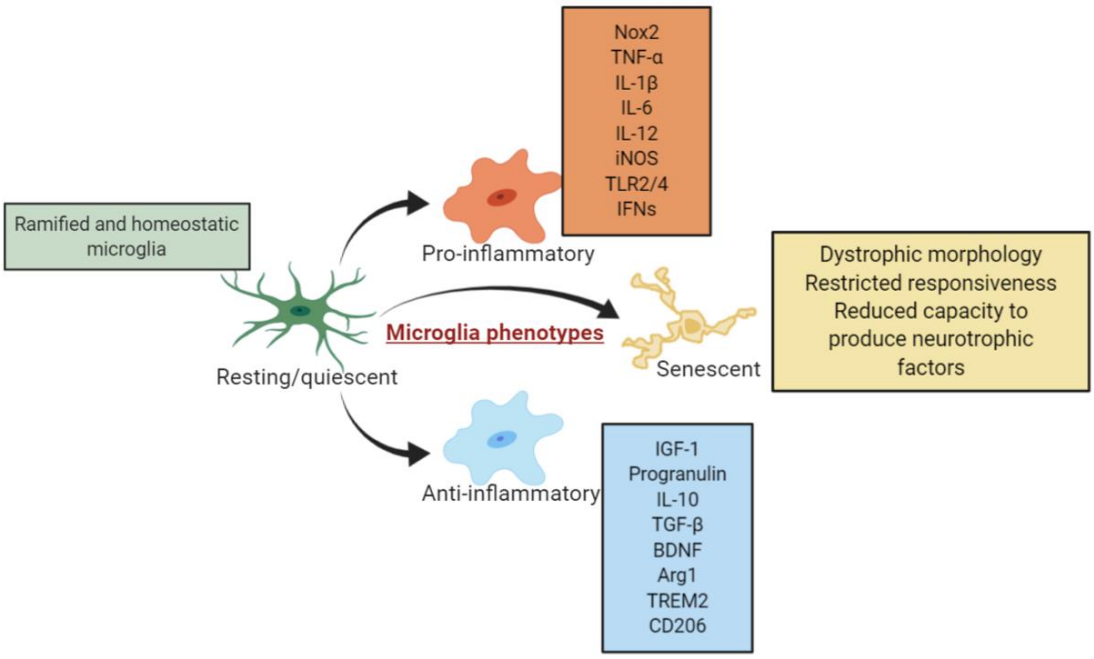

Figure I.3 - Synopsis of microglia phenotypes. Under physiologic conditions surveilling microglia exhibit a ramified morphology with enlarged cell body, with small and tick processes. Upon different stimuli microglia switch to an activated state, acquiring an amoeboid form. Two poles can be detected in this state, pro-inflammatory and anti-inflammatory microglia. Some of the molecules mostly expressed by pro-inflammatory microglia are NADPH oxidase 2 (Nox2), interleukins (IL-1 β, IL-6 and IL-12), inducible Nitric Oxide synthase (iNOs), toll-like receptors (TLR 2/4) and interferons (IFNs). These cytotoxic molecules promote the resolution of detrimental stimuli. Anti-inflammatory microglia in order to create a neuroprotective environment produce anti-inflammatory cytokines and other molecules such as insulin-like growth factor 1 (IGF-1), progranulin, IL-10, transforming growth factor βeta (TGF-β), brain-derived neurotrophic factor (BDNF), arginase 1 (Arg1), triggering receptor expressed on myeloid cells 2 (TREM2) and the mannose receptor (Cluster of differentiation 206, CD206). After a prolonged stimulus microglia become senescent, displaying dystrophic morphology, restricted responsiveness, and reduced capacity to produce neurotrophic factors. Noteworthy, microglia may display more complex phenotypes, a combination of both pro-and anti-inflammatory microglia has been noticed. (Created with BioRender.com)

1.5.2. Physiological and disease function of microglia

Microglia is a type of non-neuronal cell that derives from the hematopoietic cell lineage. They are mainly known as the primary innate immune cells of the CNS where they can present neuroprotective or neurotoxic immunological properties. Besides this, normal microglia functions include phagocytosis, synaptic pruning, chemotaxis and support the integrity of both neurons and astrocytes. Microglia represent around 10% of the total CNS cells (Komine & Yamanaka, 2015; Butovsky & Weiner, 2018).

There is a set of markers that help us to distinguish microglia from other CNS-resident cells along with infiltrating monocytes/macrophages. Some of the useful markers are ionized calcium-binding adaptor molecule 1 (Iba1), CD11b proteins and major histocompatibility complex class II (MHC-II), which are mainly microglia-exclusive in the CNS and present in higher levels in activated microglia (Kettenmann et al., 2011). Moreover, a novel marker, the fractalkine receptor

CX3CR1, has been recently nominated. Microglia are the only intrinsic brain cells that express this receptor. It seems that together with the fractalkine CX3CL1, a chemokine produced by neurons, CX3CR1 helps to support the microglia role. Studies show that microglia deficient in CX3CR1 did not offer neurotrophic support to surrounding neurons. Moreover, mice deficient in the same receptor displayed reduced connectivity between cortex and hippocampus along with impact in mouse behavior (Wolf et al., 2017).

When the blood-brain barrier (BBB) is compromised, for example in brain inflammatory diseases, monocytes, and macrophages infiltrate the CNS, which is not observed in normal circumstances. Upon different stimuli such as microbial infection, antigen-immunoglobulin complexes, cerebral microbleeds and abnormal misfolded proteins in neurodegenerative disease the microglia activation is induced. Morphology shift and migration of microglia go along with this process, with microglia changing from ramified to amoeboid form and microglia moving to the damaged cells and so, clearing the debris of the dead cells by phagocytosis. Once microglia begin to release proinflammatory cytokines, complements, ROS, and other harmful molecules the acceleration of neuronal dysfunction and death is initiated giving rise to the noble neuroinflammation (Komine & Yamanaka, 2015).

Furthermore, microglia have a role in ALS, contributing to onset and disease progression. It seems that have a protective effect on MN at an early stage. The opposite is detected in late stages, where activated microglia secrete detrimental signals and factors leading to an enhance in MN death and to a possible acceleration in disease progression (Brites & Vaz, 2014; Luo and Chen, 2012). Supporting this, data from our group showed that neurotoxic microglia leads to the stimulation of signaling pathways associated with inflammatory cascades, defective microglia function, higher phagocytic ability and a specific inflammatory miRNA profile (upregulated miR-155 and miR-146a plus downregulated miR-124) (Cunha et al., 2016). Gliosis defined as a nonspecific reactive change of glial cells in response to an injury in the CNS is recognized as a component of ALS pathology. Microgliosis and inflammation have been proven several times in lesions of mutant SOD1 mice as well as in ALS patients. The intensity of microglial activation was higher in cases where the disease was more severe which suggests an active involvement of microglial activation in ALS (Turner et al., 2004).

1.5.3. Astrocyte phenotypes

There are two major classes of astrocytes, protoplasmic and fibrous astrocytes. The first one represents the major population of astrocytes in the grey matter of the brain and of the SC. They display a spongiform morphology and are part of the neurovascular unit, a structure that integrates cellular and extracellular components being involved in the regulation of cerebral blood flow and blood–brain barrier function as well. These astrocytes are generally composed of six to seven major branches that emanate from the soma, several secondary and tertiary branches, and

thousands of smaller processes, which are required for interaction with the surrounding cells. The major branches that emanate from the soma are responsible to form an end-feet structure on blood vessels, while the others participate in other essential physiologic events (Verkhratsky & Nedergaard, 2018; Khakh & Deneen, 2019). On the other hand, fibrous astrocytes populate white matter of the brain and the SC. In contrast with protoplasmic astrocyte, they are less complex (hold fewer terminal fine processes) and exhibit less glial fibrillary acidic protein (GFAP) immunoreactive processes (Sun & Jakobs, 2012). The processes of these astrocytes are long and radially oriented in the direction of the axon bundles, where they contact with the last at the nodes of Ranvier. Moreover, these astrocytes display a distinct morphology. Although these are the two most common astrocytes there are other forms, as the radial astrocytes that occur in the developing brain (Verkhratsky & Nedergaard, 2018; Khakh & Deneen, 2019).

As formerly mentioned, inflammatory responses are essential to fight CNS insults. Besides microglia, other cells as astrocytes, have pro- and anti-inflammatory functions, thus contributing aggravate or to the resolution of the insult. Upon different stimuli, astrocytes are activated leading to a set of transcriptional, morphological, and functional alterations. Though controversial, it was indicated that at least two states of polarization, the “A1” and “A2” reactive astrocytes (a terminology that parallels the “M1” and “M2” macrophage and microglia nomenclature) are formed (Liddelow & Barres, 2017). On these situations’ astrocytes exhibit hypertrophy of both the cell body and cytoplasmic processes and an increase in expression of intermediate filament proteins, namely GFAP, vimentin and nestin as well as cytokines, proteins of the antigen presentation and complement pathways showing that astrocytes play a role in the inflammatory responses (Brites & Vaz 2014; Verkhratsky & Nedergaard, 2018). As for microglia, these phenotypes probably represent only two extremes of a continuous spectrum of reactive profiles. A1 is recognized to have harmful/toxic properties once gene transcriptome analyses show an upregulation of several injuring genes, namely those that are destructive to synapses (Liddelow & Barres, 2017). On the other hand, in A2 there is an upregulation of neurotrophic factors, factors necessary for the survival and growth of neurons as well as genes that promote synapse repair. Unlike A1, A2 seems to have a reparative/protective function (Liddelow & Barres, 2017; Verkhratsky & Nedergaard, 2018). Additionally, a recent study points to the existence of many subtypes of astrocytes (AST), including AST 1, 2, and 3 classified as mature astrocytes, AST 4 linked to neurogenesis, and AST 5, classified possible intermediate progenitors (Batiuk et al., 2020).

1.5.4. Physiological and disease functions of astrocytes

Astroglia are a type of non-neuronal cells that accounts for approximately 30% of the cell population in the mammalian CNS (Liddelow & Barres, 2017). They are highly heterogeneous in morphological and functional appearance expressing multiple receptors, channels and membrane transporters that contribute to their adaptative plasticity, which in turn support the CNS

homeostasis maintenance in development and ageing (Verkhratsky & Nedergaard, 2018). Additionally, studies have been pointing out that interactions between astrocytes and neurons are related with the development and diversity of these glial cells (Khakh & Deneen, 2019). A recent study (Stogsdill et al., 2017) supports this idea once they found that astrocytes with a complex morphology depend on direct contact with neurons, which is mediated by neuroligin(astrocyte)-neurexin(neuronal) interactions. When astrocytes become reactive, they are capable to respond to all forms of CNS insults and disease. On this circumstance, glial scar formation can be reached consequently impeding axon regeneration. In such a case, astrocyte suffers several morphological and molecular changes to begin this nonspecific, but highly characteristic cell response (Sun & Jakobs, 2012).

There is no universal marker that labels all cells of astroglial lineage. Some of the most used markers will be described hereafter. Aldh1l1 is one of the markers currently used and is considered the "new" standard marker of astrocytes once it marks both protoplasmic and fibrous astrocytes. Expression of aldehyde dehydrogenase 1 family, member L1 (Aldh1l1) is substantially broader than GFAP. However, changes in the expression of this marker with age have been detected. GFAP is an intermediate filament protein that is widely used to identify astrocytes. In CNS it is expressed in a subpopulation of astrocytes, outside the nervous system it is expressed in many other cells. Glutamate transporters, Glutamate Aspartate Transporter (GLAST) and Glutamate transporter solute carrier family 1 (GLT-1), are used to identify local subpopulations of astrocytes once several studies indicate that they are specifically expressed on astrocytes and their precursors (Verkhratsky & Nedergaard, 2018). These markers show regional variability. Protoplasmic astrocytes generally express more S100 calcium-binding protein B (S100B), a Ca^{2+}-binding protein that acts as Ca^{2+} buffer and sensor, while fibrous express more GFAP (Chaboub & Deneen 2013). Furthermore, GFAP, vimentin and S100B are generally upregulated in reactive astroglia (Verkhratsky & Nedergaard, 2018; Gomes et al., 2019).

Astrocytes present a broad variety of physiological functions. Such essential functions include the control over the BBB, ion homeostasis, energetic support, regulation of synaptogenesis and secretion of neuroactive factors. Moreover, astrocytes also contribute to the regulation of local blood flow, glycogen synthesis and storage, neurogenesis, and neurotransmitter homeostasis, as glutamate, a neurotransmitter commonly found dysregulated in ALS (Verkhratsky & Nedergaard, 2018; Khakh & Deneen, 2019). Ca^{2+} signaling has been related with multiple functions in astrocytes, namely blood vessel diameter control (Attwell et al. 2010), regulation of both neurotransmitter uptake (Shigetomi et al. 2012) and release of insult-related molecules, and inflammatory mediators (Sofroniew, 2014). Adding to this it is known that astrocytes own dozens of known Ca^{2+} binding proteins (Khakh & Deneen, 2019).

Astrocytes also have a role in neurodegenerative diseases, namely in ALS. Several studies show that astrocytes derived from $SOD1^{G93A}$ mutant mouse secrete diffusible factors that are toxic to MN reducing their survival (Di Giorgio et al., 2007; Nagai et al., 2007). Moreover, degeneration and MN dysfunction in Wt mice were observed when mutant $SOD1^{G93A}$ astrocyte-precursor cells

were transplanted into the SC of the same animals (Papadeas et al., 2011). Adding to this, abnormal astrocytes were detected in the SC of different lines of mSOD1 (ALS) mice (Yamanaka & Komine, 2018). As already mentioned, controlling, and reducing extracellular concentrations of glutamate at the synapse is an important function of astrocytes. A function that is mainly done through the glutamate transporter EAAT2. Loss of the same transporters in mSOD1 mice, as well as in sALS and other fALS patients, leads to defects in glutamate uptake by astrocytes. As a result, glutamate levels increase at the synaptic cleft. Later an excessive firing of neurons is observed increasing the influx of Ca^{2+} which can be toxic to neurons (Bruijn et al., 1997; Howland et al., 2002 & Guo et al., 2003).

As formerly mentioned, glial cells have aberrant activity contributing to ALS-related pathogenesis, reason why a therapy targeting these cells, namely microglia and astrocytes, seem feasible to prevent or rescue ALS progression.

2. MicroRNAs as potential biomarkers and targets for modulation in ALS: particular emphasis in miRNA-124

2.1. MicroRNA biogenesis and mechanism of action

MicroRNAs (miRNAs) are short non-coding RNAs (20-25 nucleotides) that act as signaling molecules by inhibiting the expression of target genes. In this process, miRNAs bind directly to mRNAs of the target genes. These molecules are found dysregulated in ALS and miRNA(miR)-124 is one of them. Once miRNA modulation (miR-124) is one of the central parts of this work a brief elucidation on how these molecules are generated and the mechanism of action of them will be done.

Two main miRNAs processing routes are known, the canonical and non-canonical pathways. Canonical animal miRNAs can be encoded in the genome as individual genes, as clusters which contain a few to several hundred different miRNAs or in introns of host genes. When they exist as clusters, mature individual miRNAs are processed from polycistronic transcripts (**Figure I.4**). Regarding non-canonical miRNAs biogenesis, several classes of Microprocessor/Drosha-independent or Dicer-independent have been characterized. “Mirtrons” are a class of short introns that are microprocessor-independent pre-miRNAs. They are originated from introns that, once spliced, functions as pre-miRNAs. After this process, cleavage by the microprocessor is not required and immediate export of these molecules for the Dicer enzyme processing in the cytoplasm is initiated. Mammals possess hundreds of mirtron loci. In comparison with the canonical pre-miRNAs, mirtron has extended hairpins, more heterogenous nucleotides at their ends and 3’ is generally uridylated. Moreover, mature miRNAs from transfer RNA (tRNA) fragments or tRNA- like RNAs, small nucleolar RNAs (snoRNA) fragments and capped hairpin transcripts can emerge from the microprocessor-independent pathway. Dicer-independent miRNA biogenesis is rare. Instead of Dicer the Ago2, an RNase H-like endonuclease, cleaves the

pre-miRNA within its stem. Eventually, the 3' end is trimmed by poly(A)-specific ribonuclease (Ha & Narry Kim, 2014; Treiber et al., 2019)

About the mechanism of miRNA function, it is accepted that miRNA guides RISC to the complementary sequences that are mostly located in the 3' untranslated region of the target mRNAs. By this way, mRNA decay and translation inhibition through deadenylation of the target mRNA is initiated. Additionally, 5'-3' exoribonuclease 1 contributes to the inhibition of miRNA target genes by the degradation of the unprotected 5' (Treiber et al., 2019). Free mature miRNAs and miRISC that are not interacting with their targets can be incorporated into multivesicular bodies (MVBs) and then sorted into small and large extracellular vesicles (sEVs/lEVS), coupled with argonaute proteins or attached to high-density lipoproteins (HDL). Alternatively, pre-miRNAs can also be released into the extracellular milieu by the previous interaction with MVBs (Brites, 2020).

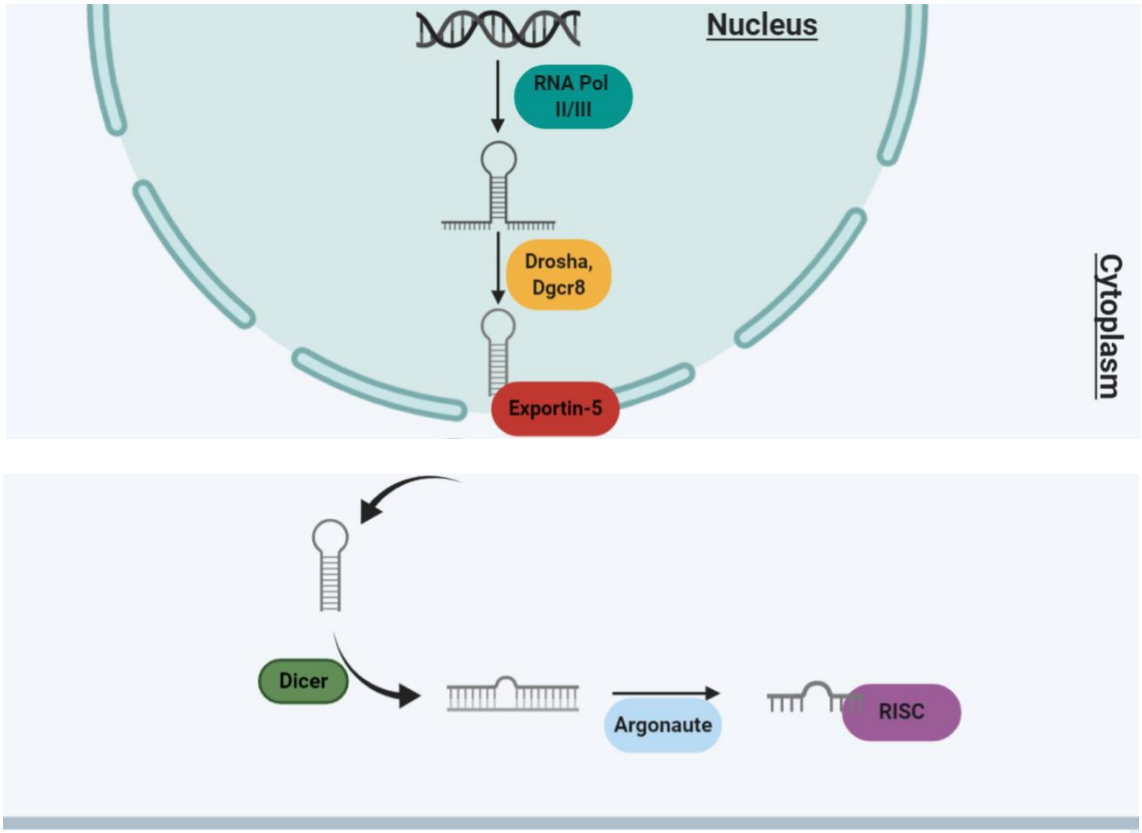

Figure I.4 - MiRNA biogenesis. In the canonical pathway RNA polymerase II/II initiate the transcription giving rise to primary polyadenylated miRNAs (pri-miRNAs). Later, the microprocessor, composed by the Drosha enzyme, Dgrc8 and several other auxiliary factors, process the pri-miRNAs to single hairpins called precursor miRNAs (pre-miRNAs). The pre-miRNAs are then exported to the cytoplasm by the interaction with Exportin-5. Here, the Dicer enzyme cleaves the pre-miRNAs within the stem close to the terminal loop giving rise to miRNA intermediate duplexes. The ultimate product is handed to the Argonaute protein. Argonaute acts by selecting one strand to become the guide strand/mature miRNA and discarding the other strand (the passenger strand). Finally, the guide strand is incorporated into the RNA-induced silencing complex (RISC). Additionally, several classes of non-cannonical miRNA pathways such as Microprocessor-independent and Dicer-independent have been characterized. Further studies must be done to clarify the alternative canonical pathways. (Created with BioRender.com)

2.2. MiRNAs are found dysregulated in ALS

It is predicted that between 5000 to 10000 miRNAs exist in mammals. These set of small RNAs regulate the expression of more than 60% of protein-coding genes in health and disease (Tahamtan et al., 2018). Moreover, it is known that one specific miRNA can be involved in the regulation of several mRNA targets, and that mRNA can also be targeted by many miRNAs (Lim et al., 2005). Cell cycle, proliferation and programmed cell death are some of the processes that these molecules participate in. They are also crucial regulators of immune cell development, inflammation, autoimmunity, and hematopoiesis, thus becoming potential tools for disease treatment, namely in neurodegenerative diseases (Tahamtan et al., 2018). Moreover, studies have shown that miRNAs are essential in both innate and adaptative immunity, acting by a negative feedback pathway. On this way, miRNAs have the potential to modulate and influence immune dysfunction and disease (Lindsay, 2008). In more detail, several miRNAs are related with the proliferation of monocytes and neutrophils, maturation of macrophages and dendritic cells, functioning of the natural killer cells, development and differentiation of B and T cells, antibody switching and in the release of inflammatory mediators, such as cytokines and chemokines (O'Connell et al., 2007; Beaulieu et al., 2013; Smyth et al., 2015). Additionally, miRNA can be transferred from cell to cell through either in the soluble form in the secretome or included in sEVs and lEVs. In this way, miRNAs can cause biological changes in the recipient cells.

MiRNA expression has been found altered in the blood and CSF of ALS patients which in turn suggest that these molecules play a role in ALS pathology (Figueroa-Romero et al., 2016; Joilin et al., 2019). For example, it seems that an overall reduction of miRNA levels in fALS and sALS cases may prevent miRNA homeostasis role, leading to synapse and neuromuscular junction structure dysfunctions, as well as impairments in neurogenesis, neurofilaments and RNA and protein metabolism. Our group has also shown that miRNAs may also be dysregulated in astrocytes and contribute to MN degeneration (Gomes et al., 2019). On the other hand, the potential of activated microglia as responsible of overexpressed miRNAs, ultimately leading to MN degeneration was also recently reviewed (Christoforidou et al., 2020). Since modulation of miR-124 is one of the key elements of the present work a further explanation on how this miRNA contributes to neuronal degeneration will be made in section **2.4.**

2.3. Role of inflammatory miRNAs in cell function and dysfunction

A set of distinct inflammatory-associated miRNAs (inflamma-miRNAs) have been associated with different phenotypes and functions of glial cells, for instance, microglia and astrocytes, as mentioned above. By acting on innate and adaptative immune responses they play a critical role in glia-mediated inflammatory responses. Once they are considered potent regulators of neuroinflammation, their modulation emerges as a possible therapeutic approach. According to that, great knowledge of their functions and identification of their targets may uncover how they

can be modulated to solve impairments and prevent exacerbated inflammatory reactions. Among inflamma-miRNAs, miR-21, miR-124, miR-125b, and miR-146a are the most studied ones and they were found to be dysregulated in neurodegenerative diseases, such as ALS (Tahamtan et al., 2018).

MiR-21 is one of the most highly expressed miRNAs in mammalian cells. It has a key role in the resolution of inflammation by negatively regulating the pro-inflammatory response (Sheedy, 2015). MiR-21 was found up-regulated in the SC of symptomatic mSOD1^{G93A} mice and in the brain of rats, where it was linked to improved neurological outcome after traumatic brain injury (Cunha et al., 2017; Ge et al., 2014). Likewise, its expression is elevated in activated immune cells (Chen et al., 2018). Caescu and co-workers found that the overexpression of miR-21 attenuates the pro-inflammatory and activates the anti-inflammatory phenotype of microglia (Caescu et al., 2015). Consequently, the secretion of IL-6 is abolished, and the production of IL-10 is enhanced (Feng et., 2014). Moreover, Zhang et al. (2012) showed that, by repressing FasL, miR-21 protects neurons from cell death induced by hypoxia-activated microglia. This miRNA is also associated with astrocytic reactivity and it was found downregulated along with miR-146a in cortical astrocytes of mSOD1^{G93A} mice (Gomes et al., 2019). Differently, miR-21 levels were found to increase in a time-dependent manner after mice SC injury (SCI). Overexpression of this miRNA in astrocytes near the injured region attenuated the hypertrophic response to SCI and caused a decrease in cell size, process thickness, and GFAP expression (Bhalala et al., 2012). Additionally, a set of studies pointed out a preventing role of miR-21 in apoptosis. There are 469 predicted targets of this miRNA, thereby, its exact functional outcome is not fully known (Brites, 2020). The inducing signal, the cell type affected, the transcriptomic profile of the cell, are some variables that affect the availability and ability to involve different target mRNAs. Thus, diverse miRNA-21 responses are expected in different conditions (Sheedy, 2015).

MiR-125b is a highly conserved miRNA that has an essential role in cell apoptosis, innate immunity, inflammation, and differentiation (Duroux-Richard et al., 2016). Enriched levels of the same miRNA are found in the nervous system tissue and neural cells, promoting neurite outgrowth in the last (Le et al., 2009). Besides, upregulated miR-125b levels are required to create a regeneration permissive environment after SCI by downregulating Sema4D and other glia-scar-related genes (Quiroz et al., 2014). Increased levels of miR-125b are also found in SOD1^{G93A} microglia, which were correlated with a constitutive nuclear factor kappa B (NF-κB) activation on these cells. By exerting its pro-inflammatory function, NF-κB signaling changes the transcriptomic profile of microglia to a more pro-inflammatory subtype (e.g. upregulation of TNF-α gene). Persistent activation of the same pathway culminates in damage and death of the surrounding MN. Parisi et al. (2016) counteracted those effects by downregulating miR-125b in SOD1^{G93A} mice. More specifically, they demonstrated that repression of A20 by the same miRNA is responsible for sustained NF-κB activity in ALS microglia. Moreover, in the same study, the authors found that miR-125b and A20 protein levels were inversely modulated in lumbar SC symptomatic SOD1^{G93A} mice (upregulation of miR-125b, whereas A20 protein was strongly

inhibited). Such results encourage modulation of this miRNA in earlier stages when perhaps the levels of the A20 protein are still prevalent and, thus, the rescue of NF-κB constitutive activation has, possibly, more strength in inhibiting disease progression. Furthermore, former studies found that other ALS causative genes, TDP43 and FUS were involved in miR-125b processing (Morlando et al., 2012; Di Carlo et al. 2013), which contributed to associate miR-125b to ALS disease. Additionally, miR-125b and miR-155 are linked to a more senescent/ dysfunctional microglia phenotypes which are believed to accelerate disease progression (Brites & Vaz, 2014).

MiR-146a is found upregulated in response to a pro-inflammatory activity, where it controls excessive inflammation by negative feedback. Studies suggest it has a modulatory role in the innate immune response and microglial activation (Saba et al. 2012). MiR-146a has 488 predicted targets (Brites, 2020). NF-κB activation induces miR-146a expression, which then restrains the translation of its two main targets, the TNF receptor-associated factor 6 (TRAF6) and the interleukin 1 receptor-associated kinase 1 (IRAK1) mRNAs (Gaudet et al., 2018). MiR-146a was found upregulated in SC tissue of symptomatic and mSOD1^{G93A} mice pups but downregulated in the brain cortex (Cunha et al., 2017; Gomes et al., 2019). Cortical astrocytes were the main cells responsible for the downregulation of miR-146a in the brain cortex when obtained from 7-day-old mSOD1 mice pups, and such dysregulation was recapitulated in cell-derived sEVs. Levels of this miRNA showed to decrease with astrocyte *in vitro* maturation when isolated from the cortical brain of WT mice, indicating that it may be essential to fulfill development processes, as well as for the regulation of inflammatory responses. However, the inverse was found to occur in the SC (Gomes et al, 2020), suggesting different regional roles. Another study demonstrated that increased levels of astrocyte miR-146a contribute to SC atrophy (Sison et al., 2017) and a decline of miR-146a levels was found in SC microglia of mSOD1 mice during disease progression (Butovsky et al., 2012). Together with miR-21, miR-146a also decreases the inflammatory response of microglia after intracerebral hemorrhage (Wang et al., 2018). Finally, upregulation of miR-146a, like miR-125b and miR-155, was associated with cell senescence, namely microglia (Brites, 2020). It was suggested that miR-146a restrain the senescence-associated secretory phenotype (SASP) by a negative feedback loop. As a result, secretion of IL-6 and IL-18 were found suppressed (Bhaumik et al., 2009). Further studies in microglia *in vivo* must be done to clarify the evidence of miR-146a role upon senescence.

2.4. Role of miR-124 in the CNS and its contribution to ALS pathogenesis

MiR-124 is the most abundant miRNA in the brain, being highly and specifically expressed in all brain regions except in the pituitary gland (Sun et al., 2015). Its expression in other tissues is nearly 100 times lower (Mishima et al., 2007). MiR-124 is also highly expressed in SC (Su et al., 2016). Regarding biogenesis, this miRNA shows specific temporal and spatial profiles in numerous cells and tissues which in turn affects an extensive biological function in the CNS. Mature miR-124 is homologous in human, mice, and rats (Sun et al., 2015). Studies have shown

its essential role in neuronal identity acquisition and maintenance (Conaco et al., 2006), a process incited by the suppression of hundreds of non-neural genes (Lim et al., 2005). Additionally, increased levels of miR-124 in non-neuronal cells lead to a shift of expression profile, approaching a neuronal phenotype (Lim et al., 2005). Although miR-124 can be found in glial cells (Wang & Wang, 2018), it is preferentially expressed in neurons (Deo et al., 2006). During CNS development and neuronal maturation, a progressive increase and accumulation of this specific molecule are observed (Sun et al., 2015). On these circumstances, miR-124 decreases the levels of polypyrimidine-tract-binding protein (PTBP), an RNA-binding protein that acts as a splicing regulator and 3' end processing. It also participates in mRNA stability and RNA localization (Sun et al., 2015). Moreover, miR-124 is responsible for the determination of the subventricular zone (SVZ), known as the largest neurogenic niche in the adult mammalian brain. MiR-124 participates in synaptic plasticity, hematopoiesis, hippocampal axogenesis and regulation of neurite outgrowth (Sun et al., 2015). Regarding its contribution to immune responses, Sun et al. (2013) found that miR-124 inhibits the production of pro-inflammatory cytokines, being important for the cholinergic anti-inflammatory action. Actually, it was evidenced that miR-124 display calming effects in microglia (Ponomarev et al., 2011). Knowing this and that miR-124 has numerous targets, miR-124 seems a potential therapeutic tool that can be used for handling a set of pathological events observed in multifactorial CNS diseases, such as ALS. Beyond the above-mentioned functions, the exact role of miR-124 in the CNS is not completely clarified.

Abnormal expression of miR-124 was found to contribute to uncontrolled CNS conditions such as neurodegeneration, neuroimmune disorders, CNS stress and brain tumors. Increased levels of miR-124 in CSF of sALS patients were detected by Waller et al. (2018). Studies from our group have shown that this miRNA is linked to diverse phenotypes and functions of microglia, as well as to symptomatic associated neuroinflammation in ALS patients (Brites & Vaz, 2014; Cunha et al. 2017). Since it was found elevated together with miR-155 and miR-146a and shown to influence microglia toward surveillance state or anti-inflammatory phenotype (Han et al., 2020), miR-124 expression may be dependent on cell requirements and pathology. Moreover, augmented levels of miR-124 were found in mSOD1 NSC-34 cells and their derived exosomes. These exosomes when internalized by microglia caused a pro-inflammatory phenotype along with a reduced phagocytic ability and increased cell senescence (Pinto et al., 2017). Additionally, after an acute pro-inflammatory response mixed microglia population composed by pro- and anti-inflammatory phenotypes along with increased levels of miR-124 in microglia were detected after engulfment of NSC-34 sEVs enriched in miR-124. Moreover, the expression of these specific miRNA in stressed neurons was linked to neurodegeneration (Sun et al., 2015). In mSOD1 mice, the elevated levels of miR-124 seem to be negatively correlated with STAT3, a transcription factor crucial for neural differentiation and cell survival (Marcuzzo et al., 2014). In opposition, Zhou et al. (2018) found diminished levels of the same miRNA in the brainstem and SC of mSOD1 mice along with an association of these altered miRNA with astrocyte differentiation. Despite these still controversial findings, it is generally accepted that the elevation of miR-124 is more closely related with the existence of neurodegeneration than with surveilling microglia (Cunha et al. 2017).

Therefore, modulation of miR-124 seems to be a viable strategy to regulate inflammatory responses and thus ameliorate deleterious features found in ALS models and patients.

2.5. Modulation of miRNAs (miR-124) as a potential application for ALS rescue

As it was mentioned in the previous section, miRNAs are short non-coding RNA molecules that act by inhibiting the expression of target genes. They are known to play a crucial role in physiological processes, as well as in pathological processes, and miR-124 has been shown to potentially contribute to ALS pathogenesis. miRNAs have been proposed not only as diagnostic biomarkers but also as therapeutic targets for neurodegenerative diseases. Among the features that characterize miRNAs as desirable molecules for drug development are that a single miRNA is capable of downregulating hundreds of targets genes, they have a short length, thus facilitating their vehiculation, they are highly conserved between species and can be delivered *in vivo* through several drug delivery systems, already approved for human use (Rupaimoole & Slack, 2017). Intracerebroventricular and intravenous injections, intrathecal and intranasal administration, virus-mediated, exosome-mediated, and stem-cell-mediated delivery are examples of delivery methods of miRNA-based drugs to the CNS (Sun et al., 2018). Focusing on the present work, a special interest in the use of EVs to antagonize pathological processes found in neurodegenerative diseases. reside on their ability to cross the BBB (Brites 2020).

MiRNA-based therapeutics include miRNA mimics, also called pre-miRNAs, and antagomiRs also called anti-miRNAs or inhibitors. MiRNA mimics are artificial small double-stranded oligonucleotides that copy miRNA precursors. After the entrance of these molecules in cells, they are recognized by miRNA biogenesis machinery and consequently processed. The strand of interest (guide strand) must be identical to the native mature miRNA. Taking this into account, if one or a set of miRNAs are diminished and correlate with disease progression, miRNA mimics can be used to compensate the functional activity of the lost miRNAs, decreasing the levels of their target genes (Sun et al., 2018). On the opposite, antagomiRs act by inhibiting the interaction between miRNAs and miRISC proteins, or between the miRISC and target mRNAs. They are single-stranded antisense oligonucleotides that target a specific mRNA to inhibit its translation into protein, or by triggering their destruction (Sun et al., 2018). As a result, increased levels of target genes are detected. Therefore, antagomiRs can be used to suppress high levels of miRNAs that appear to contribute to disease progression. Some chemical modifications, such as 2'-O-methyl, 2'-O-fluoro, or the addition of 2'-O-methyl to phosphorothioate nucleotides can be used to enhance the stability, permeability and specificity of miRNA mimics and antagomiRs. MiRNA sponges are an alternative to antisense oligonucleotides that contain multiple complementary bindings sites to a miRNA of interest. They can be produced from transgenes within the cells and act as inhibitors by decreasing the function of a specific miRNA. Additionally, miRNA sponges can be used as inhibitors of an entire family of miRNAs (Ebert & Sharp, 2010).

Increased levels of miR-124 and its contribution to ALS pathogenesis has been detected, herewith a therapy using miR-124 antagomiRs or miRNA sponges seem to be a pertinent

approach to rescue ALS progression. However, an ambiguous role of miR-124 has been argued and there is still information to be clarified, as the pathways that this molecule act in. Thus, beyond an amelioration of some pathologic features, the modulation of miR-124 could deteriorate other essential unknown features/pathways.

3. Secretome and small extracellular vesicles (sEVs): a cell-free therapeutic approach for ALS treatment

3.1. The concept of secretome and its physiologic relevance

Secretome is defined as a set of factors and molecules released by a cell, tissue, or organism into the extracellular space. EVs and soluble factors, such as cytokines, chemokines, growth factors and lipids are on its composition. As a response of fluctuations in physiologic states or pathologic conditions, secretome of individual cells and tissues suffer noteworthy content changes. Beyond the paracrine factors above-mentioned, EVs are an important component of the secretome (Mendes-Pinheiro et al., 2020).

Till the present moment, three major types of EVs were identified. They are classified as exosomes/sEVs (small size), microvesicles/lEVs (large size) and apoptotic bodies (ApoBDs) according to their size, cellular origin, protein markers and functions (Song et al., 2019). Exosomes/sEVs are the best-characterized species of EVs. They derive from intracytoplasmic MVBs and upon fusion with the plasma membrane, they are directly released into the extracellular space. sEVs dimensions range from 30 to 250 nm. Alternatively, the fusion of MVBs with Lysosomes (Lys) leads to their cargo degradation (Brites, 2020). Microvesicles/lEVs bud directly from the plasma membrane and their size range from 150 to 800 nm (Mendes-Pinheiro et al., 2020; Busatto et al., 2020). Lastly, ApoBDs which are released from cells that undergo programmed cell death range from 50 to 5000 nm in diameter (Kakarla et al., 2020). Smaller apoptotic cell derived EVs (ApoEVs) can also be found. This type of EVs usually has a maximum range diameter of 1000 nm (Brites, 2020). Lately, several studies have investigated the use of such small and large EVs as biomarkers. These sEVs and lEVs share a set of contents such as secretory proteins, DNA, non-coding RNAs (e.g. miRNAs), mRNA, sugars, and lipids (Bussato et al., 2020; Kakarla et al., 2020). Secretome also includes exomers, small nonmembranous particles (~ 35 nm) with yet nonclarified biological function (Brites, 2020).

MiRNAs besides being enriched in EVs, they can also be found as soluble molecules or complexed with proteins in cell secretome. Extracellular miRNAs are collected by the target cell through membrane fusion, endocytosis, phagocytosis, or receptor interaction. Therefore, these molecules exert a paracrine effect by local regulation of RNA availability and protein translation on the host cell (Brites, 2020). Globally, the secretome participates in cell-to-cell and cell-to-microenvironment communication, namely in neuron-microglia communication. Secretome signaling is important in several physiological processes, such as immune system activation,

coagulation, and tissue regeneration. Moreover, it influences cell fate, function, and plasticity (Mendes-Pinheiro et al., 2020; Busatto et al., 2020).

Microglia are classified as better recipients of secretome/EVs in comparison with neurons and astrocytes, being successfully activated by the secretome/EVs (Pinto et al., 2017; Li et al., 2018). Additionally, former studies demonstrated that EVs mediate phenotypic changes in microglia and surrounding cells. Bahrini et al. (2015) showed that neuronal sEVs facilitated synaptic pruning by increasing complement factors in microglia. Moreover, neurons-derived EVs were shown to be enriched in miR-124 and miR-9. Veremeyko and co-workers (2019) suggested that both miRNAs were responsible to maintain microglia in a deactivated state. In another study, miRNA-9 derived from EVs of astrocyte cells triggered microglial migration activity (Yang et al., 2018). Lastly, microglia derived EVs have been associated with both pro-inflammatory (Kumar et al., 2017) and anti-inflammatory (Huang et al., 2018) effects.

Multiple different messengers can be carried in secretome/Evs to long distances from the vesicular origin and thus EVs also contribute to the maintenance and spread of pathological processes that depend on cell-to-cell communication (Bussato et al., 2020). Knowing these, secretome is a powerful tool to explore the mechanisms of ALS homeostatic imbalance and cell interaction in ALS models, either using isolated cells in culture, animals, organoids, spheroids or organotypic cultures (OCs).

3.2. Pathological process spreading and therapeutic application in neurodegenerative diseases

Secretome/Evs derived from diseased cells were found to be implicated in the spread of pathological processes and disease dissemination. Pinto et al. (2017) disclosed that mSOD1 exosomes were enriched in miR-124 and able to cause microglia dysfunction. A 50% reduction in microglia phagocytic ability and increase in senescent cells were detected. Moreover, increased levels of miR-124 in exosomes may consist in a potential biomarker of MN degeneration in ALS and its modulation (downregulation) can be beneficial by decreasing exosomal-inflammatory-miRNA dissemination and result in beneficial paracrine influence toward microglia functional recovery. Additionally, the same study supported the secretome relevance in the signaling mechanisms that underlie HMGB1 (High Mobility Group Box 1)-induced microglia activation. It is important to mention that increased levels of HMGB1 cytokine were found to be released by injured neurons and activated microglia (Brites & Vaz, 2014; Cunha et al., 2016). Vaz et al., (2019) revealed that by secreting increased levels of pro-inflammatory markers (TNF-a/IL-1β/HMGB1/S100B/iNOS) along with enriched levels of SOD1 and HMGB1 proteins and inflamma-miRs miRs-146a/155 in $SOD1^{G93A}$ microglia exosomes, mutant microglia could be contributing to disease propagation and neuroinflammation. Additionally, and supporting the contribution of secretome/Evs to disease dissemination, deleterious exosomes were found to be

transferred from mSOD1 astrocytes to MN (Basso et al., 2013). Those sEVs also contribute to mSOD1 propagation (Grad et al., 2014).

Furthermore, Morel et al. (2013) found that miR-124a carried in exosomes derived from neurons were able to increase the levels of GLT-1 in astrocytes, thus reinforcing miR-124a as an interesting therapeutic target. A second study showed that secretome from mesenchymal stem cells, fibroblasts, neural stem cells and astrocytes rescue cortical neurons from glutamate toxicity by increasing neurite outgrowth and reducing lactate dehydrogenase (LDH) and caspase 3/7 activity (Maguire et al., 2019). Moreover, exosome from murine adipose-derived stromal cells showed to protect NSC-34 cells from oxidative damage by increasing cell viability (Bonafede et al., 2016). In a more recent study, it was demonstrated that neural stem cell (NSC)-sEVs significantly reduced the extent of SCI, microglial activation, neuroinflammation, and neuronal apoptosis, and improved functional recovery in rats submitted to traumatic SCI (Rong et al., 2019). It was also demonstrated that by inducing autophagy, the NSC-sEVs can regulate apoptosis and inflammatory processes. Autophagosome formation was promoted by increased levels of autophagy marker proteins beclin-1 and LC3B. This study showed that treatment with NSC-sEVs reduced apoptosis and neuroinflammation at an early stage of SCI by promoting autophagy. With these findings, the authors demonstrate a future possible therapeutic approach for SCI and possibly neurodegenerative disease, such as ALS, based on sEVs.

Once Secretome/Evs can carry diverse manufactured cargoes they are considered as promising vehicles for drug delivery, as well as for regenerative strategies, therefore bearing therapeutic molecules to inaccessible regions of the CNS. Stem cell secretome has been used as a therapeutic approach to ameliorate CNS complications, such as stroke, traumatic BI, SCI, and neurodegenerative diseases by decreasing inflammation and increasing angiogenesis, neurogenesis, axonal regeneration and oligodendrogenesis (Mendes-Pinheiro et al., 2020). In conclusion, secretome/Evs derived from modulated cells with a specific miRNA seem to be potential vehicles that can be used to lighten ALS progression, pathology, and symptoms mainly through regulation of inflammatory responses.

4. Models to study ALS

Numerous models carrying different mutations in *SOD1*, as well as mutations in other genes such as *C9ORF72*, *TARDBP* and *FUS*, have been developed for clarification of ALS pathological mechanisms. These models include cell lines, such as MN NSC-34 and microglia N9, as well as primary cell cultures and OCs.

Studies across the globe rely on many species such as *Drosophila melanogaster*, *Caenorhabditis, Danio rerio*, *Mus musculus* and *Rattus norvegicus*, being *Mus musculus* the most widely used. Together these diversities of models have allowed the unveiling of molecular,

cellular, and systemic mechanisms that support/trigger ALS onset and progression. However, not always they exhibit all the features found in ALS patients carrying the corresponding mutation (Van Damme et al., 2017). Thus, there is a lack of a trustworthy model for the identification of reliable biomarkers and development of proper therapies.

NSC-34 cell line is the most used MN-like cell line. It results from a fusion between MN of the SC of embryonic mice with neuroblastoma cells (Berthod & Gros-Louis, 2012). NSC-34 stably expressing hSOD1^{G93A} mimics several aspects of MN degeneration, for that reason they are widely used for the study of molecular mechanisms of MN degeneration (Gomes et al., 2008). Supporting this, data from our group show decreased mitochondria viability, apoptotic nuclei, activation of caspase-9 along with ATP depletion, high levels of nitrites and metalloproteinase-9 activation in the extracellular media of NSC-34 cells expressing hSOD1^{G93A} (Vaz et al., 2015).

Additionally, microglial N9 cell line and glial primary cell cultures, as well as OCs and patient-derived cells are used as complement models for studying other molecular mechanisms as well as complex processes linked to ALS pathogenesis.

Patient-derived cells, such as induced pluripotent cells (iPSCs), are obtained from somatic cells of a patient affected by a specific disease. Those cells are reprogrammed preserving the patient genotype. They provide a source that recapitulates the pathological background and allows the study of sALS cases, in opposition to the mice model for example. Moreover, they may eradicate the chances of immune rejection during the transplantation process by using patient own cells (Singh et al., 2015). Knowing this, patient-derived neural cells seem to be a potential reliable model for the study of neurodegenerative diseases such as ALS.

4.1. SOD1^{G93A} mice model

Mutations in *SOD1* are the second most common cause of fALS (accounting for approximately 15%). They can also appear in sALS cases as well (Mathis et al., 2019). SOD1^{G93A} model is currently the most widely used in ALS research and drug testing, thus allowing the comparison between several studies across the globe. Hence transgenic models carrying autosomal dominant mutation such as SOD1^{G93A} has been developed to unveil pathways that are impaired in ALS, allowing a better understanding of the disease. First reported in 1994, SOD1^{G93A} expresses large amounts of mSOD1 and develops adult-onset neurodegeneration of spinal MN and progressive motor deficits leading to paralysis (Gurney et al., 1994). The model was originally developed on a mixed SJL and C57BL6 background and it was the first to have its genome sequenced. However, the present strain is refractory to several tumors (The Jackson Laboratory). On the present thesis, the B6SJL strain will be used in further experiments. For that reason, we may summarize some crucial features. B6SJL mice are hemizygous for human SOD1^{G93A} (human SOD1^{G93A}) and were classified as viable and fertile. Moreover, similarly to the first, it possesses a high number of transgenes copy and a phenotype like the one found in human ALS. Paralysis

can occur in one or more limbs because of SC MN loss. Neuropathology appears in ULM as well. It generally takes place at about five months after the onset of SC MN degeneration and does not progress to absolute neuronal loss. Moreover, the proliferation of reactive astrocytes and microglia have shown to develop in parallel with SC MN degeneration. Since 50 % survive at 128.9 ± 9,1 days it is considered to have an abbreviated life span. For experimental design, a balanced group of male and female mice from the same littermate although with a relative number of male animals (maximum 4) since it was reported as particularly aggressive and quantitative genotyping to ensure transgene copy number (given the importance of copy number) should be considered. Finally, because of the high copy number, a large amount of SOD1 protein is produced. This, in turn, may lead to misinterpretation since ALS patients only hold one allele mutated (The Jackson Laboratory; Alzaforum-Networking for a cure).

4.2. Organotypic cultures (OCs) and relevance in ALS

OCs, 3D culture or organoid culture is defined as the culture of a collected organ derived from an organism. It is an *ex vivo* model that preserves the basic structure and connective organization of a specific tissue or organ covering the gap between the *in vitro* and *in vivo* models (Cavaliere et al., 2016). Former studies showed that interactions between neurons, and neurons and glial cells were effectively maintained in organotypic slices (Lossi et al., 2009). Organotypic slices can be obtained from the brain, SC, and other organs (Shamir & Ewlad, 2014). There are two major types of preparations, acute and chronic OCs. The first are short-living preparations that range between hours and a few days, whereas chronic OCs can be cultivated from a couple of days to several weeks or even more than 2 months with a virtuous morphology (Jackson et al., 2002). Acute OCs slices are mostly done in young pups once they present greater cell viability. On these preparations, the cytoarchitectonic fundaments are established in almost all areas of the tissue/organ. However, a distorted and/or poorly preserved OC may occur on the first development stages. Another factor that contributes to neuroanatomic deformation is the brief time-lapse that these OCs have to recover from the trauma cut. The above-mentioned deformations are less frequent in chronic OCs (Lossi et al., 2009).

In the ’90s a method where explants were cultivated in an air-liquid interface in a semi-porous membrane was developed (Stoppini et al., 1991). Since then this method has been widely used and improved by several research groups once the explants are well oxygenated and receive adequate nutrition from the medium underneath the membrane. Moreover, with this technology cells can be cultured in the lower compartment while slices from a tissue/organ can be cultured on the upper membrane, allowing the study of the impact of cells that are absent in the tissue/organ of interest under normal and pathological conditions (Humpel, 2015). Moreover, in comparison with the roller tube procedure, the air-liquid procedure allows reduced glial cells migration after architectural disruptions (Lossi et al., 2009). OCs have a simple way of preparation and allows the preservation of several aspects of the structural and synaptic organization. Besides

that, they allow the evaluation of a wide range of cellular interactions (Cavaliere et al., 2016). Proliferation and cell death studies are also possible in this type of culture (Lossi et al., 2009).

However, like any model, OCs have limitations. Slices derived from young postnatal animals has a significant reduction in thickness over time. Slices from adult animals preserve their thickness, however necrosis of the central cellular layers and a low tissue survival are observed (Cavaliere et al., 2016). The neurons are the type of cells most affected over time. Tissue age, slice thickness, medium composition, sterility, and health of the donor animals are some parameters that can restrict the survival of this type of cells. Moreover, long-term cultures are time-consuming. On these circumstances, the sterility is arduous to maintain as well (Humpel, 2015). Lastly, loss of tissue structure emerges as one of the big limitations once it may compromise the biological significance of the results. As a result of mechanical damage, MN loss, and neuronal circuit rearrangement are commonly found on SCOCs. Later, the fast rise of glutamate concentration and the consecutive over-activation of glutamate receptors propagate the insult. It was demonstrated that the Tumor Necrosis Factor-α (TNF-α) can act synergistically with the neurotransmitter glutamate to induce MN degeneration. Consequently, these types of neurons end up dying (Albin & Greenamyre, 1992; Lossi et al., 2009). Oxygen and glucose deprivation also contribute to a profound neuron disfunction and apoptosis (Miyata et al., 2002). Another study noticed that microglia participate in glutamate homeostasis and contribute to nitric oxide (NO) production and cellular collapse (Sandra et al., 2012). Those results demonstrate that microglia have a crucial role in this process, suggesting that after a MN insult it acts as a modulator of neurite growth impairments and mediate cell death. A more complex dendritic ramification pattern can also be obtained since damaged axons recover from the injury and start to reroute their processes, thereby, producing new neuronal connections (Lossi et al., 2009).

SCOCs have been used as *ex vivo* models of ALS to study cellular interactions under ALS pathological-like conditions (Berthod & Gros-Louis, 2012), as well as the impact of IgG (Li et al., 2008). More recently, OCs from mSOD1 pups were used to detect of altered glycinergic inhibition in spinal microcircuits (Medelin et al., 2016). Therefore, the examination of MN degeneration and glial cell reactivity in SC slices derived from $SOD1^{G93A}$ mice may open new avenues on the discovery of novel pathophysiological mechanisms in ALS.

II. AIMS

ALS is a neurodegenerative disease that affects UMN and LMN, but evidence shows that glial cells also play a role in the disease onset and progression. We have found overexpression of miR-124 in NCS-34 MN expressing mSOD1 (MN ALS model) and in the spinal cord of mSOD1 mice during the symptomatic stage. In addition, we have identified the presence of this miR-124 in MN-derived sEVs and showed their paracrine influence in determining acute and delayed phenotypic alterations in microglia. Secretome, containing sEVs, is a vehicle that holds a variety of biological molecules, such as cytokines, chemokines, growth factors and miRNAs that reflect the state of the donor cell. Under pathological conditions, they may influence disease progression in ALS. We showed that anti-miR-124 in MN prevents their degeneration and can decrease the levels of this miR-124 in the secretome toward the normal levels. Therefore, we hypothesized that such secretome could have therapeutic properties. To explore this issue, we decided to treat SCOCs from WT and transgenic mice with secretomes from modulated and non-modulated MN. Modulated cells included the WT MN treated with pre-miR-124 to induce a phenotype like that of pathological MN, and the mSOD1 MN that were treated with anti-miR-124 to restore their steady state function. With this in mind, we intend to further explore the harmful effects of upregulated miR-124 in MN as a pathological event in ALS and to assess its restoration toward normal levels would prevent SC cell dysfunction and dysregulated signaling. If we succeed, we may use this rescued secretome as a therapy for the prevention and or delay of ALS progression through the modulation of miR-124 in ALS MN. To achieve that, secretomes will be incubated in lumbar SCOCs of early symptomatic mice (10-12 weeks $SOD1^{G93A}$ or TG animals) and age-matched controls (WT animals).

The specific aims of the present master thesis are to:

1. Evaluate neuron-glia-associated pathological alterations between TG mice at the onset of the disease using SCOCs of 10-12 weeks-old animals and matched WT controls (WT and TG mice OCs exposed to culture media);
2. Unveil if TG SCOCs show less pathological characteristics upon the addition of WT MN-secretome and a neuron-glia metabolism closer to their respective controls (WT slices);
3. Assess if the secretome from NSC-34 MN-like cells expressing mSOD1 (mSOD1 MN) cause dysregulation of cellular and molecular mechanisms in the WT and TG SCOCs;
4. Certify if pre-miR-124 treated WT MNs produce a secretome with the same pathological characteristics of the mSOD1 MN-secretome after its incubation in WT SCOCs;
5. Validate if TG MN secretome paracrine pathology is abrogated when TG MNs are treated with anti-miR-124, after their incubation with WT SOCS, and if such modulation can rescue neurodegeneration and glial cell aberrancies in SCOCs from the mSOD1 mice at the early onset of the disease.

III. MATERIALS AND METHODS

1. Material

1.1. Biological

1.1.1. Animals

Ethics statement

The present study was performed according to the European Community guidelines (Directives 86/609/EU and 2010/63/EU, Recommendation 2007/526/EC, European Convention for the Protection of Vertebrate Animals used for Experimental or Other Scientific Purposes ETS 123/Appendix A) and Portuguese Laws on Animal Care (Decreto-Lei 129/92, Portaria 1005/92, Portaria 466/95, Decreto-Lei 197/96, Portaria 1131/97). All the protocols used in this study were approved by the Portuguese National Authority (General Direction of Veterinary) and the Ethics Committee of the Instituto de Medicina Molecular (iMM) João Lobo Antunes of the Faculty of Medicine, Universidade de Lisboa, Lisbon, Portugal. Every effort was made to minimize the number of animals used, according to the 3R's Principle.

The $SOD1^{G93A}$ (mSOD1) mice is a well-characterized transgenic model of ALS that has been extensively used to study the neuropathological mechanism of ALS. The present model recapitulates widely the human disease, showing progressive degeneration of both ULMs and LMN (Özdinler et al., 2011) as well as glial reactivity and alterations in the inflammatory-miRNA profile in either pre- and symptomatic stages of disease progression (Cunha et al, 20017, Gomes et al 2019). Transgenic B6SJL-TgN 1Gur/J males (Jackson Laboratory, No. 002726) overexpressing $hSOD1^{G93A}$ and WT B6SJLF1/J females were purchased from The Jackson Laboratory (Bar Harbor, ME, USA). Mice were bred at Instituto de Medicina Molecular João Lobo Antunes rodent facilities, where a colony was established. The B6SJL background was maintained by breeding $SOD1^{G93A}$ males with WT females. Experiments were conducted in early-symptomatic mice (10-12 weeks-old animals) and age-matched controls (WT) and both males and females were used in our experiments. Reverse transcription-PCR (RT-qPCR) from a section of the distal phalanx collected at 5-8 days after birth was made to identify the genotype of the mice.

1.2. Supplements and chemicals

Dulbecco's modified Eagle's medium (DMEM) high glucose with glutamine and without pyruvate, penicillin/streptomycin (Pen/Strep), non-essential amino acids (NEAA), glycerol, L-glutamine, 4',6-diamidino-2-phenylindole (DAPI), Isofluorane , Triton X-100 and absolute ethanol were acquired from Merck (Darmstadt, Germany). Trypsin-ethylenediamine tetra acetic acid (trypsin-EDTA) solution, bovine serum albumin (BSA), Poly-D-Lysine (PDL) and XtremeGENE™ HP DNA Transfection Reagent and 4-(2-hydroxyethyl)-1-piperazine ethanesulfonic acid (HEPES) were obtained from Sigma-Aldrich (St. Louis, MO, USA). Geneticin 418 sulfate (G418) was purchased from Calbiochem (Darmstadt, Germany). DMEM-Ham's F-12 without glutamine, Hank's balanced salt solution (HBSS), Neurobasal medium, Opti-MEM™, Fetal Bovine Serum (FBS), Heat-inactivated horse serum, B-27 serum-free supplemented with vitamin A and TRIzol® were from Life Technologies (Waltham, Massachusetts, USA). Xpert cDNA Synthesis Mastermix kit and Xpert Fast SYBR Mastermix BLUE kit were purchased from GRiSP (Porto, Portugal). miRCURY® LNA® RT Kit and primer mix for miRNAs and SNORD were obtained from Qiagen (Hilden, Germany). Power SYBR™ Green PCR Master Mix was from Applied Biosystems (Massachusetts, USA). Pre-miR™ miRNA precursor 124 (mimic) and Anti-miR™ miRNA Inhibitor 124 were from Ambion (Massachusetts, USA). All the SCOCs slices staining procedures were mounted using Fluoromount-G (Southern Biotech, Birmingham, AL). All the other commonly used reagents were purchased either from Sigma-Aldrich or Merck.

1.3. Primers

The set of primers used to amplify protein-coding genes (Thermo Scientific) are listed in Table III.1, whereas primer mix used to amplify miRNAs (miR-21, miR-124, miR-125b, and miR-146a), from Qiagen, are listed in Table III.2.

Table III.1 - List of primer sequence used in RT-qPCR to amplify protein-coding genes.

Gene	**Forward primer** (5'-3')	**Reverse primer** (5'-3')
iNOS	ACCCACATCTGGCAGAATGAG	AGCCATGACCTTTCGCATTAG
IL-1β	CAGGCTCCGAGATGAACAAC	GGTGGAGAGCTTTCAGCTCATA
IL-10	ATGCTGCTTGCTCTTACTGA	GCAGCTCTAGGAGCATGTGG
HMGB1	CTCAGAGAGGTGGAAGACCATGT	GGGATGTAGGTTTTCATTTCTCTTTC
CX3CR1	ATGGGGTCTCTGTCTGCTCT	TACTGGCAATGGGTGGCATT
CX3CL1	CTCACGAATCCCAGTGGCTT	TTTCTCCTTCGGGTCAGCAC
S100B	GAGAGAGGGTGACAAGCACAA	GGCCATAAACTCCTGGAAGTC
GFAP	CAAACTGGCTGATGTCTACC	GCTTCATCTGCCTCCTGTCTA
DLG4	GAGGCTGGCGGCCAGTACACCAG	ACAGAGCAGGCGGTCAG
SYP	GACGTTGGTAGTGCCTGTG	GCACAGGAAAGTAGGGGGTC
MFG-E8	AGCCTGAATGGTAGGGTTGG	GAGACTGCATCCTGCAACCA
GLT-1	GTGAACAGGCCAAGCTGATG	CGTACCACAGCGCCATTACA
TREM2	GTGGCCAGTGGGCTAGACT	CTCTGGGTCCAGTGAGGA
MFN2	CAGAGCAGAGCCAAACTGCT	AACATGTTGAGTTCGCTGTCC
DRP1	GCTCAGTGCTGGAAAGCCTA	TCCATGTGGCAGGGTCATTT
β-actin	GCTCCGGCATGTGCAA	AGGATCTTCATGAGGTAGT

RT-qPCR, reverse transcription-quantitative polymerase chain reaction; **iNOS,** inducible nitric oxide synthase; **IL-1β**, interleukin 1-beta; **IL-10**, interleukin-10: **HMGB1**, high mobility group box 1; **CX3CR1**, C-X3-C motif chemokine receptor 1; **CX3CL1**, C-X3-C motif chemokine ligand 1/fractalkine; **S100B**, S100 calcium-binding protein B; **GFAP**, glial fibrillary acidic protein; **DLG4**, discs large MAGUK scaffold protein 4 (that encodes for postsynaptic density protein 95, PSD-95); **SYP**, synaptophysin; **MFG-E8**, milk fat globule-EGF factor 8; **GLT-1**, glutamate transporter-1, **TREM2**, triggering receptor expressed on myeloid cells 2; **MFN2**, mitofusin-2; **DRP1**, dynamin-related protein 1; **β-actin**, beta-actin.

Table III.2 - List of primer sequences used in RT-qPCR to amplify miRNAs.

miRNAs	**Target sequence** (5'-3')
hsa-miR-21-5p	UAGCUUAUCAGACUGAUGUUGA
hsa-miR-124-3p	UAAGGCACGCGGUGAAUGCC
hsa-miR-125b-5p	UCCCUGAGACCCUAACUUGUGA
hsa-miR-146a-5p	UGAGAACUGAA UUCCAUGGGUU
SNORD110	Reference gene
Unisp6	Spike in quality control gene

RT-qPCR, reverse transcription-quantitative polymerase chain reaction; **miRNA**, microRNA; **hsa,** homo sapiens.

1.4. Primary and secondary antibodies

The antibodies used for immunohistochemistry studies, as well as its respective sources, species and dilutions, are listed in **Table III.3.**

Table III.3 - List of primary and secondary antibodies used in Immunohistochemistry.

Antibodies		Source	Species	Dilution
Primary	**GFAP**	NovoCastra, GFAP-GA5-6035278	Mouse	1:100
	Iba-1	Wako, 019-19741	Rabbit	1:250
Secondary	**Alexa 647 anti-mouse**	Invitrogen, A21236	Goat	1:500
	Alexa 594 anti-rabbit	Invitrogen, A111012	Goat	1:500

GFAP, glial fibrillary acidic protein; **Iba-1**, ionized calcium-binding adapter molecule 1.

2. Methods

2.1. NSC-34 MN-like cell line cultures

Mouse NSC-34 MN-like cell line, stably transfected with hSOD1, either WT (WT MN) or mutated in G93A ($SOD1^{G93A}$/mSOD1 MN) was used as usual in our laboratory (Vaz et al., 2015; Pinto et al., 2017). This hybrid cell line was produced by the fusion of MN from the SC embryos with N18TG2 neuroblastoma cells (Cashman et al., 1992) and exhibits properties of MN after differentiation and maturation protocols, except for glutamate-induced excitotoxicity (Madji Hounoum et al., 2016). Moreover, studies have been made to assess neurotoxicity/neuroprotection by using this cell line (Maier et al., 2013; Vaz et al., 2015). Additionally, reduced survival, time-consuming extraction protocols, low purity, and yield of primary spinal MN cultures (Stifani & Mobility, 2014) along with immature phenotype of MN differentiated from embryonic stem cells (Bucchia et al., 2018) or made from induced pluripotent stem cells (Ho et al., 2016) make the adoption of the above-mentioned models difficult. In this way, MN-like NSC-34 is broadly used to study the molecular and cellular alterations of MN that occurs in ALS.

WT and mSOD1 NSC-34 cells were seeded in PDL-coated plates (10 µg/ml) a concentration of 5 × 10^4 cells/ml and maintained at 37ºC in a humidified atmosphere of 5% CO_2 in proliferation medium [DMEM high glucose with glutamine, without pyruvate, supplemented with 10% of FBS and 1% of Pen/Strep, and G418 at 0.5 mg/ml for selection] (Vaz et al., 2015; Pinto et al., 2017). Differentiation was induced after 48 h by changing medium for DMEM-F12 plus 1% of FBS, 1% of NEAA, 1% of Pen/Strep and 0.5 mg/ml of G418, as determined by (Cho et al., 2011), which corresponded to 0 days *in vitro* (DIV). At 2 DIV, WT and mSOD1 MN were transfected with 15 nM of miRNA Pre-miR miRNA Precursor 124 (mimic) or Anti-miR miRNA Inhibitor 124, respectively, by using XtremeGENE HP DNA Transfection Reagent in a proportion of 1:2 and diluted in Optimem. After 12 h of transfection, media was replaced by a new differentiation medium, this time FBS-exosome depleted, and cells were cultured for additional 2 DIV. Cells and secretome were then collected after 4 DIV of differentiation, a timepoint previously established to induce SOD1 accumulation and miR-124 overexpression in mSOD1 cells (Vaz et al., 2015; Pinto et al., 2017). Secretomes were collected from WT and mSOD1 MN and incubated in spinal cord organotypic cultures. A schematic representation of this model is indicated in **Figure III.1**.

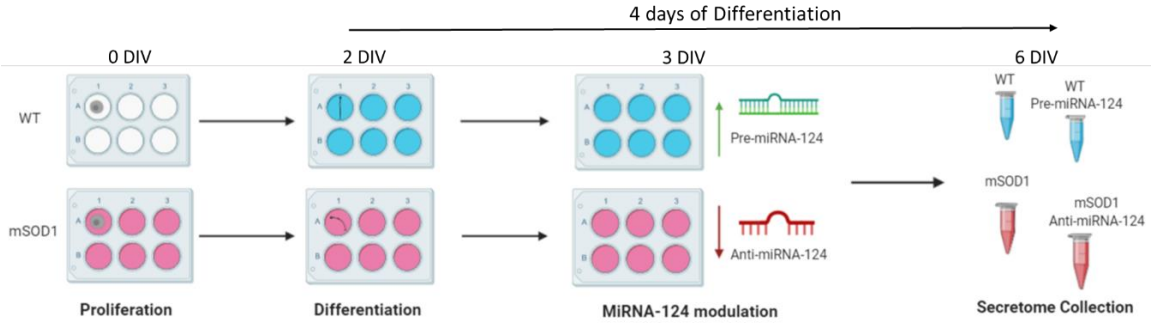

Figure III.1 - Schematic illustration of miR-124 modulation in WT and mSOD1 NSC-34 MN cell line. Wild type (WT) and $SOD1^{G93A}$/mSOD1 motor neurons (MN) were plated in PDL coated plates and maintained for 48h in proliferation media. The differentiation was induced in the time considered as 0 days of differentiation (0 DIV) and at 2 DIV WT MN were transfected with pre-miR-124 and mSOD1 MN with anti-miR-124. New differentiation media was added 12h after and cells were maintained for more 2 DIV. Finally, WT, WT pre-miR-124, mSOD1, and mSOD1 anti-miR-124 secretome were collected at 4 DIV and later incubated in spinal cord organotypic cultures (SCOCs). (Created with BioRender.com)

2.2. Spinal cord organotypic cultures (SCOCs)

SCOCs were used to explore ALS homeostatic imbalance and cell pathology when obtained from the $SOD1^{G93A}$ mice model relatively to matched controls. OC is a strong model that conserves the basic structure and connective organization of a specific tissue or organ of interest (Cavaliere et al., 2016). Moreover, interactions between neurons, neurons and glial cells and paracrine signaling (our point of interest) are effectively maintained in this *ex vivo* model (Lossi et al., 2009).

Thus, WT and TG (mSOD1) early symptomatic animals (10-12 weeks old mice) were used in our experiments. Animals were anesthetized with inhalant isoflurane prior sacrifice. Dissected

lumbar portions of the spinal cords were embedded in ice-cold HBSS medium (with 6mg/ml of glucose and 5% of Pen/Strep) to simulate *in vivo* pH and osmotic balance and maintain the tissue consistency. Transversal SCOCs slices of 350 µm were obtained by using a McIlwain Tissue Chopper® (Gomshall, Surrey, UK). Next, a set of 4 slices were placed in the upper face of the insert membrane (BD Falcon, #353493, Lincoln Park, NJ, USA) and cultured on the surface of 0.4 µm pores inserts membrane. The inserts were then placed in 6-well plates with culture medium (Neurobasal medium plus 2% of B27, 1,33 % of glucose, 1,5% of Pen/Strep and 1% of L-glutamine) during 3 DIV for trauma cut recovery. Fresh culture medium was added each 24 h and SCOCs slices were cultivated at 37ºC in a humidified atmosphere of 5% CO_2 in the air-liquid interface. At 3 DIV, WT and TG SCOCs were incubated with secretome described in section 2.1. SCOCs were collected after 4 h and 24 h of incubation and non-treated WTOC or WTOC incubated with WT MN secretome were used as controls. Slices were collected and stained with propidium iodide (PI) for assessment of non-viable cells, with GFAP and Iba-1 antibodies for assessment of GFAP- and Iba-1 -positive cells, or in Trizol for RNA isolation with later quantification by RT-qPCR. No change in color and transparency was detected during the culture under the light microscope. A schematic representation of the model is indicated in **Figure III.2**.

Cell cultures (NSC-34 MN-like cell line) and SCOCs were handled in sterile conditions in a Holten Lamin Air HVR 2460 (Allerod, Denmark) and maintained in HERA cell 150 incubators (Thermo Scientific, Waltham, MA, USA) in stable and optimal conditions for cell growth (37ºC, 5% CO2).

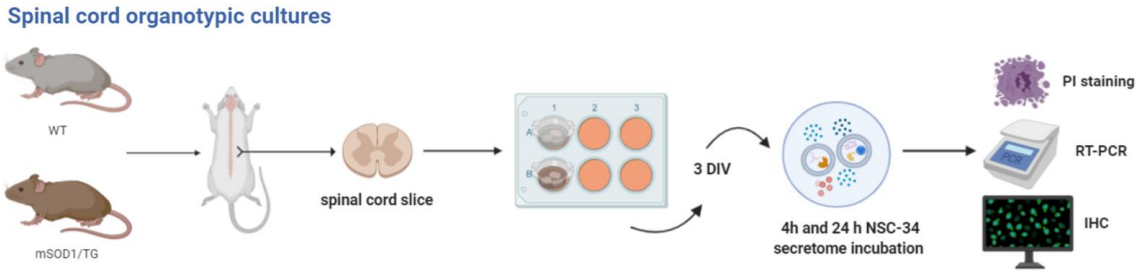

Figure III.2 - Schematic representation of WT and TG (mSOD1) spinal cord slices acquisition and MN secretome incubation. Transgenic (TG) mice at an early symptomatic stage (10-12 weeks-old animals) and aged-matched controls (wild type [WT] animals) were used in our experiments. The lumbar region of the spinal cords of the above-mentioned mice was dissected and divided transversally into 350 µm slices by using a McIlwain Tissue Chopper. Slices were then placed and cultivated in tissue inserts that were positioned in 6-well plates. SCOCs were maintained for 3 DIV in culture medium before 4h and 24h MN secretome incubation. Non-treated WTOC or WTOC incubated with WT MN secretome were used as our controls. Finally, SCOCs were collected for RNA isolation and subsequent RT-qPCR, for propidium iodide (PI) staining and immunohistochemistry (IHC) assay. (Created with BioRender.com)

2.3. Assessment of cell death by necrosis

Necrotic cell-like death was determined by monitoring the cellular uptake of the fluorescent dye propidium iodide (PI). Propidium iodide is membrane impermeant and therefore excluded from viable cells. It binds to DNA by intercalating between the bases, thereby binding both DNA and RNA. When bound to DNA, this dye emits red fluorescence (630 nm) (Givan, 1992). After

incubation with MN secretome, unpermeabilized slices were incubated with the PI solution for 15 minutes at 37ºC in a humidified atmosphere of 5% CO_2 in absence of light. For the achievement of the last step, a stock PI solution [0.5 mg/ml] were diluted 1:20 in the culture medium. Slices were then washed with PBS and fixed with PFA 4% in PBS for 1 h in room temperature in absence of light. After a previous wash with PBS, slices were stained with DAPI (1:1000 in PBS) for 5 minutes. Slices were again washed with PBS and immediately mounted using Fluoromount-G for fluorescence/confocal microscopy. Images of at least 5 ventral horn fields per condition were obtained with 40 x magnification in at least three independent samples (n≥ 3). A threshold of mean fluorescence ≥ of 100 pixels was established for PI-positive cells. Moreover, particles between 3 and 50 μm^2 size co-stained with blue (DAPI) and red (PI) were considered dead cells. Fluorescence images were acquired by using Leica DMi8-CS inverted microscope with Leica LAS X software and the different z-stacks were merged and analyzed with ImageJ (Fiji Is Just) software.

2.4. Immunohistochemistry assay (GFAP- and Iba-1 positive cells)

For immunostaining procedure, slices were washed with Phosphate-Buffered Saline (PBS) solution and immediately fixed with Paraformaldehyde (PFA) 4% in PBS for 1 h at room temperature. Later, the slices were washed one more time with PBS and cut out from the insert, placed into glass slides and blocked for 3 h at room temperature with blocking solution (2% of heat-inactivated horse serum, 10 % of FBS, 1 % of BSA, 0.25 % of Triton X-100 and 1 nM of HEPES). Slices were subsequently incubated with primary antibodies (**Table III.3**) diluted in blocking solution on a moist bed at 4°C for 48 h. Afterwards, SCOCs slices were washed 3 times for 20 minutes with 0.01 % Triton X-100 in PBS solution and incubated with secondary antibodies (**Table III.3**) diluted in blocking solution for 24 h at 4°C. Slices were washed in the same conditions and cell nuclei stained with DAPI (1:1000 in PBS) for 5 minutes. Slices were again washed 3 times, this time with PBS. Lastly, slices were mounted with one drop of Fluoromount-G and one lamella for fluorescence/confocal microscopy. Images of at least 5 ventral horn fields (n≥ 3) per condition were obtained with 40x magnification. Fluorescence images were acquired by using Leica DMi8-CS inverted microscope with Leica LAS X software and the different z-stacks were merged and analyzed with ImageJ (Fiji Is Just) software.

2.5. Reverse transcription-quantitative PCR

Following incubation with MN secretome, SCOCs were washed once with PBS and collected in Trizol reagent for RNA isolation. Sample homogenates were obtained by using a Pellet Mixer (VWR Life Science, EUA) and total RNA was extracted and quantified as usual in our laboratory.

NanoDrop ND100 Spectrophotometer (NanoDrop Technologies, Wilmington, USA) was used for RNA quantifications of SCOCs slices homogenates Samples with a yield ≥ to 500 ng/µl of total RNA were used for quantification of mRNA expression by converting it into complementary DNA (cDNA). For genes, the Xpert cDNA Synthesis Mastermix kit was used. Later, RT-qPCR was performed by using an Xpert Fast SYBR Mastermix BLUE kit. The sequences of the primers that were used are listed in **Table III.1**. RT-qPCR was performed in 384-well plates and each sample was quantified in duplicate. Non-template controls (NTC) for each amplification product were used as well under optimized conditions: 50ºC for 2 min, 95ºC for 2 min, followed by 45 amplification cycles at 95ºC for 5 seconds and 62ºC for 30 seconds. A melting curve analysis was done after the amplification to verify specificity. β-actin was used as an endogenous control to normalize each gene expression level.

MiRNAs expression was also achieved by RT-qPCR. In the same way, total RNA was extracted from the SCOCs after homogenization of the slices. After RNA quantification, 5 ng of total RNA was converted to cDNA by using the miCURY LNA™ RT Kit under the following conditions: 60 min at 42ºC succeeded by heat-inactivation of the reverse transcriptase for 5 min at 95 ºC. Subsequently, RT-qPCR was performed by using Power SYBRTM Green PCR Master Mix in combination with the primers listed in **Table III.2**. The reaction conditions consisted of polymerase activation/denaturation under the following conditions: 95 °C for 10 min, followed by 50 amplification cycles at 95 °C for 10 s and 60 °C for 1 min. A melting curve analysis was done as well after the amplification to verify specificity. Here, SNORD was used as a reference control to normalize each miRNA expression level.

Relative mRNA/miRNA concentrations are represented as fold change which was determined by the $2^{-\Delta\Delta CT}$ method as previously performed in our studies (Cunha et al., 2017). A total of 4 or more mice per group (randomly chosen) were used and data normalized to the average of age-matched WT mice for each PCR plate. cDNA synthesis from RNA samples was performed in a thermocycler (Biometra®, Göttingen, Germany). Later, we used the QuantStudio 7 Flex Real-Time PCR System (Applied Biosystems, Life Technologies) to determine mRNA and miRNA expression by reverse transcription-quantitative PCR (RT-qPCR).

2.6. Statistical analysis

Statistical analysis was performed using GraphPad Prism 7 (GraphPad Software, San Diego, CA, USA). Data of, at least, three different experiments were expressed as mean ± SEM. Differences between WT and TG ($SOD1^{G93A}$) non-treated SCOCs, as well as between WT and TG SCOCs incubated with MN secretomes were determined by unpaired Student's *t*-test. Welch's *t*-test correction was applied when variances were different between the two groups. Two-tailed Mann-Whitney test was applied when data did not assume a Gaussian distribution. Moreover, comparisons of more than two groups were done by one-way ANOVA followed by multiple comparisons Bonferroni post hoc correction. Values of $p < 0.05$ were considered statistically significant.

IV. RESULTS

Previous data from our group demonstrated NSC-34-MN-like cell line overexpressing the hSOD1^{G93A} mutation (mSOD1 MN) had increased levels of miR-124 comparatively to the non-mutated ones overexpressing hSOD1^{WT} (WT MN). Such miR-124 upregulation was similarly observed in both exosomes and secretome from the mSOD1 MN (Pinto et al, 2017; Colaço, Master Thesis 2020), suggesting that the transference of this miRNA can have important paracrine signaling effects to the neighbor cells. In addition, recent data from the group showed that several mechanisms involved in mSOD1 MN dysfunction, such as dysregulation of mitochondrial dynamics, axonal transport and synaptic signaling, were prevented upon transfection with anti-miR-124 (Vizinha, Master Thesis, 2018). Moreover, mSOD1 MNs-derived secretome induced microglia and astrocyte reactivity, an effect that was abolished when the glial cells were incubated with secretome from mSOD1 MNs modulated with anti-miR-124, confirming the crucial role of this miRNA in inducing either MN dysfunction in ALS and in promoting glial reactivity in cellular models.

The present work aimed to further explore the consequences of the anti-miR-124 strategy in ALS models by using for the first time the OCs of the spinal cord of mSOD1 mice at the early onset of the disease, i.e., at 10-12-weeks-old. Specifically, the present work aims to assess: (i) Pathological differences in TG SCOCs relatively to the matched WT samples at the early onset of the disease; (ii) Beneficial therapeutic effects of the secretome from healthy MNs on the pathological features of TG SCOCs from mice at 10-12-weeks-old; (iii) Adverse effects of the mSOD1 MN secretome on healthy WT SCOCs from young adult mice; (iv) Pathological consequences of the secretome enriched in miR-124 on WT SCOCs from adult mice; (v) Therapeutic advantage of the secretome from mSOD1 MNs downregulated for miR-124 in the recovery of pathological features of TG SCOCs at the early onset of the disease.

1. SCOCs from TG mice show elevation of cell demise, changes in inflammatory-associated miRNAs and neuron/glia-dysregulated genes at the onset of the disease

First, we intended to establish which pathological changes could be observed in the transgenic mice relatively to its matched control, using SCOCs obtained at the onset of the disease (10-12-weeks old), by assessing mediators of neurodegeneration and glial cell aberrancies, namely those associated to astrocyte reactivity and microglia activation. As so, 350 µm SC lumbar slices were maintained in culture during 3 DIV for trauma cut recovery. Afterwards, SCOCs were exposed to an additional 24h of culture medium to evaluate whether the presence of the ALS pathology at this stage was reflected in (i) increased cell death by necrosis; (ii)

reduction of GFAP staining, a characteristic of astrocyte aberrancy in ALS; (iii) microgliosis, by the number of Iba-1^{+} cells; and (iv) pathological transcriptomic profiling.

A representative image of slice resultant from a SCOCs is presented in **Figure IV.1**, where we were able to observe GFAP and Iba-1 staining preferentially in the ventral region. Moreover, Dapi staining was identified not only at the edge but also in the center of the slice, indicating that other cells than Iba-1- and GFAP-positive cells are also preserved in the SCOCs.

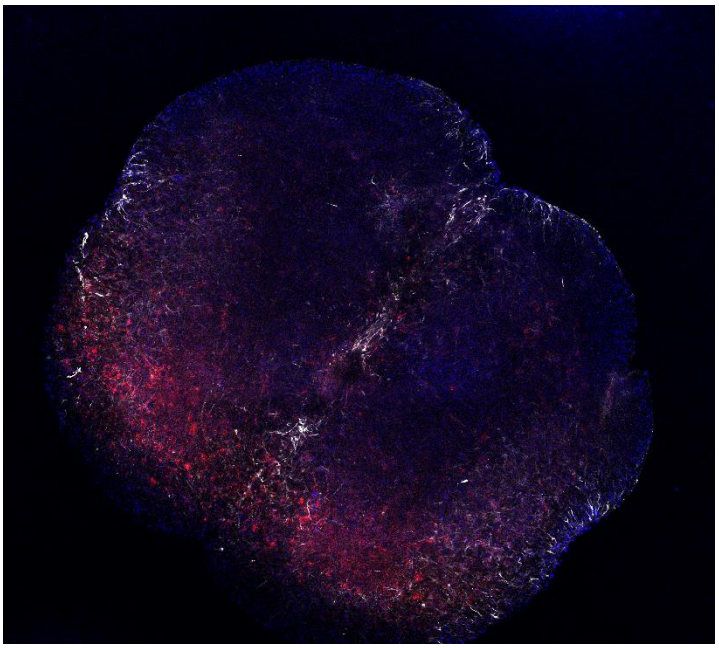

Figure IV.1 - Representative image of a transversal spinal cord slice stained for microglia and astrocytes. Nuclei are in blue (Dapi), microglia in red (Iba-1) and astrocytes in white (GFAP).

1.1. SCOCs from TG mice show increased cell necrosis and proneness to astrocyte reduced GFAP staining at the onset of the disease

To assess the presence of necrosis, we used the PI staining. As shown in **Figure IV.2A** we were able to observe that an increased number of cells (approximately 15%) were suffering necrosis in the SCOCs from the TG mice relatively to the WT animals ($p<0.05$). Elevated co-localization of DAPI (blue) and PI probe (red) in the cell's nuclei TG slices could be observed evidencing the penetration of the dye trough cell and nucleus membranes, as expected in non-viable cells suffering the necrotic process (Givan 1992). Once the loss of MNs is a characteristic feature of ALS and results are from SC ventral horn fields, we hypothesize that this finding may result from their degeneration, which was previously identified by staining for neurofilaments in the SC of TG mice at the symptomatic stage (Cunha et al., 2017, Turner and Talbot 2008).

Preliminary data obtained by immunohistochemistry do not suggest the presence of microgliosis or astrocytosis at the onset of the disease (**Figure IV.2B**). GFAP$^+$ and Iba-1$^+$ cells, occupy near 25% and 10%, respectively, of the WT SCOCs area. Such density is near the one previously indicated, i.e. 30% and 10% of total mammalian CNS cells population (Liddelow & Barres, 2017; Komine & Yamanaka, 2015; Butovsky & Weiner, 2018). A decrease of GFAP$^+$ of near 10% is apparent in the TG SCOCs and is in line with the downregulation of GFAP previously observed in the cortical and spinal astrocytes of rodent mSOD1 ALS models, mainly during the symptomatic stage (Yoshii et al., 2011; Díaz-Amarilla et al., 2011; Gomes, 2020).

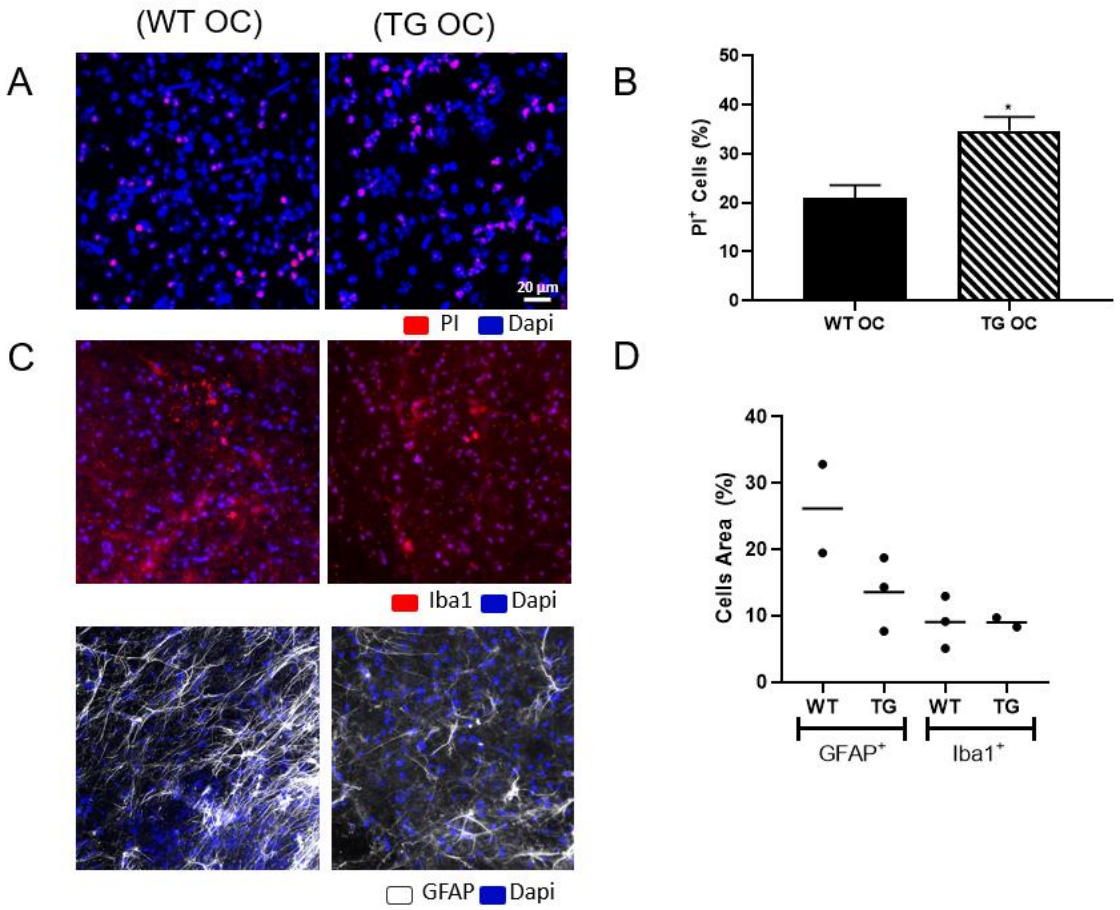

Figure IV.2 - Spinal cord organotypic cultures (OCs) of ALS transgenic mice show increased cell demise and an apparent reduction of GFAP staining. On the fourth day of culture, wild Type (WT) and transgenic (TG) slices (overexpressing hSOD1^{G93A}) were incubated with the propidium iodide (PI) probe for 1h to assess cell demise. (**A**) Representative images of ventral horn regions of WT and TG slices stained for PI (red, dead cells) with the cell nuclei in blue (DAPI). (**B**) Results are mean ± SEM of 4 independent experiments for the percentage of dead cells (co-stained cell nuclei) per condition. *p<0.05 *vs.* WTOC using two-tailed unpaired Student's *t*-test with Welch's correction when required. (**C**) Representative immunohistochemistry images for GFAP (white, astrocytes) and for Iba-1 (red, microglia)-positive cells in WT and TG spinal cord organotypic cultures (OCs). (**D**) Percentage of the area occupied by GFAP and Iba1-positive cells by individual evaluation in duplicates and triplicates (represented as dots) in ventral horn fields of SCOCs, and respective average (line). Scale bar: 20 µm. **GFAP**, glial fibrillary acidic protein; **Iba-1**, ionized calcium-binding adapter molecule 1.

1.2. SCOCs from TG mice show immune dysregulation, activation of compensatory mechanisms and disturbed neuronal function at the onset of the disease

Once we could observe some early pathological changes in the TG SCOCs, we decided to assess whether alterations of inflammatory-associated miRNAs (miR-21, miR-124, miR-125b and miR-146a) could be noticed, as well.

Globally, TG SCOCs showed a dysregulated signature of inflammatory miRNAs (inflamma-miRs) that included upregulated miR-21 ($p<0.05$) and miR-146a ($p<0.05$), but no alterations for miR-124 and miR-125b (**Figure IV.3A** and heat map in **Figure IV.3C**). This profile points to the presence of an anti-inflammatory status that may precede the occurrence of neuroinflammation, probably as a defensive mechanism. Indeed, such miRNAs are known to target genes associated with immune dysregulation.

Having observed the dysregulation of inflamma-miRs, next we explored several genes associated with neurodegeneration, as well as to astrocyte and microglia polarized cells. Polarization towards activation is suggested by elevated levels of IL-1β ($p<0.01$), CX3CR1 ($p<0.05$) and TREM2 ($p<0.05$) (**Figure IV.3B,C**). Nevertheless, other genes of inflammation were found unchanged (MFG-E8) or decreased (iNOS and HMGB1, $p<0.05$), and the IL-10, a cytokine with anti-inflammatory properties (though a matter of controversy), was upregulated, thus reinforcing the homeostatic imbalance and the decompensated immunoinflammatory status. Relatively to astrocytes, we could validate the reduced GFAP mRNA ($p<0.001$), while S100B was not altered, and GLT-1 was overexpressed ($p<0.05$), again suggesting the activation of mechanisms of reparation. Now, and related with neuronal function, we obtained a downregulation of CX3CL1 ($p<0.01$), suggesting compromised neuronal-microglial CX3CL1-CX3CR1 axis, together with that of Dlg4 ($p<0.05$) that encodes for the PSD-95 post-synaptic protein. In contrast, we identified an upregulated SYP gene that encodes for the pre-synaptic protein synaptophysin, suggesting a mechanism to counterbalance the disturbed post-synaptic signaling. Increased transcript levels of TREM2 ($p<0.05$), impairments at the synaptic level and increase in necrosis are consistent with data achieved in other neurodegenerative pathologies (Lue et al., 2015). To further understand alterations of fusion-fission dynamics in neuronal mitochondria we assessed the expression of related genes, respectively MFN2 and DRP1 (**Figure IV.3B,C**). While the first was unchanged, the later was overexpressed ($p<0.05$) indicating an acute and adaptive response to maintain mitochondrial and MN integrity upon injury (Kiryu-Seo et al., 2016).

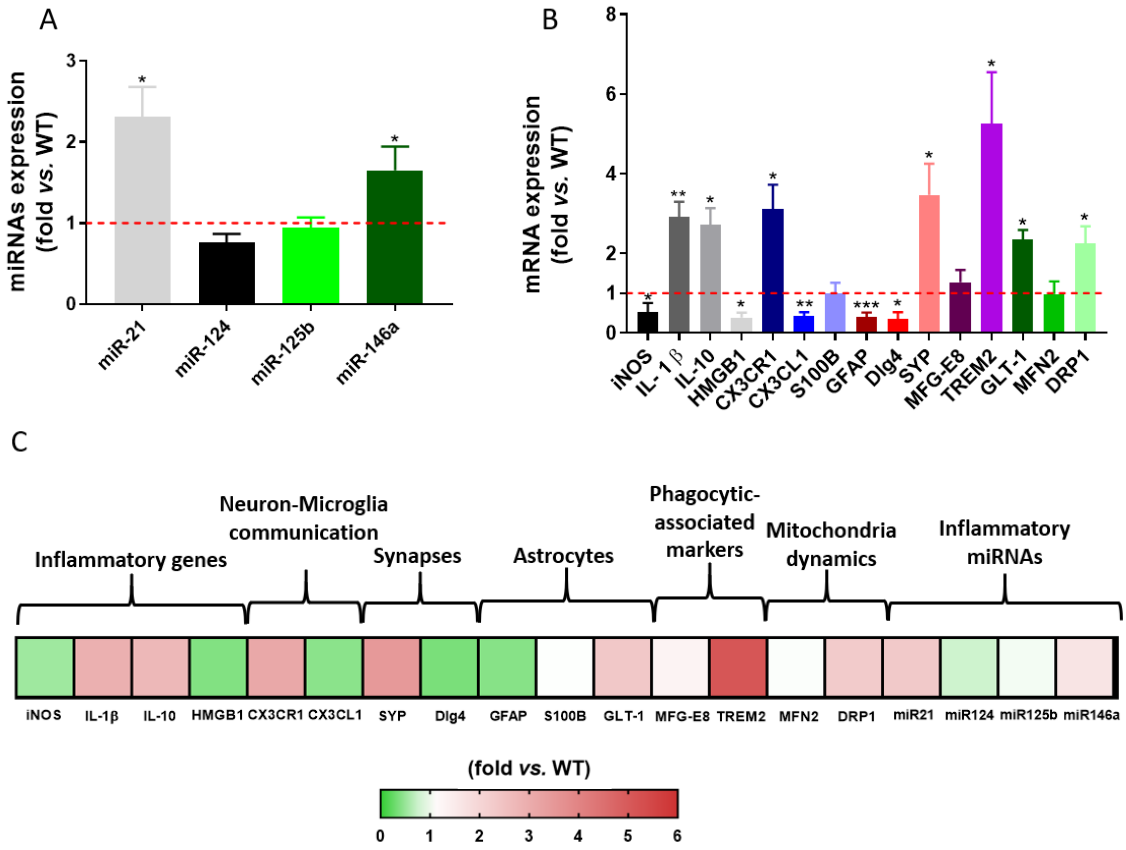

Figure IV.3 - Spinal cord organotypic cultures of ALS transgenic mice show dysregulated inflammatory-associated mediators, including miRNAs, as well as adaptative responses to neuronal damage by the transcriptomic profiling. After 3 days in culture and 24 h incubation with culture medium (4 DIV), WT (wild type) and TG (transgenic) spinal cord organotypic cultures were collected in Trizol for reverse transcription-quantitative polymerase chain reaction (RT-qPCR) analysis. β-actin was used as an endogenous control for protein-coding genes while SNORD was used as a reference gene for miRNAs. MiRNA levels of miR-21, miR-124, miR-125b, and miR-146a and mRNA levels of iNOS, IL-1β, IL-10, HMGB1, CX3CR1, CX3CL1, S100B, GFAP, Dlg4, SYP, MFG-E8, GLT-1, TREM2, MFN2, and DRP1 of TG slices *vs.* WT OC are depicted, respectively, in (**A**) and (**B**). Results are mean ± SEM of, at least, 4 independent experiments. **p*<0.05, ***p*<0.01 and ****p*<0.001 *vs.* WTOC (red dashed line) were obtained by using two-tailed unpaired Student's *t*-test with Welch's correction when required. (**C**) Heat map summarizing the distinct transcriptomic profile of early symptomatic SCOCs. **iNOS,** inducible nitric oxide synthase; **IL-1β**, interleukin-1 beta; **IL-10**, interleukin-10; **HMGB1**, high mobility group protein 1; **CX3CR1**, C-X3-C motif chemokine receptor 1; **CX3CL1**, C-X3-C motif chemokine ligand 1; **S100B**, S100 calcium-binding protein B; **GFAP**, glial fibrillary acidic protein; **Dlg4**, discs large MAGUK scaffold protein 4 (or PSD-95, postsynaptic density protein 95); **SYP**, synaptophysin; **MFG-E8**, milk fat globule-EGF factor 8; **GLT-1**, glutamate transporter 1, **TREM2**, triggering receptor expressed on myeloid cells 2; **MFN2**, mitofusin-2; **DRP1**,

2. WT MN secretome has a neuroprotective effect on TG SCOCs by circumventing cell death and immune dysregulation

Once we have been working with the secretome of miR-124 MN modulated cells, and before assessing whether it could be used for their potential therapeutic benefits, we next determined if the secretome from the non-treated NSC-34 MN-like cells added to SCOCs obtained from the TG mice could by itself have a beneficial influence on cell demise and neuroimmune imbalance. For comparison, we evaluated the effects also produced on SCOCs from WT mice. For that, the

secretomes from naïve NSC-34 cells were incubated for 24 h after the 3 day recover of SCOCs obtained from either WT or TG mice.

2.1. WT NSC-34 MN secretome prevents cell necrosis in SCOCs from TG mice after 24 h incubation

Results show that WT MN secretome has beneficial effects in TG SCOCs by sustaining the cell viability in a similar way to data of WT slices. This finding is evident when comparing the representative images of ventral horn regions of WT and TG slices stained for PI (red, dead cells) with the cell nuclei in blue (DAPI) after the addition of the secretome from WT MNs (**Figure IV.4A).** Also, by assessing the cell demise in folds, considering the WT SCOCs as fold 1 (control), it is clear from **Figure IV.4B** that no changes were obtained for the WT SCOCs treated with WT MN secretome relatively to WT SCOCs. However, it is manifest that the increased fold of TG SCOCs ($p<0.05$), was prevented by the addition of the WT MN secretome ($p=0.09$ Anova; and $p<0.05$ by *t* student analysis when comparing the secretome treated TG SCOCs with the non-treated one), thus maintaining the levels near to the control ones. No changes were obtained relatively to the number of $GFAP^+$ or $Iba1^+$ cells (data not shown).

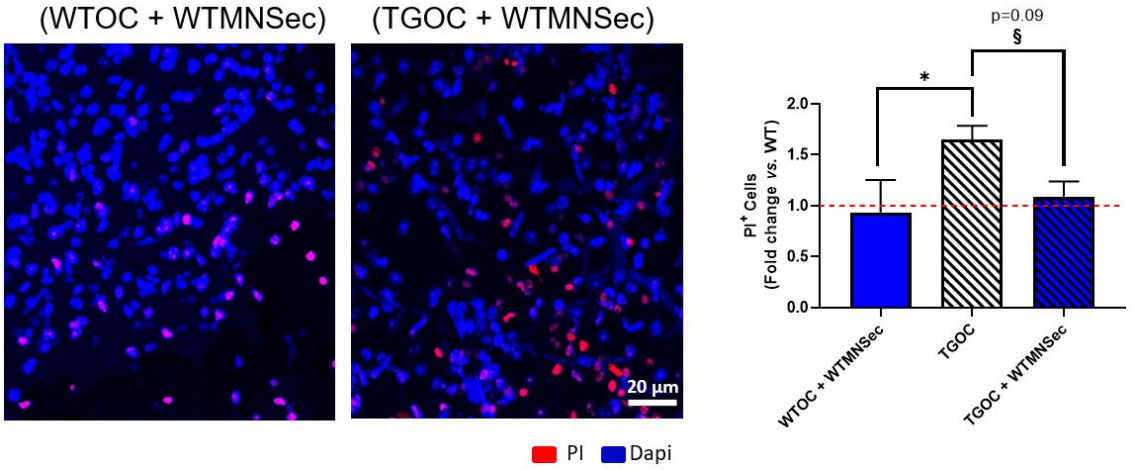

Figure IV.4 - Cell demise in spinal cord organotypic cultures (OCs) of ALS transgenic mice was prevented by 24 h treatment with the secretome (Sec) of NSC-34 MN-like cells. After 24h addition of wild type (WT) Motor Neuron (MN) Sec to WT or transgenic (TG) OCs we proceed to the incubation with the propidium iodide (PI) probe for 1h. (**A**) Representative images of ventral horn regions of WT and TG slices treated with the WT MN secretome and stained for PI (red, dead cells) with the cell nuclei in blue (DAPI). (**B**) Results are mean fold change ± SEM of, at least, 3 independent experiments. **p*<0.05 and p=0.09 *vs.* WTOC (red dashed line) using one-way ANOVA followed by multiple comparisons Bonferroni post hoc correction. $^{\S}p<0.05$ *vs.* TGOC using two-tailed unpaired Student's *t*-test with Welch's correction when required. Scale bar: 20 µm.

2.2. WT MN secretome has a protective effect in neuroimmune dysregulation of SCOCs from TG mice after 24 h incubation

As before, we then assessed the influence of the WT MN secretome on the TG SCOCs for miRNAs, and after 24 h incubation, we observed an upregulation of miR-124 and miR-125b two miRNAs commonly found in neuronal cells (Deo et al., 2006; Le et al., 2009) which are both known to regulate microglia activation (Parisi et al., 2016; Ponomarev et al., 2011), being the later also involved in axonal regeneration (Quiroz et al., 2014) (**Figure IV.5A,C**). However, excessive upregulation of such miRNAs can bring problematic situations. Indeed, the elevation of miR-124 has been linked to the acquisition of neurodegenerative traits than with microglia surveilling state (Cunha et al. 2017). Further studies are needed to better clarify the toxicity mediated by miR-124 elevation. Additionally, both miR-21 and miR-146a remained unchanged, as compared with untreated SCOCs (**Figure IV.3A**).

When the TG SCOCs treated with WT MN secretome were analyzed for the glial and neuronal gene profile as in **Figure IV.3B** we could observe that the majority were unchanged, supporting that some of the pathological adaptive mechanisms prevailed. However, both IL-1β and IL-10 genes decreased ($p<0.05$) and a further reduction in iNOS ($p<0.001$) and HMGB1 ($p<0.01$) levels were observed, suggesting that WT secretome may have a calming influence in some of the immunoregulatory genes of TG SCOCs, at least in this early disease stage.

An additional comparison between WT and TG non-treated OCs and WT and TG slices exposed to WT MN secretome was made regarding the expression of genes and miRNAs. The same table shows the beneficial effects of this secretome in SCOCs (please see **Supplementary tables**).

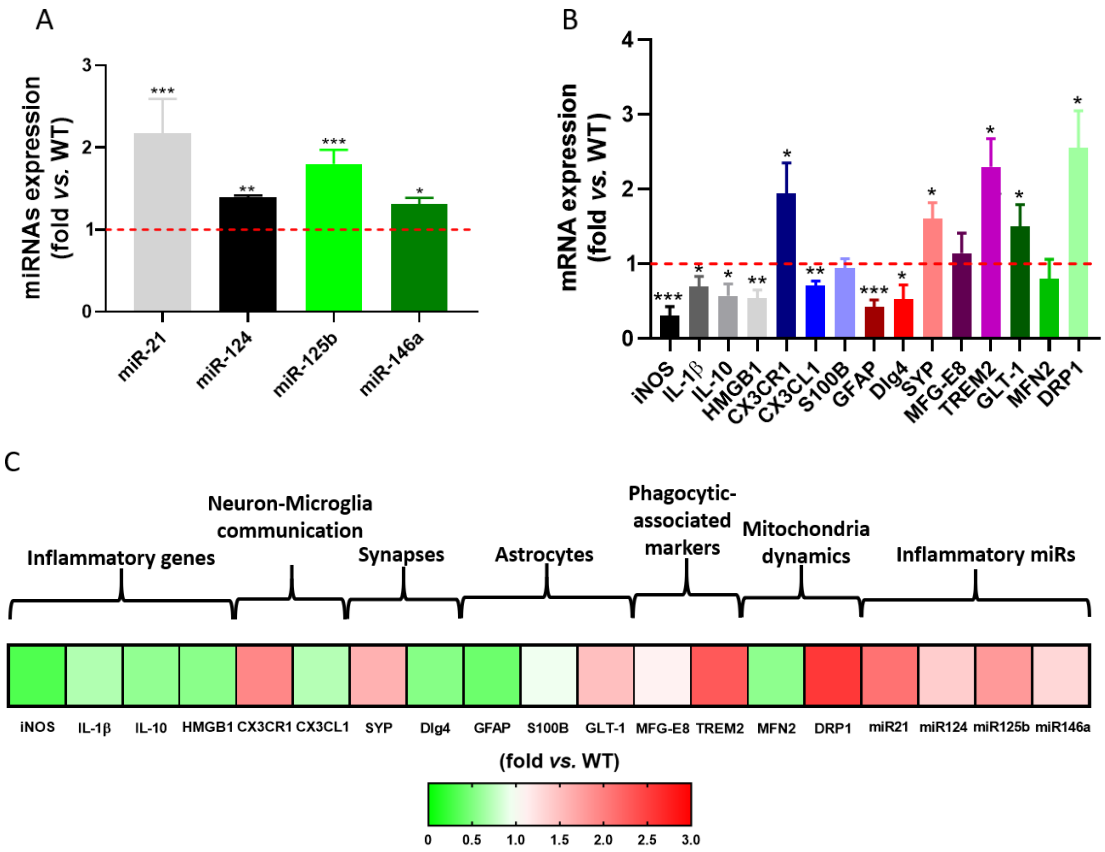

Figure IV.5 - Secretome from wild type (WT) motor neurons shows a mild protective effect on the spinal cord organotypic cultures (SCOCs) of ALS transgenic (TG) mice, by somehow counteracting immune imbalance causative mediators. After 3 days in culture, SCOCs from WT and TG mice at early disease onset were incubated for 24 h with the secretome from WT NSC-34 motor neuron-like cells (4 DIV) and then collected in Trizol for reverse transcription-quantitative polymerase chain reaction (RT-qPCR) analysis. β-actin was used as an endogenous control for protein-coding genes while SNORD was used as a reference gene for miRNAs. MiRNA levels of miR-21, miR-124, miR-125b, and miR-146a and mRNA levels of iNOS, IL-1β, IL-10, HMGB1, CX3CR1, CX3CL1, S100B, GFAP, Dlg4, SYP, MFG-E8, GLT-1, TREM2, MFN2, and DRP1 of TG slices *vs.* WT OC treated with WT MN secretome are depicted, respectively, in (**A**) and (**B**). Results are mean ± SEM of, at least, 4 independent experiments. **p*<0.05, ***p*<0.01 and ****p*<0.001 *vs*. WTOC (red dashed line) were obtained by using two-tailed unpaired Student's *t*-test with Welch's correction when required. (**C**) Heat map summarizing the transcriptomic profile of early symptomatic SC slices exposed to healthy MN secretome. **iNOS,** inducible nitric oxide synthase; **IL-1β**, interleukin-1 beta; **IL-10**, interleukin-10; **HMGB1**, high mobility group protein 1; **CX3CR1**, C-X3-C motif chemokine receptor 1; **CX3CL1**, C-X3-C motif chemokine ligand 1; **S100B**, S100 calcium-binding protein B; **GFAP**, glial fibrillary acidic protein; **Dlg4**, discs large MAGUK scaffold protein 4 (or PSD-95, postsynaptic density protein 95); **SYP**, synaptophysin; **MFG-E8**, milk fat globule-EGF factor 8; **GLT-1**, glutamate transporter 1, **TREM2**, triggering receptor expressed on myeloid cells 2; **MFN2**, mitofusin-2; **DRP1**, dynamin-related protein 1.

3. Secretome from TG MNs causes neurodegenerative and neuroimmune dysregulated profiling in WT SCOCs like that of TG SCOCs, which instead reveal many reactive disabilities

In the previous section, we have shown that the secretome of MN healthy cells has a neuroprotective role over dysfunctional neurons and glial cells of SCOCs from TG mice, mainly

by reducing the inflammatory status. In contrast, as already mentioned, TG MNs (NSC-34 MN-like cells overexpressing mSOD1) and its derived secretome possess increased levels of miR-124 (Colaço, Master Thesis, 2020) and showed to be linked to detrimental outcome in MNs and glial cells, namely, in microglia (Pinto et al., 2017, Vizinha, Master Thesis, 2018, Colaço, Master Thesis, 2020). However, all these studies were performed with cell lines or primary cultures in mono- or co-cultures. Now, we had a better ALS 3D model that recapitulate the pathological mechanisms of all the cells as in the original architectural space of diseased SC. In this way, we decided to assess how the secretome from the TG MNs was able to disturb the neuronal and glial function in either WT or TG SCOCs. The treatment was realized at the third day of culture for 24h and evaluations comprised the necrotic cell death, the percentage of Iba-1$^+$ and GFAP$^+$ cells, inflamma-miR and transcriptomic profile, similarly to previous sections.

3.1. Secretome from mSOD1 MNs reduces the cell viability of WT and TG spinal cord organotypic cultures from 10-12-weeks-old mice

Firstly, we started to examine whether the cell viability was differently affected in WT and TG SCOCs after treatment with the secretome from TG MN (NSC-34 MN-like cells overexpressing mSOD1). The treatment was performed at the third day of culture during 24 h and the parameters evaluated were the same as described for the previous sections. Slices were stained with PI probe as previously proceeded. In WT and TG slices, there was a notorious enhancement in the co-localization of DAPI and PI with TG MN secretome (**Figure IV.6A**) in comparison with respective slices treated with the secretome from WT MNs (**Figure IV.4**). Nearly 2-fold increase was observed in the number of cells that died by necrosis in either WT or TG SCOCs (**Figure IV.6B**).

Additionally, exploratory immunohistochemistry data indicated that the addition of the secretome from TG MNs may have a high effect in reducing the number of GFAP$^+$ cells mainly in the WT SCOCs (**Figure IV.6C,D**). However, no marked changes were observed for GFAP$^+$ cells in the TG SCOCs or for Iba$^+$ cells in WT and TG SCOCs. Therefore, the MN pathological secretome may account for aberrancies in WT astrocyte, without modifying the number of Iba$^+$ microglial cells.

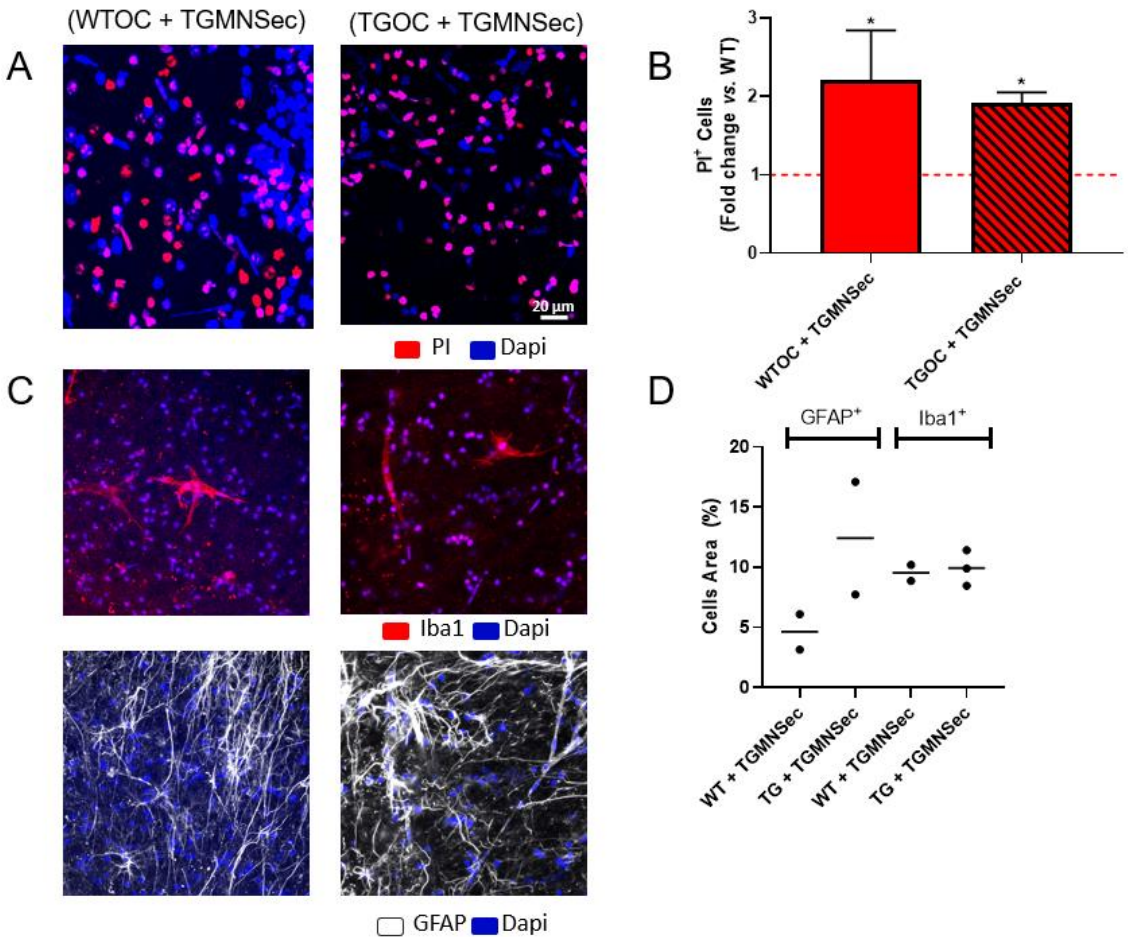

Figure IV.6 - Secretome (Sec) from transgenic motor neurons (TG MNs) exacerbate cell death in both wild type (WT) and TG spinal cord organotypic cultures (SCOCs), while weakening the number of GFAP$^+$ cells only in WT SCOCs, after 24 h incubation. After 24h incubation of TG MN secretome, WT and TG slices (overexpressing hSOD1^{G93A}) were incubated with the propidium iodide (PI) probe for 1h to assess cell demise. (**A**) Representative images of ventral horn regions of WT and TG slices stained for PI (red, dead cells) with the cell nuclei in blue (DAPI). (**B**) Results are mean fold change ± SEM of, at least, 3 independent experiments. *p<0.05 *vs*. WTOC (red dashed line) using one-way ANOVA followed by multiple comparisons Bonferroni post hoc correction. (**C**) Representative immunohistochemistry images for GFAP (white, astrocytes) and for Iba-1 (red, microglia)-positive cells in WT and TG spinal cord organotypic cultures (OCs). (**D**) Percentage of area occupied by GFAP and Iba1-positive cells by individual evaluation in duplicates and triplicates (represented as dots) in ventral horn fields of SCOCs, and respective average (line). Scale bar: 20 µm. **GFAP**, glial fibrillary acidic protein; **Iba-1**, ionized calcium-binding adapter molecule 1.

3.2. Secretome from mSOD1 MNs enhances the expression of inflammatory-associated miRNAs in WT and TG spinal cord organotypic cultures from 10-12-weeks-old mice

Next, we proceeded with the evaluation of inflammatory-associated miRNAs (miR-21, miR-124, miR-125b and miR-146a) in WT and TG slices exposed to TG MN secretome. It is possible to observe that such secretome led to an upregulation of such miRNAs in WT SCOCs (at least $p<0.05$), as depicted in **Figure IV.7**.

Regarding TG SCOCs, and comparing with data from **Figure IV.3**, we now obtained an increased upregulation for all the miRNAs assessed, including miR-124 and miR-125b, as formerly observed in our group (Cunha et al., 2017). The most increased was again the miR-21,

consistent with previous data from sections 1 and 2. In addition, the increase of miR-21 and miR-146a were higher than in matched WT SCOCs, though not statistically significant. These findings suggest that the secretome from TG MNs exacerbates the dysregulation of inflamma-miRs in both WT and TG SCOCs.

Knowing this and that miR-125b has a stressful (Parisi et al., 2016) and miR-21 and miR-146a a calming effect in immune response (Sheedy, 2015; Brites, 2020) and miR-124 a mixed role in inducing microglia to acquire either pro- or anti-inflammatory phenotypes (Pinto et al., 2017), our results point again to a heterogeneous and dysregulated immune response in spinal cord OCs from transgenic mice. Importantly, they also suggest that regenerative mechanisms already took place to compensate those of neurodegeneration.

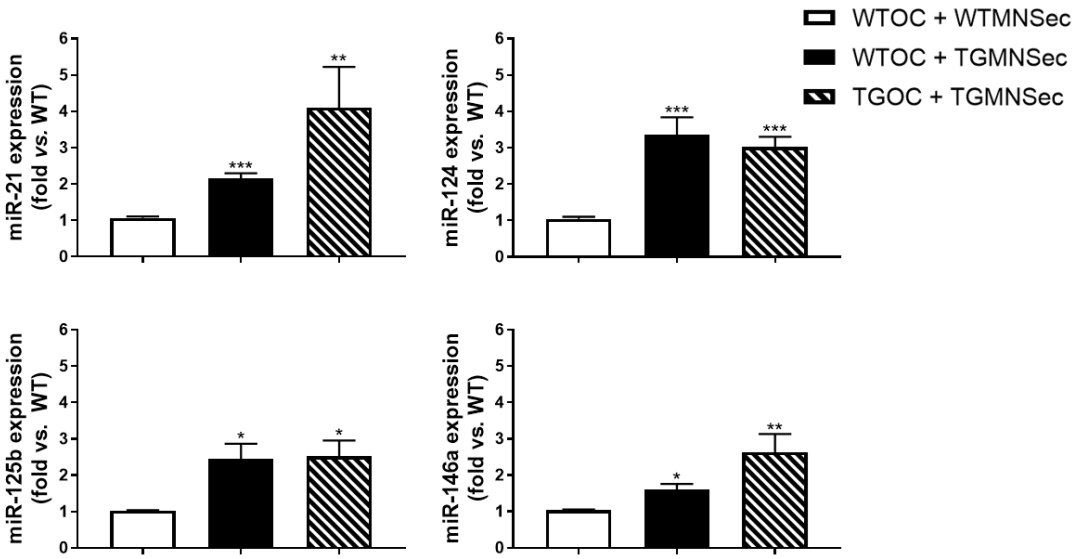

Figure IV.7 - Secretome (Sec) from transgenic motor neurons (TG MNs) upregulate inflammatory-associated miRNAs in wild type (WT) and transgenic (TG) organotypic cultures (SCOCs), after 24 h incubation. After 3 days in culture and 24 h incubation with TGMNSec, WT and TG SCOCs were collected in Trizol for reverse transcription-quantitative polymerase chain reaction (RT-qPCR) analysis, where SNORD was used as a reference gene. MiRNA levels of miR-21, miR-124, miR-125b, and miR-146a of WT and TG slices *vs.* control (WTOC treated with WTMNSec) are depicted in the present figure. Results are mean ± SEM of, at least, 4 independent experiments. **p*<0.05, ***p*<0.01 and ****p*<0.001 *vs.* WTOC treated with WT MN secretome using One-way ANOVA followed by Bonferroni's multiple comparisons post hoc correction.

3.3. Increase of iNOS and IL-1β gene expression by the secretome from mSOD1 MNs only in WT organotypic cultures support an immunogenic compromised glia phenotype in TG slices

To further investigate the influence of the secretome of ALS MNs in our WT and TG organotypic cultures we explored a set of inflammatory-related markers (iNOS, IL-1β, IL-10, and HMGB1). Before RT-qPCR quantification, slices were treated with culture medium for 3 DIV and, subsequently, incubated with either WT or TG MN secretome for 24 h. In **Figure IV.8.** it is possible to observe an overexpression of iNOS ($p<0.01$) and IL-1β ($p<0.05$) in WT slices exposed to the

pathogenic secretome, but no changes for IL-10 or HMGB1. Such markers were found upregulated in N9 hSOD1^{G93A} (a microglia cell line) in comparison with N9 hSOD1^{WT} (Vaz et al. 2019). Importantly, we were unable to see any change on TG SCOCs from the early symptomatic mice what may be due to an irresponsive/deactivated glia phenotype and suggest an inability to mount a reparative response toward the detrimental stimulus by the secretome from TG MNs, thus accounting to allow the progression of the neurodegenerative mechanisms.

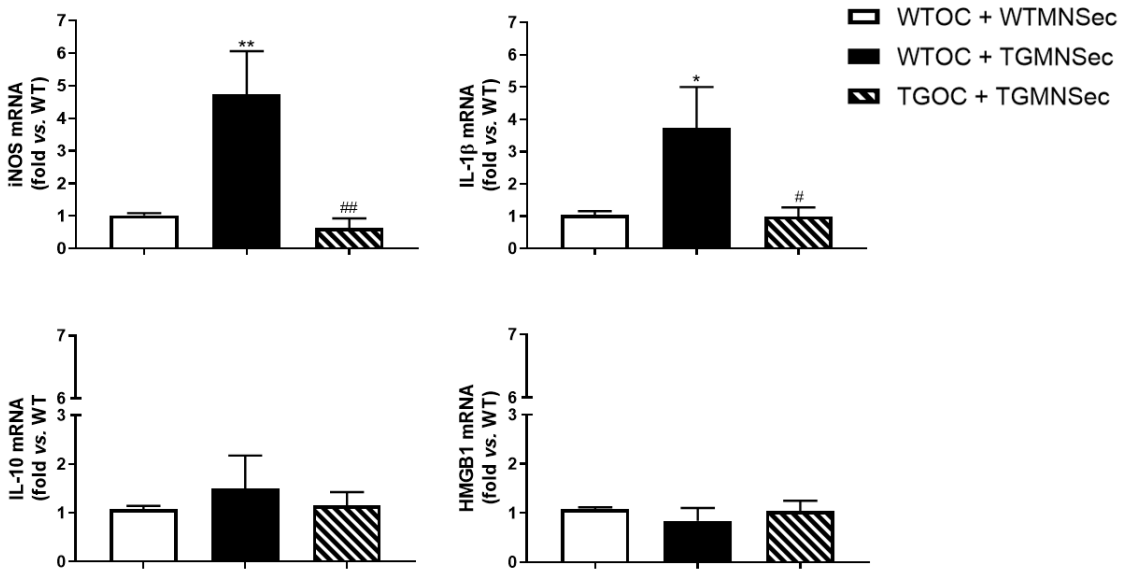

Figure IV.8 - Secretome from mSOD1 MNs leads to the overexpression of iNOS and IL-1β in spinal cord organotypic cultures (SCOCs) from wild type (WT) mice with 10-12-weeks-old, but not in those from transgenic (TG) animals, after 24 h incubation. After 3 days in culture and 24 h incubation with TGMN secretome (Sec), WT and TG SCOCs were collected in Trizol for reverse transcription-quantitative polymerase chain reaction (RT-qPCR) analysis, where β-actin was used as an endogenous control. WT and TG slices mRNA levels of iNOS, IL-1β, IL-10, and HMGB1 *vs.* control (WT OC treated with WT MN secretome) are represented in the present figure. Results are mean ± SEM of, at least, 4 independent experiments. *p<0.05, **p<0.01 *vs.* WTOC treated with WT MN secretome and $^{\#}p$<0.05, $^{\#\#}p$<0.01 *vs.* WTOC exposed to TG MN secretome were obtained by using One-way ANOVA followed by Bonferroni's multiple comparisons post hoc correction. **iNOS,** inducible nitric oxide synthase; **IL-1β**, interleukin-1 beta; **IL-10**, interleukin-10; **HMGB1**, high mobility group protein 1.

3.4. TG MN secretome leads to upregulation of CX3CL1-CX3CR1 axis only in WT organotypic cultures, supporting an immunogenic compromised glia phenotype in TG slices

Later we studied neuron-microglia intercommunication to uncover if the harmful effect was noticed by glial cells, namely microglia. For that, mRNA levels of fractalkine CX3CL1 and its cognate receptor CX3CR1 were analyzed by RT-qPCR after 24h incubation of TG MN secretome in SCOCs. These molecules are constant, and respectively, expressed by neurons and microglia (Wolf et al., 2017) and were found upregulated in the SC of SOD1^{G93A} mice during the symptomatic stage (Cunha et al., 2017). By expressing higher levels of fractalkine, it can be cleaved from neurons starting to act as a signaling molecule and mediating microglial activation through interaction with CX3CR1 (Zhang et al., 2018). Both were found upregulated only in WT

slices exposed to TG MN secretome (p<0.05) (**Figure IV.9.**). Again these results reinforce that the TG SCOCs are unable to react to the pathogenic secretome from the TG MNs, and unable to activate reparative mechanisms when stimulated.

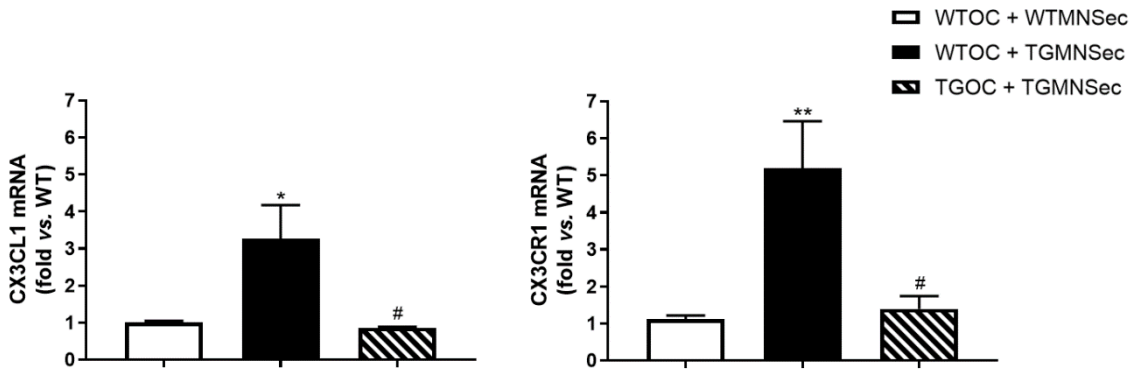

Figure IV.9 - TG MN secretome only enhances transcript levels of fractalkine and CX3CR1 in WT organotypic cultures. After 3 days in culture and 24 h incubation with TGMN secretome (Sec), WT and TG SCOCs were collected in Trizol for reverse transcription-quantitative polymerase chain reaction (RT-qPCR) analysis, where β-actin was used as an endogenous control. WT and TG slices mRNA levels of CX3CL1 and CX3CR1 *vs.* control (WT OC treated with WT MN secretome) are represented in the present figure. Results are mean ± SEM of, at least, 4 independent experiments. **p*<0.05, ***p*<0.01 *vs.* WTOC treated with WT MN secretome and $^{\#}p$<0.05 *vs.* WTOC exposed to TG MN secretome were obtained by using One-way ANOVA followed by Bonferroni's multiple comparisons post hoc correction. Kruskal-Wallis test was applied when data did not assume a Gaussian distribution (CX3CR1 gene). In that case, Dunn´s test post host correction was applied. **CX3CL1**, C-X3-C motif chemokine ligand 1; **CX3CR1**, C-X3-C motif chemokine receptor 1.

3.5. TG MN secretome stimulates the expression of pre-synaptic elements in both WT and TG organotypic cultures, while decreases the post-synaptic one only in the later

In this section, we explored whether the secretome from pathological MNs was able to modify the synaptic dynamics of WT SCOCs or eventually aggravate that of TG SCOCs. For that, we evaluated the expression of pre- (SYP, encoding for synaptophysin) and post-synaptic (Dlg4, encoding for PSD-95) markers by RT-qPCR. We observed overexpression of SYP (p<0.05) in both WT and TG slices when compared with the control condition (WT slices treated with WT MN secretome). The post-synaptic marker (Dlg4) only diminished in the TG SCOCs treated with the pathological secretome (p<0.05) (**Figure IV.10**). These findings are consistent with data from **Figures IV.3B** and **IV.5B**, for TG slices non-treated or treated with WT secretome. Moreover, increased SYP (Vizinha, Master Thesis, 2018) and reduced levels of Dlg4 (Vizinha, Master Thesis, 2018; Gomes, 2020) in mSOD1 MN were already observed in our group. These data indicate that secretome from ALS MNs causes alterations in synaptic dynamics, reinforcing pre-synaptic signaling, but impairing post-synaptic ones.

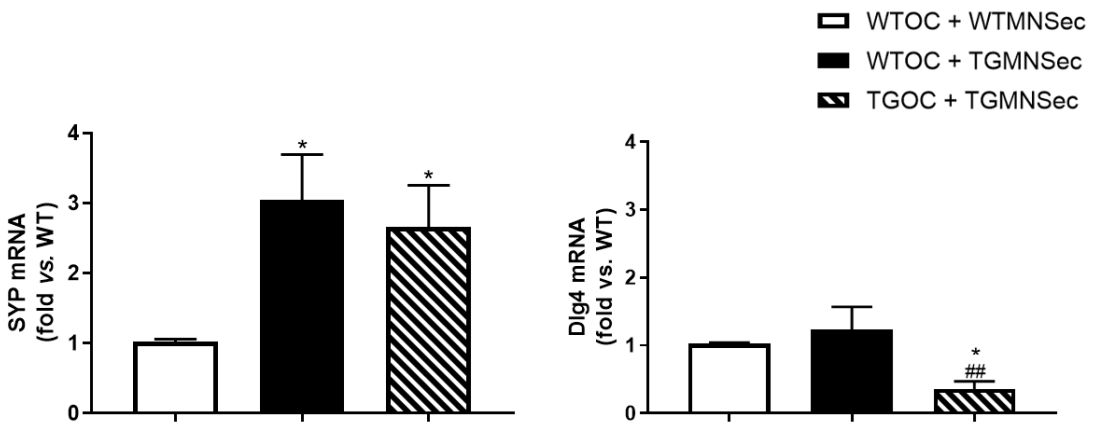

Figure IV.10 - TG MN secretome incubation drives alterations in the expression of pre- and post-synaptic markers. After 3 days in culture and 24 h incubation with TGMN secretome (Sec), WT and TG SCOCs were collected in Trizol for reverse transcription-quantitative polymerase chain reaction (RT-qPCR) analysis, where β-actin was used as an endogenous control. WT and TG slices mRNA levels of SYP and Dlg4 *vs.* control (WT OC treated with WT MN secretome) are represented in the present figure. Results are mean ± SEM of, at least, 4 independent experiments. *p<0.05 *vs.* WTOC treated with WT MN secretome and $^{\#\#}$p<0.01 *vs.* WTOC exposed to TG MN secretome were obtained by using One-way ANOVA followed by Bonferroni's multiple comparisons post hoc correction. **SYP**, synaptophysin; **Dlg4**, discs large MAGUK scaffold protein 4 (or PSD-95, postsynaptic density protein 95).

3.6. TG MN secretome stimulates the gene expression of GLT-1 in both WT and TG SCOCs, while GFAP is decreased in WT and increased in TG samples

Glial cells, especially astrocytes, play a pivotal in synaptogenesis modulation (Verkhratsky & Nedergaard, 2018; Khakh & Deneen, 2019). However, by presenting aberrant phenotypes and thus secreting toxic factors in SC of rodent models these cells have been pointed as important contributors of MN neurodegeneration and disease progression (Trias et al., 2017). Thus, we here explored whether the ALS MN pathological secretome also causes harmful effects in WT and TG SCOCs, by assessing GFAP and GLT-1.

Regarding GFAP, we observed a decreased expression in WT SCOCs (p<0.05) upon incubation with TG MN secretome *vs.* WT SCOCs treated with healthy secretome (**Figure IV.11**). However, the opposite was observed for TG SCOCs, where an overexpression was achieved (p<0.05). These findings may indicate direct and indirect influences depending on the homeostatic balance or imbalance of WT and TG SCOCs, considering the healthy and the aberrant astrocyte phenotypes that will be influenced by the ALS MN secretome. The naïve ones presenting the common ALS aberrancy of the downregulated GFAP after treatment with the ALS MN secretome, while in the later we cannot exclude some benefits from the growth factors of the secretome over the dysfunctional astrocytes. This finding was somehow suggested in the preliminary data indicated in **Figure IV.6D**. Such hypothesis may also explain the elevation in the gene expression of GLT-1 (p<0.05) in both WT and TG OC (**Figure IV.11)** as a compensatory mechanism.

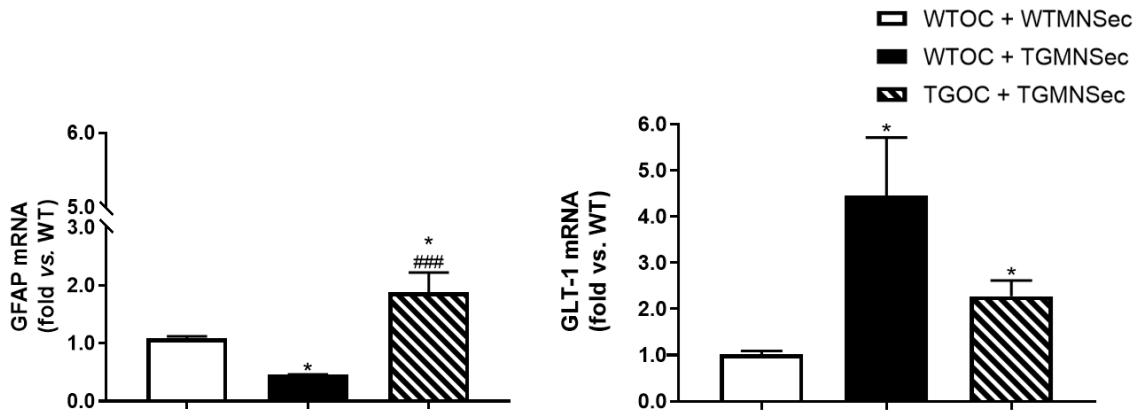

Figure IV.11 - Secretome (Sec) from transgenic (TG) motor neurons (MNs) impacts on astrocyte protein-coding genes in the spinal cord organotypic cultures (SCOCs). After 3 days in culture and 24 h incubation with TGMN secretome (Sec), WT and TG SCOCs were collected in Trizol for reverse transcription-quantitative polymerase chain reaction (RT-qPCR) analysis, where β-actin was used as an endogenous control. WT and TG slices mRNA levels of GFAP and GLT-1 vs. control (WT OC treated with WT MN secretome) are represented in the present figure. Results are mean ± SEM of, at least, 4 independent experiments. *p<0.05 vs. WTOC treated with WT MN secretome and $^{\#\#}$p<0.01 vs. WTOC exposed to TG MN secretome were obtained by using One-way ANOVA followed by Bonferroni's multiple comparisons post hoc correction. **GFAP**, glial fibrillary acidic protein; **GLT-1**, glutamate transporter 1.

3.7. TG MN secretome stimulates microglia phagocytosis in both WT and TG organotypic cultures from 10-12-weeks-old mice

Knowing that the phagocytosis is a process almost restricted to microglia, we investigated whether the ALS MN secretome was able to induce changes in genes associated with such property, after TG MN incubation in WT and TG SCOCs.

We observed an increase of both MFG-E8 and TREM2 ($p<0.05$) in either WT or TG SCOCs (**Figure IV.12**), which were shown to enhance microglia phagocytic ability (Chiu et al., 2013). Data indicate that the ALS MN secretome stimulates microglia to act for restoring homeostasis and for the clearance of cell debris, an effect that is presented by microglia from either WT or TG SCOCs. The present feature indicates that phagocytosis is preserved in microglia from TG SCOCs at disease onset, in contrast with their inability to be immunostimulated as presented in **Figure IV.8** and also in prior data reported in the pre-symptomatic mSOD1 mice (Cunha et al, 2017).

The increase in TREM2 associated with ALS pathology seems to be a consistent finding in this study, if we consider also the results depicted in **Figures IV.3B** and **IV.5C**. Accordingly, Cady and co-workers (2014) also found elevated levels of TREM2 in ALS patients and SOD1^{G93A} mice, which suggest TREM2 as a consistent biomarker in several ALS-like conditions.

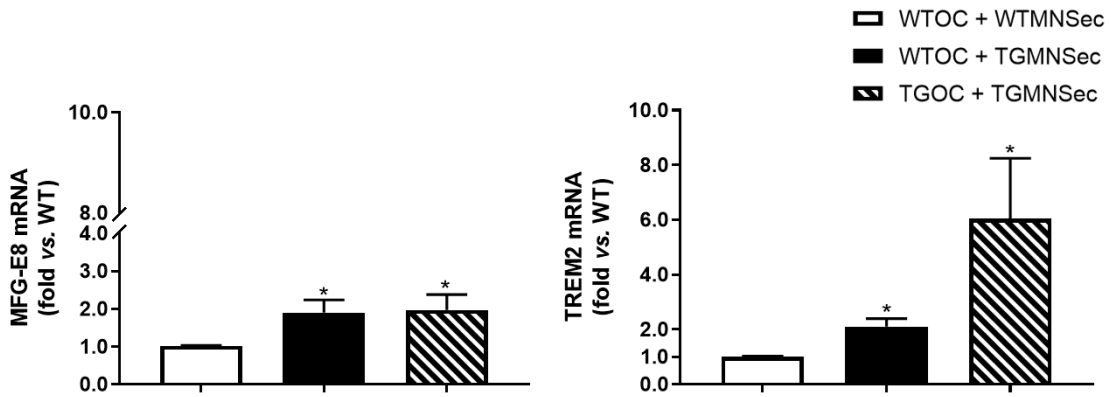

Figure IV.12 - Secretome (Sec) from transgenic (TG) motor neurons (MNs) stimulates microglia phagocytosis by upregulating MFG-E8 and TREM2 genes in the spinal cord organotypic cultures (SCOCs). After 3 days in culture and 24 h incubation with TGMN secretome (Sec), WT and TG SCOCs were collected in Trizol for reverse transcription-quantitative polymerase chain reaction (RT-qPCR) analysis, where β-actin was used as an endogenous control. WT and TG slices mRNA levels of MFG-E8 and TREM2 vs. control (WT OC treated with WT MN secretome) are represented in the present figure. Results are mean ± SEM of, at least, 4 independent experiments. *p<0.05 vs. WTOC treated with WT MN secretome were obtained by using One-way ANOVA followed by Bonferroni's multiple comparisons post hoc correction. **MFG-E8**, milk fat globule-EGF factor 8; **TREM2**, triggering receptor expressed on myeloid cells 2.

3.8. TG MN secretome stimulates mitochondrial dysfunction in both WT and TG organotypic cultures, from 10-12-weeks-old mice

Dysregulation of fusion and fission mechanisms is linked to an impairment of the mitochondrial dynamics, and acquisition of aberrant functions compromising the ability to maintain its size, shape, and cell energy requirements (Smirnova et al., 2001). A more fragmented network by the overexpression of both fusion and fission proteins was reported in the ALS murine model (Liu et al., 2013).

Here we determined the expression of fusion (MFN2) and fission (DRP1) protein-coding genes, as also performed in previous sections of this study. Again, but now at the neuronal level, we observed that the secretome from mSOD1 MNs also stimulated the expression of these genes **(Figure IV.13**), supporting mechanisms of mitochondria fusion and fission. We observed an increase in both MFN2 and DRP1 ($p<0.05$) in WT and TG SCOCs. The overexpression of DRP1 was previously noticed in the untreated TG SCOCs and after treatment with the secretome from WT MNs (**Figures IV.3** and **IV.5**). In sum, this increase in MFN2 and DRP1 reinforce the stimulation of compensatory responses triggered by the TG MN secretome. It seems that besides its toxic stimulus, the TG MN secretome also produces acute and adaptive responses probably as an attempt to sustain MN function.

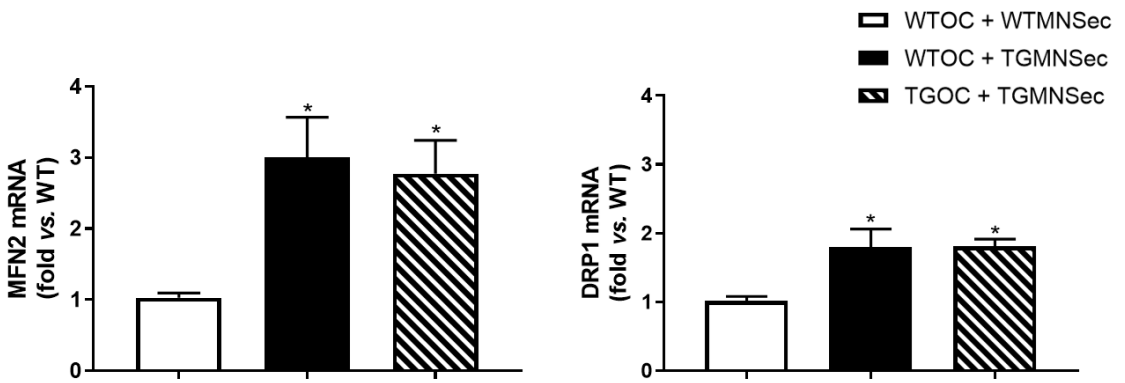

Figure IV.13 - Secretome (Sec) from transgenic (TG) motor neurons (MNs) stimulates mitochondria fusion/fission mechanisms by upregulating MFN2 and DRP1 in the spinal cord organotypic cultures (SCOCs). After 3 days in culture and 24 h incubation with TGMN secretome (Sec), WT and TG SCOCs were collected in Trizol for reverse transcription-quantitative polymerase chain reaction (RT-qPCR) analysis, where β-actin was used as an endogenous control. WT and TG slices mRNA levels of MFN2 and DRP1 *vs.* control (WT OC treated with WT MN secretome) are represented in the present figure. Results are mean ± SEM of, at least, 4 independent experiments. *p<0.05 *vs.* WTOC treated with WT MN secretome were obtained by using One-way ANOVA followed by Bonferroni's multiple comparisons post hoc correction. **MFN2**, mitofusin-2; **DRP1**, dynamin-related protein 1.

3.9. Acute TG MN secretome triggers a more restricted immune response in TG slices regarding the one achieved after 24h incubation

Data from **Figure IV.8** showed that TG SCOCs were unable to mount an immune response when treated with the secretome from TG MNs. Data from **Figure IV.9** reinforced a lower stimulation in TG SCOCs as compared to WT ones, upon the addition of the same secretome from pathological ALS MNs. Moreover, our previous data on SC of pre- and symptomatic mice evidenced a decrease of MFG-E8 (Cunha et al., 2017). Based on that we wonder whether the data here presented (**Figure IV.12**) resulted from the 24 h incubation instead of using a shorter time incubation, which has shown to only have microglia immunostimulation at early time points (Pinto et al., 2017). With this in mind, we decided to use an incubation of only 4 h to check the variations in the above-mentioned parameters by RT-qPCR.

Data from **Table IV.1** indicate that such acute incubation leads to the downregulation of IL-1β, HMGB1, CX3CL1, CX3CR1 and MFG-E8 genes ($p<0.05$) in TG slices treated with TG MN secretome relatively to its respective control (WT OC exposed to WT MN secretome during 4 h). Moreover, this downregulation was higher at 4 hours in comparison with the 24 h treatment, except for IL-1β, supporting the idea of deterioration of a proper inflammatory response in the TG SCOCs even at for shorter periods of time. To note, however, that we now obtained a downregulation of MFG-E8 mRNA highlighting the plasticity of microglia to adopt different phenotypes depending on the diseased conditions, stimuli, and duration.

Table IV.1 - Expression of immune-associated markers in transgenic (TG) organotypic culture (OC) supporting the acute neuronal/glial dysfunction induced by 4h of incubation with TG motor neuron (MN) secretome.

Gene	**Fold change** (TGOC + TGMNSec *vs*. WTOC + WTMNSec; [4h]) **Mean ± SEM**	***p* values** (*vs*. WTOC + WTMNSec [4h])	***p* values** (*vs.* TGOC + TGMNSec [24h])
IL-1β	**0.13 ± 0.01**	**0.0001**	0.11
HMGB1	**0.15 ± 0.02**	**0.01**	**0.02**
CX3CL1	**0.28 ± 0.05**	**0.0005**	**0.0002**
CX3CR1	**0.03 ± 0.02**	**< 0.0001**	**0.04**
MFG-E8	**0.60 ± 0.06**	**0.05**	**0.04**

Comparisons were made in pairs between transgenic (TG) slices treated with TG motor neuron (MN) secretome (4 h) and respective control (wild type (WT) slices exposed to WT MN secretome), and between the first and TG OC incubated with TG MN secretome during 24 h. mRNA expression levels were evaluated by reverse transcription-quantitative polymerase chain reaction (RT-qPCR) analysis and data are expressed as fold change. The *p* values of the above-mentioned comparisons are present in the same table, in bold are the ones statistically significant. The values were calculated using the Student's *t*-test. Results are from, at least, 3 independent experiments, except for IL-1β (2 independent experiments). **IL-1β**, interleukin 1 beta; **HMGB1**, high mobility group protein 1; **CX3CL1**, C-X3-C motif chemokine ligand 1; **CX3CR1**, C-X3-C motif chemokine receptor 1; **MFG-E8**, milk fat globule-EGF factor 8.

4. Increased levels of miR-124 play a critical role in TG MN secretome-associated alterations in SCOCs

Our previous data, as already mentioned, suggest that the overexpression of miR-124 in mSOD1 MNs may be linked to some pathological features presented by the ALS MNs, but also to exert harmful effects on astrocytes and microglia mediated by paracrine signaling. When we overexpressed miR-124 in WT MNs such detrimental effects were observed and recapitulated those induced by the ALS MNs. To assess the consequences of such modulation in our 3D SCOCs we used healthy (WT) MN and transfected them with pre-miR-124, as mentioned in **Figure III.1** (methods section). Subsequently, the secretome from these WT MNs was collected and incubated in WT slices for 24 h.

4.1. Secretome from pre-miR-124 treated WT MNs slightly induces cell death by necrosis in WT SCOCs

We started by comparing the cell viability of WT slices exposed to TG MN secretome (see **Figure IV.6**) with those treated with WT MN secretome (see **Figure IV.4**) that revealed no differences when compared to non-treated WT SCOCs. As previously indicated, the TG MN secretome increased in almost 2-fold the number of dying cells ($p<0.05$, **Figure IV.14**). Now it is interesting to note that although not achieving the same levels of cell death, the transfection of WT MNs with pre-miR-124 originated a secretome that also induced some cell death (**Figure IV.14**), although at lower levels and not achieving statistical significance ($p=0.06$ ANOVA; $p<0.01$ by *t* test and compared with WTOC+WTMNSec).

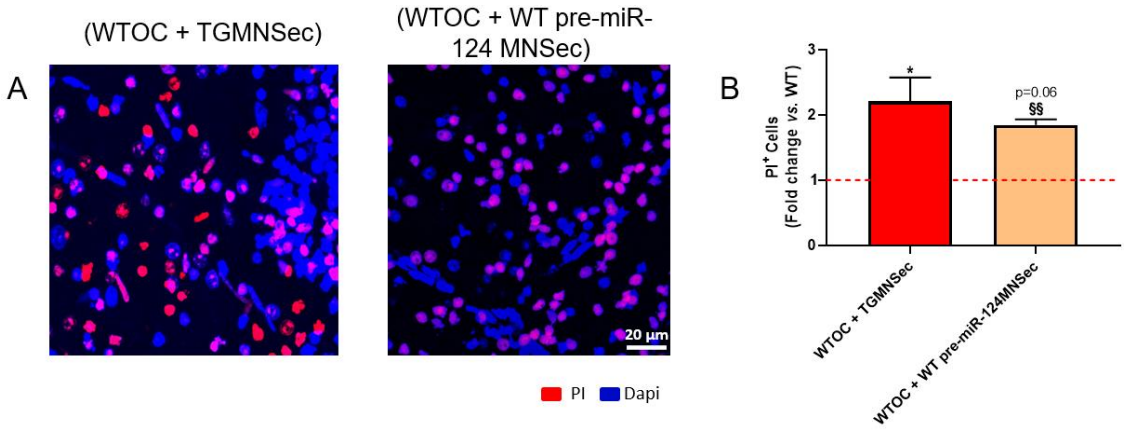

Figure IV.14 - Comparative effects of the secretome from transgenic (TG) motor neurons (MNs) and the secretome from wild type (WT) MN treated with pre-miR-146a on cell death by necrosis in WT organotypic cultures (OCs). After 24h incubation of transgenic (TG) and wild type (WT) pre-miR-124 motor neuron (MN) secretome, WT slices were incubated with the PI probe for 1h. (**A**) Representative images of ventral horn fields of WTOC treated with WT pre-miR-124 and TG MN secretome (for comparison) and stained for PI (red, dead cells) with the cell nuclei in blue (DAPI). **B**) Results are mean fold change ± SEM of, at least, 3 independent experiments. **p*<0.05 and p=0.06 *vs.* WTOC treated with WT MN secretome (red dashed line) using one-way ANOVA followed by multiple comparisons Bonferroni post hoc correction. §§*p*<0.01 *vs.* WTOC exposed to WT MN secretome (red dashed line) using two-tailed unpaired Student's *t*-test with Welch's correction when required. Scale bar: 20 µm.

4.2. Secretome from WT MNs treated with pre-miR-124 causes changes in neuro-immune markers mostly like those produced by the secretome from TG MNs

Next, we evaluated the expression of miRNAs and protein-coding genes already evaluated in previous sections. Results of WT slices exposed to WT pre-miR-124 MN secretome are represented as fold change *vs.* WT OC treated with WT MN secretome. Next, a comparison between WT slices exposed to WT pre-miR-124 MN secretome and WT slices treated with TG MN secretome was made. Green bars represent a recap similar to that obtained with TG MN secretome incubation. On the other hand, the red ones do not recapitulate the profile induced by TG MN secretome incubation. Regarding miRNAs, overexpression of miR-21 ($p<0.001$), miR-124 ($p<0.001$) and miR-125b ($p<0.01$) was observed **(Figure IV.15A**). No difference in miR-146a was

detected. In sum, we may say that the overexpression of miR-124 in WT MNs leads to a secretome that induced immune-dysregulated miRNAs and neuronal/glial gene profile with similarities to those found with the secretome from ALS MNs. This finding suggests that the increase of miR-124 observed in ALS MNs, and in its secretome (Colaço, Master Thesis, 2020)] is responsible, at least in part, for the inflamma-miR imbalance here observed.

Now considering the protein-coding genes (**Figure IV.15B**), most of them obtained with the secretome from TG MN were recapitulate by the secretome enriched in miR-124 [enhanced levels of IL-1β ($p<0.05$), CX3CR1 ($p<0.001$), TREM2 ($p<0.001$) and DRP1 ($p<0.01$); decreased levels of GFAP ($p<0.01$)]. Additionally, the genes iNOS, IL-10, CX3CL1, SYP, GLT-1, MFG-E8 and MFN2 were differently modified by the overexpression of miR-124 in comparison with the TG MN secretome incubation. Anyway, we may conclude that enriched levels of miR-124 play a role in disease-related dysfunctions, being responsible for a large portion of the toxic effects observed by the mSOD1 MN secretome incubation in SCOCs.

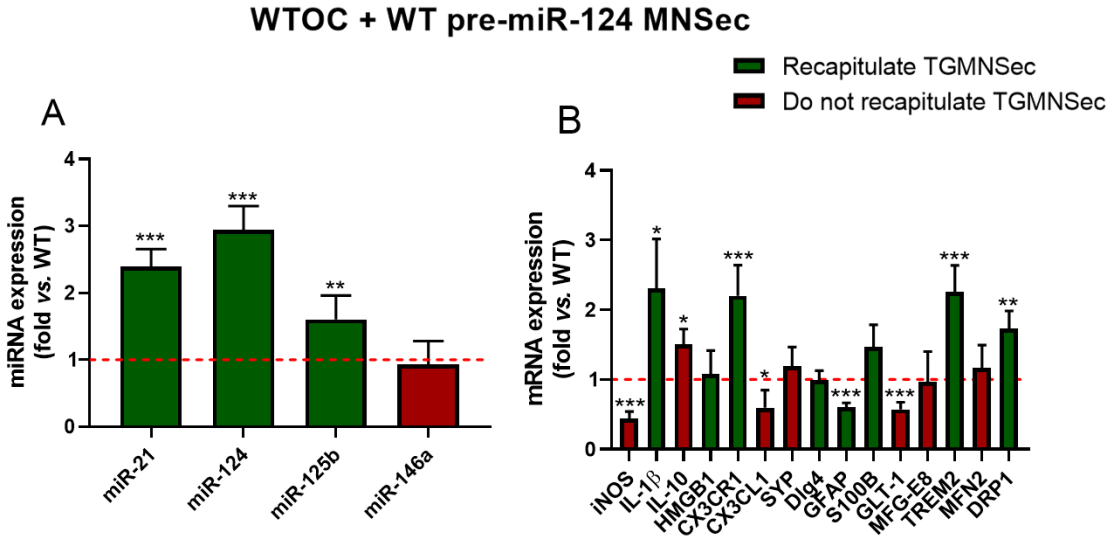

Figure IV.15 - Treatment of wild type (WT) motor neurons (MNs) with pre-miR-124 leads to a secretome that impairs neuro-immune balance in WT spinal cord organotypic cultures (SCOCs) with similarities to the one caused by the secretome from transgenic (TG) MNs. After 3 days in culture, WT SCOCs were incubated for 24 h with the secretome from WT pre-miR-124 NSC-34 motor neuron-like cells (4 DIV) and then collected in Trizol for reverse transcription-quantitative polymerase chain reaction (RT-qPCR) analysis. β-actin was used as an endogenous control for protein-coding genes while SNORD was used as a reference gene for miRNAs. MiRNA levels of miR-21, miR-124, miR-125b, and miR-146a and mRNA levels of iNOS, IL-1β, IL-10, HMGB1, CX3CR1, CX3CL1, S100B, GFAP, Dlg4, SYP, MFG-E8, GLT-1, TREM2, MFN2, and DRP1 *vs.* WT OC treated with WT MN secretome are depicted, respectively, in (**A**) and (**B**). Results are mean ± SEM of, at least, 4 independent experiments. *$p<0.05$, **$p<0.01$ and ***$p<0.001$ vs. WTOC (red dashed line) were obtained by using two-tailed unpaired Student's t-test with Welch's correction when required. Green bars represent a recapitulation of TG MN secretome incubation while red ones the cases that different expression was achieved. **iNOS,** inducible nitric oxide synthase; **IL-1β**, interleukin-1 beta; **IL-10**, interleukin-10; **HMGB1**, high mobility group protein 1; **CX3CR1**, C-X3-C motif chemokine receptor 1; **CX3CL1**, C-X3-C motif chemokine ligand 1; **S100B**, S100 calcium-binding protein B; **GFAP**, glial fibrillary acidic protein; **Dlg4**, discs large MAGUK scaffold protein 4 (or PSD-95, postsynaptic density protein 95); **SYP**, synaptophysin; **MFG-E8**, milk fat globule-EGF factor 8; **GLT-1**, glutamate transporter 1, **TREM2**, triggering receptor expressed on myeloid cells 2; **MFN2**, mitofusin-2; **DRP1**, dynamin-related protein 1.

5. Secretome from anti-miR-124 treated mSOD1 MNs has a deactivation effect on WT organotypic cultures stimulated with mSOD1 MN-derived secretome and in TG slices at early disease onset

In this section, we explored the potential benefits of using anti-miR-124 as a therapeutic approach for neuroprotection in ALS. This aim results from our previous data showing that increased levels of miR-124 in MNs are linked to a significant number of malfunctions in these and glial cells, such as astrocytes and microglia (Pinto et al., 2017, Vizinha, Master Thesis, 2018, Colaço, Master Thesis, 2020). Thus, the objective of downregulating this miRNA is to essentially halt or prevent the progression of ALS, as well as excessive cell metabolization and accumulation of toxic proteins. This modulation always will have in consideration to allow the maintenance of expression at normal levels or slightly below to preserve the important functions of miR-124 in the CNS. Actually, the knockout of miRNA-124 would have severe consequences in precluding neurogenesis (Conaco et al., 2006), but also as an immunomodulator (Qin et al., 2016), and in regulating synaptic homeostasis. However, elevated levels of miR-124 are also linked to poorer neurological outcomes in some conditions, such as cardiac arrest and acute ischaemic stroke (Devaux et al., 2016; He et al., 2019). It inhibits cell proliferation by downregulating Rho-associated protein kinase 1 (ROCK1) (Zhou et al., 2016), suppresses ionotropic glutamate receptors and restricts synaptic plasticity and spatial learning (Hu & Li, 2017; Rajasethupathy et al., 2009). Here we incubated WT SCOCs with the secretome from mSOD1 MNs that we know to be enriched in miR-124, as well as with the secretome from anti-miR-124 treated mSOD1 MNs, as depicted in **Figure III.1**, to assess the effects produced in several inflammatory mediators and markers of neuronal function. This same secretome was later incubated with TG SCOCs, obtained at early disease onset, for the same parameters and compared to those obtained in non-treated original TG SCOCs (**Figure IV.3**).

5.1. Secretome from TG MNs treated with anti-miR-124 slightly reduces necrotic cell death in WT spinal cord organotypic cultures stimulated with ALS MN secretome

We started by evaluating the extent of dead cells in WT and TG slices incubated with the secretome from anti-miR-124 treated mSOD1 MNs, by using the PI probe as before. Although we did not observe statistical differences after using secretome from mSOD1TG MN modulated with anti-miR-124), a slight prevention from cell death in TG OC toward the one found in WT slices treated with culture medium (**Figure IV.16A,B**). Immunohistochemistry data for GFAP+ and Iba-1+ cells (**Figure IV.16C**) display no significant changes in their extent in SCOCs from WT or TG treated with TG anti-miR-124 MN secretome (**Figure IV.6D**). However, a slight increase in GFAP+ cells was noticed in WT slices relatively to TG ones. The treatment with anti-miR-124 has a smaller effect in reducing their cell area average and deserve further confirmation.

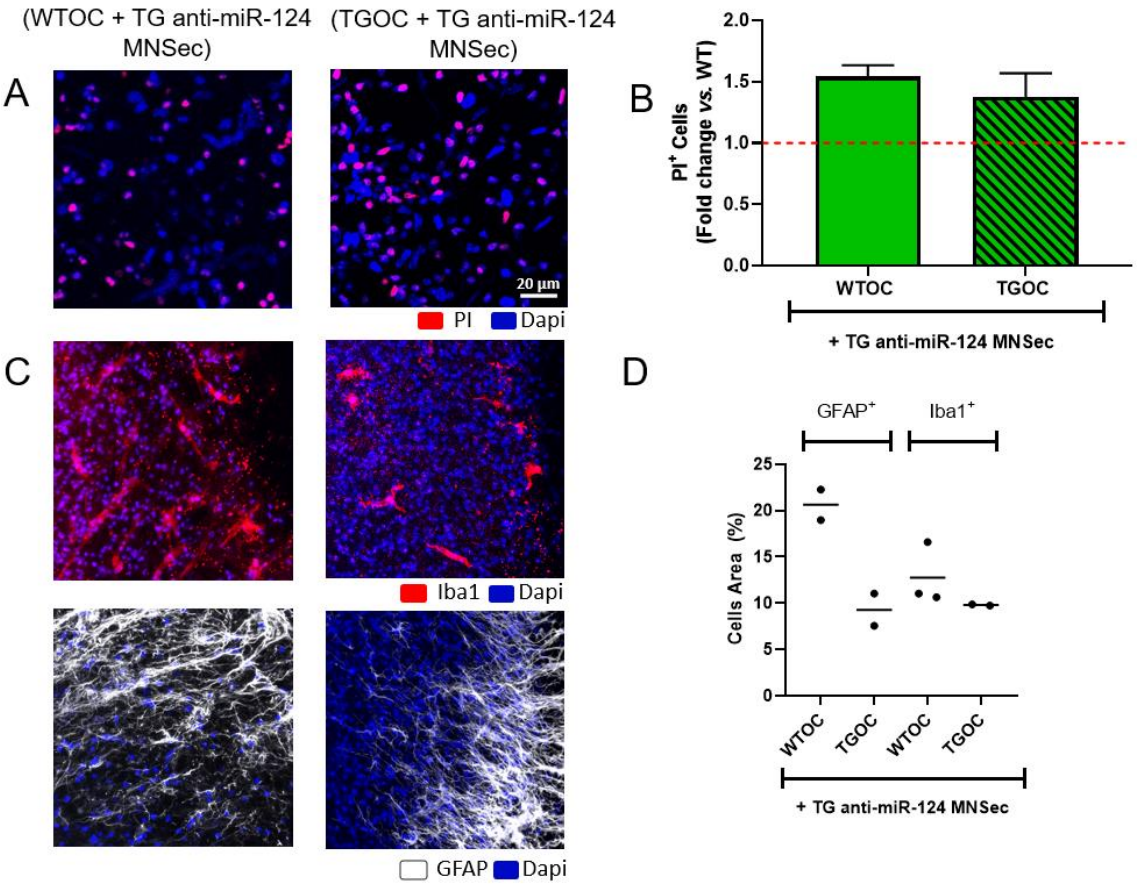

Figure IV.16 - Evaluation of cell demise, and GFAP⁺ and Iba-1⁺ cells in WT and TG spinal cord organotypic cultures (OCs) following incubation with secretome from anti-miR-124-treated TG MNs. After 24h incubation of transgenic (TG) anti-miR-124 motor neuron (MN) secretome, wild type (WT) and transgenic (TG) slices (overexpressing hSOD1^{G93A}) were incubated with the propidium iodide (PI) probe for 1h to assess cell demise. (**A**) Representative images of ventral horn regions of WT and TG slices stained for PI (red, dead cells) with the cell nuclei in blue (DAPI). (**B**) Results are mean fold change ± SEM of, at least, 3 independent experiments. (**C**) Representative immunohistochemistry images for GFAP (white, astrocytes) and for Iba-1 (red, microglia)-positive cells in WT and TG spinal cord organotypic cultures (OCs). (**D**) Percentage of the area occupied by GFAP and Iba1-positive cells by individual evaluation in duplicates and triplicates (represented as dots) in ventral horn fields of SCOCs, and respective average (line). Scale bar: 20 µm. **GFAP**, glial fibrillary acidic protein; **Iba-1**, ionized calcium-binding adapter molecule 1.

In the following sections, we will evaluate if the downregulation of miR-124 is enough to abrogate the negative effects caused by the TG MN secretome in WT slices. As so, the same set of miRNAs and neuronal/glial-related genes were assessed under 24 h exposure of TG anti-miR-124 MN secretome.

5.2. Secretome from TG MNs treated with anti-miR-124 reduces all inflamma-miRs in WT spinal cord organotypic cultures stimulated with ALS MN secretome

First, we evaluated the expression of the miRNAs already studied in WT treated with mSOD1 anti-miR-124 MN secretome *vs.* TG non-modulated MN secretome incubation. Results are fold change *vs.* TG MN secretome treatment. We observed a decrease in the expression of miR-21, miR-124, miR-125 and miR-146a (all $p<0.05$) (**Figure IV.17**) upon incubation with modulated TG MN secretome. Data indicate that the reduction of miR-124 in sick MNs lead to a secretome that is able to cause a general deactivation of all the inflamma-miRs, as depicted in **Figure IV.7**.

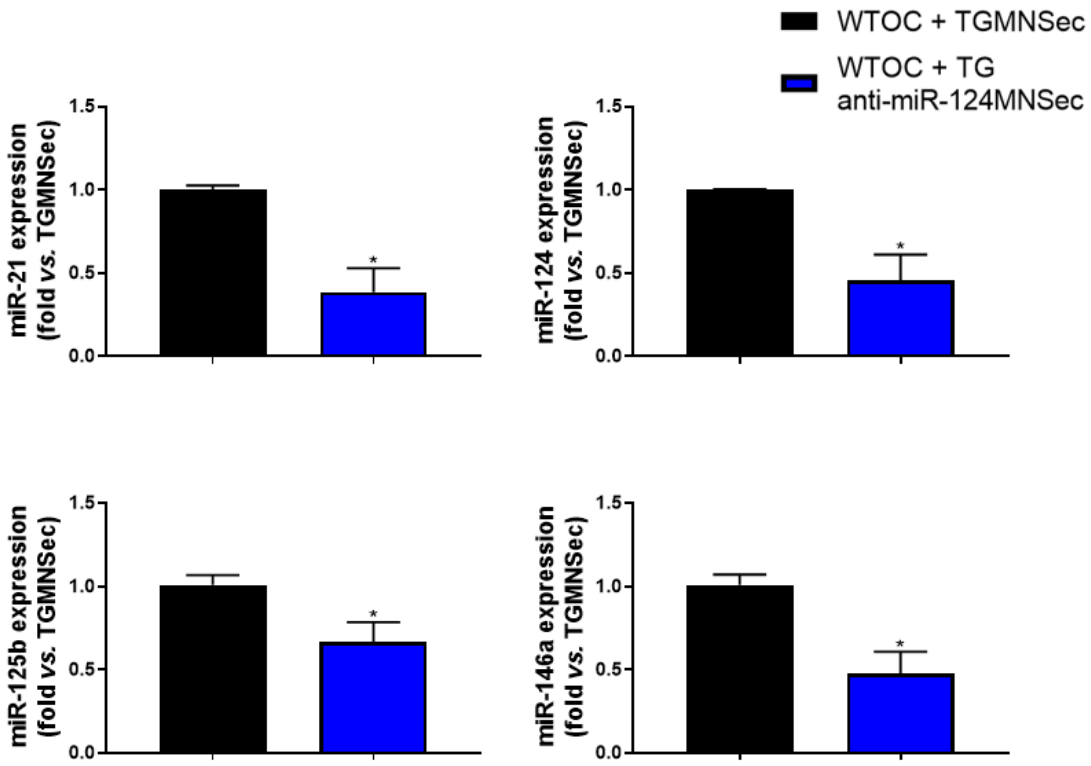

Figure IV.17 - Secretome from anti-miR-124-treated mSOD1 MNs is able to reduce all miRNAs that were overstimulated in WT SCOCs upon the addition of the secretome from non-treated ALS MNs. After 3 days in culture and 24 h incubation with transgenic (TG) anti-miR-124 motor neuron (MN) secretome, wild type (WT) spinal cord organotypic cultures (SCOCs) were collected in Trizol for reverse transcription-quantitative polymerase chain reaction (RT-qPCR) analysis, where SNORD was used as a reference gene. MiRNA levels of miR-21, miR-124, miR-125b, and miR-146a *vs.* WT OC treated with TG MNs secretome are depicted in the present figure. Results are mean ± SEM of, at least, 4 independent experiments. *$p<0.05$ vs. WT OC treated with TG MN secretome were obtained by using two-tailed unpaired Student's *t*-test with Welch's correction when required.

5.3. Secretome from anti-miR-124-treated TG MNs reduces the gene expression of iNOS and IL-1β, but causes an elevation of the alarmin HMGB1, in WT spinal cord organotypic cultures stimulated with ALS MN secretome

Later we investigated the expression of selected inflammatory-related genes. We observed downregulation of iNOS ($p<0.001$) and IL-1β ($p<0.05$) indicating that the anti-miR-124 treatment was able to induce a paracrine modulatory effect on neuroinflammation produced by the pathological secretome on the WT SCOCs (**Figure IV.18; Figure IV.8**). However, we found that some stimulation of the alarmin HMGB1 was produced ($p<0.05$). The same gene encodes for a protein that it is critical to the cell's response to stress and indicates an alert signal. This finding is interesting since no elevation of HMGB1 was observed in TG SCOCs (**Figure IV.3**).

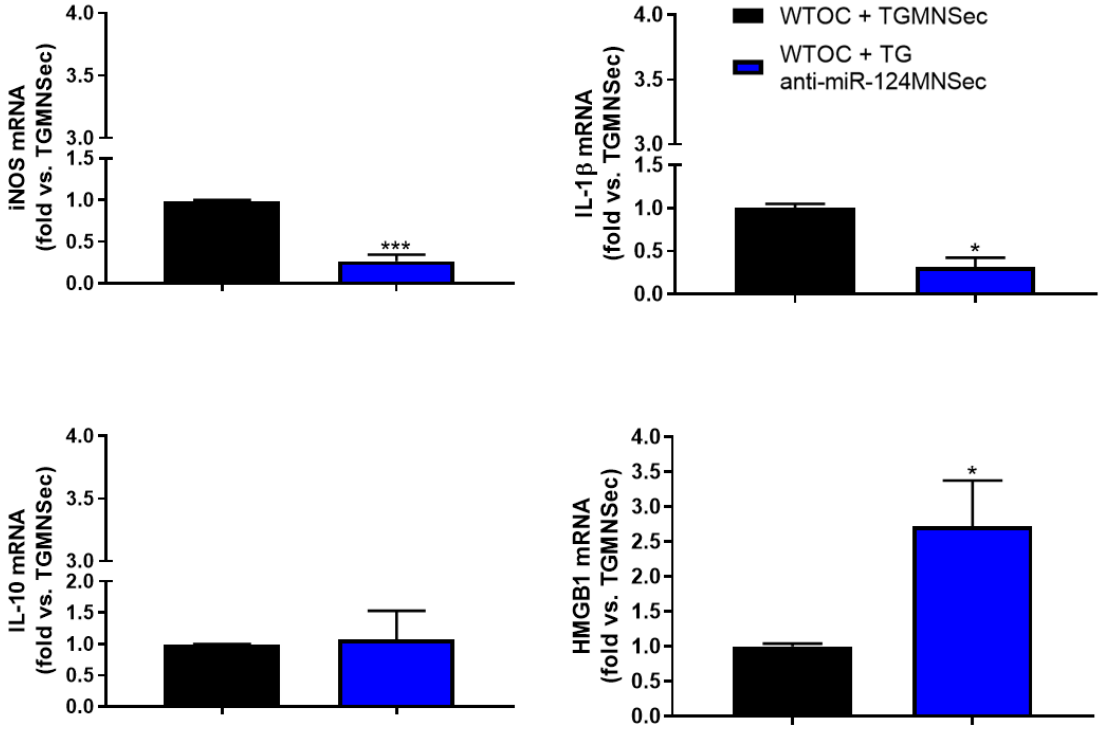

Figure IV.18 - Secretome from anti-miR-124-treated mSOD1 MNs is able to transcriptionally downregulate iNOS potentially mediated by IL-1β reduction, while caused a nuclear elevation of HMGB1 relatively to WT SCOCs exposed to the secretome from non-treated ALS MNs. After 3 days in culture and 24 h incubation with transgenic (TG) anti-miR-124 motor neuron (MN) secretome (Sec), wild type (WT) and spinal cord organotypic cultures (SCOCs) were collected in Trizol for reverse transcription-quantitative polymerase chain reaction (RT-qPCR) analysis, where β-actin was used as an endogenous control. WT mRNA levels of iNOS, IL-1β, IL-10, and HMGB1 vs. WT OC exposed to mSOD1 MNs secretome are represented in the present figure. Results are mean ± SEM of, at least, 4 independent experiments. *$p<0.05$, ***$p<0.001$ vs. WT OC treated with TG MN secretome and were obtained by using two-tailed unpaired Student's t-test with Welch's correction when required. **iNOS,** inducible nitric oxide synthase; **IL-1β**, interleukin-1 beta; **IL-10**, interleukin-10; **HMGB1**, high mobility group protein 1.

5.4. Secretome from anti-miR-124-treated TG MNs reduces fractalkine and its cognate microglial receptor CX3CR1 in WT spinal cord organotypic cultures stimulated with ALS MN secretome

Next, the expression of genes related to neuron-microglia interconnectivity was studied in WT SCOCs treated with TG anti-miR-124 MN secretome. As previously, CX3CL1-CX3CR1 axis was assessed after 24 h of incubation of the above-mentioned secretome. Decreased transcript levels of fractalkine ($p<0.01$) and CX3CR1 ($p<0.01$) were detected (**Figure IV.19A**). The downregulation of miR-124 in TG MN prevents the stimulation of such neuronal-microglial axis resultant of the paracrine signaling derived from the MN ALS pathological secretome (**Figure IV.9**).

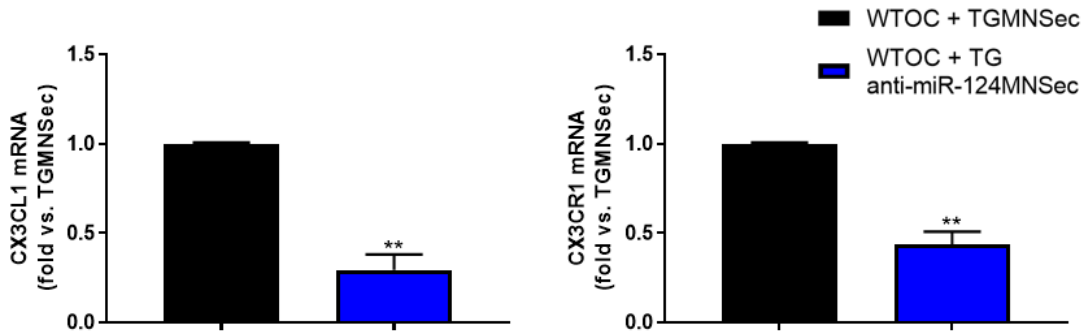

Figure IV.19 - Secretome from anti-miR-124-treated mSOD1 MNs is able to lower activated CX3CL1-CX3CR1 in WT SCOCs upon the addition of the secretome from non-treated ALS MNs. After 3 days in culture and 24 h incubation with transgenic (TG) anti-miR-124 motor neuron (MN) secretome (Sec), wild type (WT) SCOCs were collected in Trizol for reverse transcription-quantitative polymerase chain reaction (RT-qPCR) analysis, where β-actin was used as an endogenous control. Transcript levels of CX3CL1 and CX3CR1 in WT slices *vs.* WT OC exposed to TG MN secretome are represented in the present figure. Results are mean ± SEM of, at least, 4 independent experiments. **p<0.01 *vs*. WT OC treated with TG MN secretome were obtained by using two-tailed unpaired Student's *t*-test with Welch's correction when required. **CX3CL1**, C-X3-C motif chemokine ligand 1; **CX3CR1**, C-X3-C motif chemokine receptor 1.

5.5. Secretome from anti-miR-124-treated TG MNs reduces the pre-synaptic gene SYP that encodes for synaptophysin in WT spinal cord organotypic cultures stimulated with ALS MN secretome

Synaptic alterations (increased SYP and diminished levels of Dlg4) were obtained in section (**3.5.**) upon TG MN secretome incubation. As so, we also evaluated the expression of these markers upon incubation with secretome for TG MN transfected with anti-miR-124.

In WT SCOCs, we obtained a reduction in SYP ($p<0.01$) and no changes in Dlg4 levels (**Figure IV.20**) after the addition of the secretome from the modulated ALS MNs. One more time modulated diseased MN secretome was able to prevent the increased levels of SYP in WT SCOCs exposed to mSOD1 MN secretome (**Figure IV.10**). This finding should be envisaged in parallel with previous data on the TG SCOCs (**Figure IV.3**), upon the addition of the secretome from WT MNs to TG slices (**Figure IV.5**) and treatment with the pathological secretome from MNs (**Figure IV.7**), where this gene associated with the pre-synaptic protein synaptophysin was

observed consistently elevated. However, this finding should be further explored and analyzed together with the other assessed markers to conclude whether our findings should be interpreted as a positive or harmful effect of anti-miR in mSOD1 MNs.

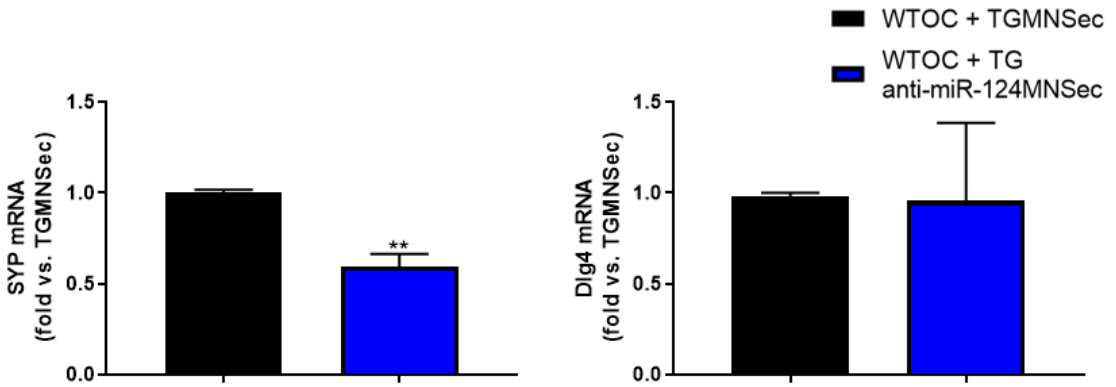

Figure IV.20 - Secretome from anti-miR-124-treated mSOD1 MNs decreases the expression of SYP mRNA toward normal levels upon the addition of the secretome from non-treated ALS MNs. After 3 days in culture and 24 h incubation with transgenic (TG) anti-miR-124 motor neuron (MN) secretome (Sec), wild type (WT) spinal cord organotypic cultures (SCOCs) were collected in Trizol for reverse transcription-quantitative polymerase chain reaction (RT-qPCR) analysis, where β-actin was used as an endogenous control. Transcript levels of SYP and Dlg4 in WT slices *vs*. WT OC exposed to TG MN secretome are represented in the present figure. Results are mean ± SEM of, at least, 4 independent experiments. ***p*<0.01 *vs.* WT OC treated with TG MN secretome was obtained by using two-tailed unpaired Student's *t*-test with Welch's correction when required. **SYP**, synaptophysin; **Dlg4**, discs large MAGUK scaffold protein 4 (or PSD-95, postsynaptic density protein 95).

5.6. Secretome from anti-miR-124-treated TG MNs enhances GFAP gene expression that is reduced in WT spinal cord organotypic cultures stimulated with ALS MN secretome

Regarding WT SCOCs, TG anti-miR-124 MN secretome induced upregulation of GFAP ($p<0.05$) while no changes were observed in GLT-1, the first downregulated and the second upregulated upon the incubation of slices with the pathological MN secretome (**Figure IV.21A; Figure IV.11**). The same representation was observed in the TG SCOCs (**Figure IV.3**) and in WT SCOCs after the addition of the WT MN secretome to TG slices (**Figure IV.5**). Therefore, it seems that the anti-miR-124 modulation is able to counteract these features. Again, the benefits or harmful consequences of it should be explored in future studies.

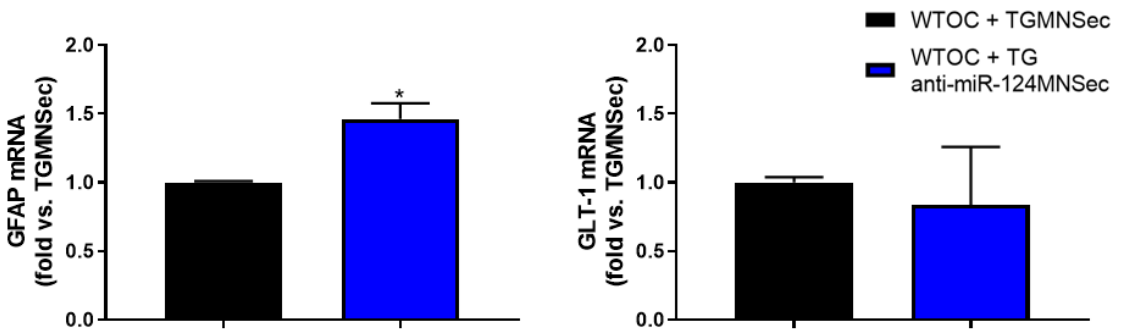

Figure IV.21 - Secretome from anti-miR-124-treated mSOD1 MNs increases the expression of GFAP mRNA toward normal levels in WT SCOCs upon the addition of the secretome from non-treated ALS MNs. After 3 days in culture and 24 h incubation with transgenic (TG) anti-miR-124 motor neuron (MN) secretome (Sec), wild type (WT) spinal cord organotypic cultures (SCOCs) were collected in Trizol reverse transcription-quantitative polymerase chain reaction (RT-qPCR) analysis, where β-actin was used as an endogenous control. Transcript levels of GFAP and GLT-1 in WT slices *vs*. WT OC exposed to TG MN secretome are represented in the present figure. Results are mean ± SEM of, at least, 4 independent experiments. *p<0.05 *vs.* WT OC treated with TG MN secretome was obtained by using two-tailed unpaired Student's *t*-test with Welch's correction when required. **GFAP**, glial fibrillary acidic protein; **GLT-1**, glutamate transporter 1.

5.7. Secretome from anti-miR-124-treated TG MNs reduces MFG-E8 gene expression in WT spinal cord organotypic cultures stimulated with ALS MN secretome

As mentioned in (section **3.7.**) diseased MN secretome induced an increase in microglial phagocytosis by overexpressing the mRNA levels of MFG-E8 and TREM2 in SC slices. Here, we investigated the impact of the secretome from mSOD1 MNs downregulated for miR-124 in the WT SCOCs treated with the pathological MN untreated secretome in the expression of the same parameters. Regarding WT SCOCs, the levels of MFG-E8 were diminished ($p<0.05$), while no changes were observed for TREM2 levels (**Figure IV.22A**). If beneficial, the modulation with anti-miR-124 was able to restore the normal levels of MFG-E8 that we found to be enhanced by the TG MN secretome, but the same was not obtained for TREM2 that was found to be upregulated by this secretome in both WT and TG SCOCs (please see **Figure IV.12**).

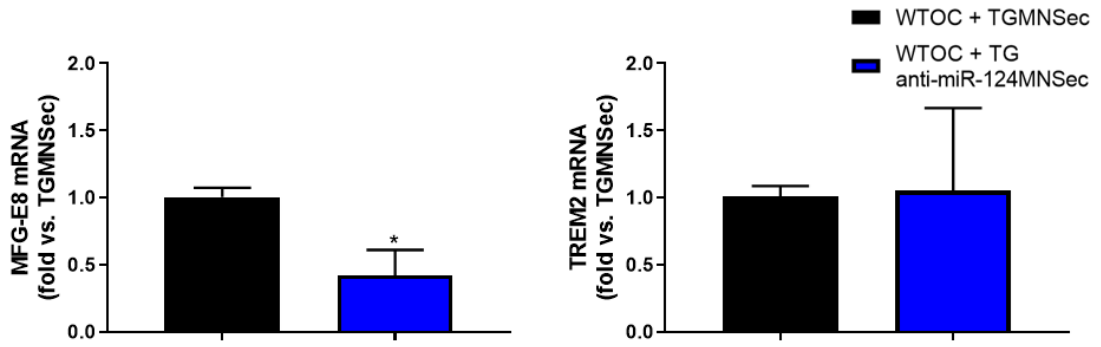

Figure IV.22 - Secretome from anti-miR-124-treated mSOD1 MNs decreases the expression of MFG-E8 mRNA toward normal levels in WT SCOCs upon the addition of the secretome from non-treated ALS MNs, but not TREM2 levels. After 3 days in culture and 24 h incubation with transgenic (TG) anti-miR-124 motor neuron (MN) secretome (Sec), wild type (WT) spinal cord organotypic cultures (SCOCs) were collected in Trizol reverse transcription-quantitative polymerase chain reaction (RT-qPCR) analysis, where β-actin was used as an endogenous control. Transcript levels of MFG-E8 and TREM2 in WT slices *vs*. WT OC exposed to TG MN secretome are represented in the present figure. Results are mean ± SEM of, at least, 4 independent experiments. *p<0.05 *vs.* WT OC treated with TG MN secretome was obtained by using two-tailed unpaired Student's *t*-test with Welch's correction when required. **MFG-E8**, milk fat globule-EGF factor 8; **TREM2**, triggering receptor expressed on myeloid cells 2.

5.8. Secretome from anti-miR-124-treated TG MNs restores MFN2 gene expression in WT spinal cord organotypic cultures stimulated with ALS MN secretome, but does not modify DRP1 one

In section (**3.9.**) we detected increased levels of MFN2 and DRP1 under incubation of diseased MN secretome in both WT and TG SCOCs. Here, the downregulation of miR-124 toward physiological levels in mSOD1 MNs led to a secretome that once added to TG slices was able to abrogate the increase of MFN2 gene expression triggered by the secretome from ALS MNs (MFN2, p<0.05, **Figure IV.23;** please compare with **Figure IV.13).** DRP1 was found elevated in the ALS SCOCs, either without (**Figure IV.3**) or with the addition of WT MN secretome (**Figure IV.5**). Therefore, these findings suggest a recovery only in mitochondrial fusion dynamics by the secretome derived from the modulation of anti-miR-124 in the diseased MNs.

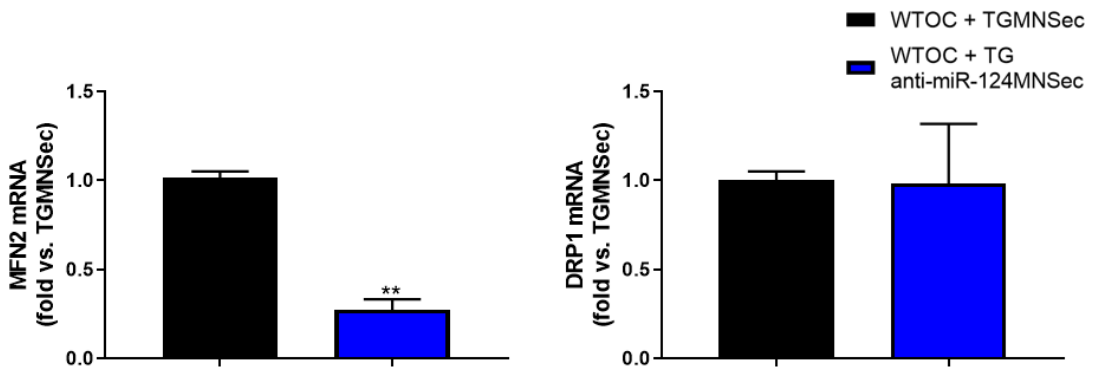

Figure IV.23 - Secretome from anti-miR-124-treated mSOD1 MNs decreases the expression of MFN2 toward normal levels in WT SCOCs upon the addition of the secretome from non-treated ALS MNs, but not DRP1 levels. After 3 days in culture and 24 h incubation with transgenic (TG) anti-miR-124 motor neuron (MN) secretome (Sec), wild type (WT) spinal cord organotypic cultures (SCOCs) were collected in Trizol for reverse transcription-quantitative polymerase chain reaction (RT-qPCR) analysis, where β-actin was used as an endogenous control. Transcript levels of MFN2 and DRP1 in WT slices *vs*. WT OC exposed to TG MN secretome are represented in the present figure. Results are mean ± SEM of, at least, 4 independent experiments. ***p*<0.01 *vs.* WT OC treated with TG MN secretome was obtained by using two-tailed unpaired Student's *t*-test with Welch's correction when required. **MFN2**, mitofusin-2; **DRP1**, dynamin-related protein 1.

5.9. Anti-miR-124 treatment represses the transcriptomic profile of early symptomatic mice

In the last part of this project, we decided to validate if the modulation of the miR-124 in the ALS MNs would translate into a secretome with neuroprotective and anti-inflammatory properties. For that, we will incubate such secretome in the TG SOCS at the early onset of the disease, which constituted the first piece of the Results (**Figure.IV.3**). TG anti-miR-124 MN secretome was obtained and incubated in TG SCOCs for 24 as previously performed.

Regarding miRNAs, results showed a decrease of miR-21 ($p<0.05$) and miR-124 ($p<0.001$), which was expected given the use of anti-miR-124 (**Figure.IV.24A**). Moreover, the extent of miR-125b remained the same and miR-146a was no longer significantly upregulated. Thus, we could find a suppression of inflamma-miRs probably indicating that the homeostatic inflammatory balance was somehow solved, indicating that the immune dysregulation triggered by the diseased secretome was, at least in part, prevented. We may assume that the need to react to the insult was reduced by the incubation of a secretome with less neurotoxic and neuroinflammatory properties. This was further corroborated by the transcriptomic profile evidencing that almost all the related genes involved in such processes were repressed (**Figure.IV.24B**). As already mentioned, such profile may indicate the presence of compensatory and adaptative mechanisms attempting to halt the progression of the disease and the accumulation of the mutant protein, leading to a depressed cellular metabolism. Globally the results highlight the beneficial consequences that the modulation of miR-124 toward reduced levels may have as a therapeutic

strategy. If true we may use secretome impoverished in miR-124 or exosomes containing anti-miR-124 in patients presenting elevated levels of miR-124 in circulating exosomes.

Accordingly, inflammatory-associated genes, such as iNOS, IL-1β and CX3CR1 were decrease (at least $p<0.05$) (**Figure.IV.24B**). With such a decrease, it was expected that IL-10 was also reduced, what was also observed ($p<0.05$). The same was observed for the reactive genes in astrocytes, S100B, GFAP and GLT-1 (at least $p<0.05$). Genes associated with synaptic dynamics were also reduced such as SYP and Dlg4 ($p<0.001$). Whether these results may have harmful consequences should be explored in the future, mainly in a late disease stage, e.g. mice with 12-14 weeks-old or even during the symptomatic stage (14-16 weeks-old) (Rocha et al., 2013; Nascimento et al., 2014). In such stages, we observe an exacerbated inflammatory status with elevation of all inflamma-miRs, neuronal loss, astrocyte reactivity and microglia activation (Cunha et al., 2017).

Mitochondria dynamics maintained unchanged with normal levels of MFN2 and DRP1. Corroborating a less activated stage, it is also the observed decrease in genes that codify for proteins involved in phagocytosis such as MFG-E8 or TREM2, indications that a more homeostatic calming balance was achieved.

Another point that should be later investigated is whether this depressed profile is suggestive of a more steady state of the cells, or whether the cells switched to a more irresponsive phenotype. This issue may be tested by challenging the TG SCOCs with LPS, or TNF-α+IL1β, or even H2O2, in the presence and in the absence of the secretome from the modulated MNs with anti-miR-124. Only by performing such experiments, we can expand our knowledge on the benefits, or not of anti-miR-124 in the ALS disease.

In sum, our results suggest that downregulation of miR-124 in TG MNs toward physiologic levels acquire the ability to counteract most of the abnormalities found in the SCOCs from TG animals, but also in those from WT mice after the harmful stimulus caused by the presence of the neurotoxic and immunostimulatory secretome from diseased ALS MNs. Indeed, an overall rescue of the inflammatory status of glial cells along with a supply in neuronal protection in comparison with non-modulated TG MN secretome was observed. These findings reinforce that the downregulation of miR-124 may be a helpful therapeutic strategy whenever such biomarker is found elevated in the circulation of ALS patients, what may indicate a poorer outcome in ALS, as in other conditions (Devaux et al., 2016; He et al., 2019).

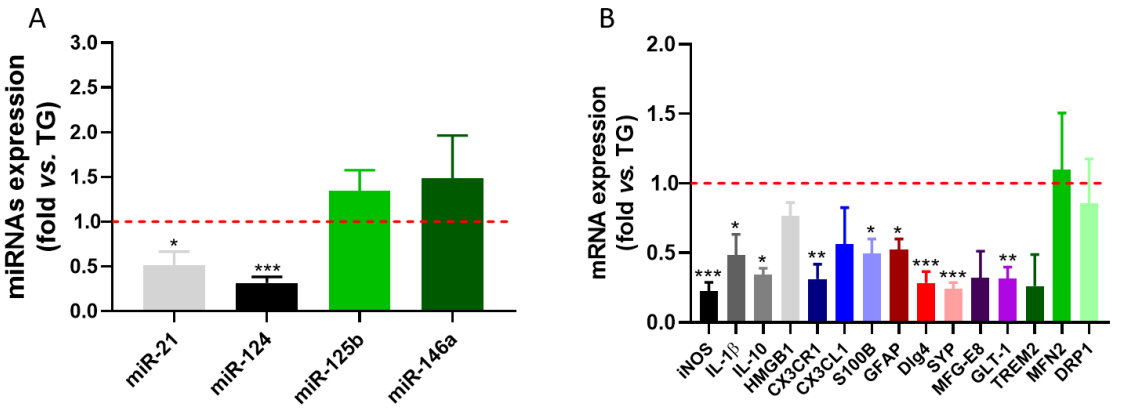

Figure IV.24 - Secretome from anti-miR-124-treated mSOD1 MNs has a broad suppressive effect on inflammatory-associated mediators, astrocyte reactive markers, synaptic dynamics and immune signaling in TG SCOCs upon the addition of the secretome from non-treated ALS MNs. After 3 days in culture and 24 h incubation with culture medium (4 DIV), transgenic (TG) spinal cord organotypic cultures (SCOCs) were collected in Trizol for reverse transcription-quantitative polymerase chain reaction (RT-qPCR) analysis. β-actin was used as an endogenous control for protein-coding genes while SNORD was used as a reference gene for miRNAs. MiRNA levels of miR-21, miR-124, miR-125b, and miR-146a and mRNA levels of iNOS, IL-1β, IL-10, HMGB1, CX3CR1, CX3CL1, S100B, GFAP, Dlg4, SYP, MFG-E8, GLT-1, TREM2, MFN2, and DRP1 *vs.* TG OC treated with culture medium are depicted, respectively, in (**A**) and (**B**). Results are mean ± SEM of, at least, 4 independent experiments. *p<0.05, **p<0.01 and ***p<0.001 *vs.* TGOC (red dashed line) were obtained by using two-tailed unpaired Student's *t*-test with Welch's correction when required. **iNOS,** inducible nitric oxide synthase; **IL-1β**, interleukin-1 beta; **IL-10**, interleukin-10; **HMGB1**, high mobility group protein 1; **CX3CR1**, C-X3-C motif chemokine receptor 1; **CX3CL1**, C-X3-C motif chemokine ligand 1; **S100B**, S100 calcium-binding protein B; **GFAP**, glial fibrillary acidic protein; **Dlg4**, discs large MAGUK scaffold protein 4 (or PSD-95, postsynaptic density protein 95); **SYP**, synaptophysin; **MFG-E8**, milk fat globule-EGF factor 8; **GLT-1**, glutamate transporter 1, **TREM2**, triggering receptor expressed on myeloid cells 2; **MFN2**, mitofusin-2; **DRP1**, dynamin-related protein 1.

V. DISCUSSION

ALS is a progressive neurodegenerative disease, complex and multifactorial that affects UPM and LMN. It is nowadays accepted that glial cells, namely astrocytes and microglia, have a key role in disease onset and progression and several pathological mechanisms have been implicated (Rothstein et al., 1992; Bruijn et al., 1997; Wang et al., 2011; Brites and Vaz, 2014). However, it is still uncertain which are the triggers and consequent major causes of the disease. Alterations of miRNAs in ALS patients and disease models have been identified and related with cell survival and neuroinflammation (Rajgor, 2018; Brites 2020). MiRNAs were found altered in the blood and CSF of ALS patients highlighting their implication in ALS pathology (Figueroa-Romero et al., 2016; Joilin et al., 2019) and showing the ease of track and measurement of these potential biomarkers. The same molecules play a role in the acquisition of dysfunctional properties, namely in MN and glial cells. Therefore, its modulation toward physiologic levels to restore the cellular homeostasis has been remarkably studied. MiR-124 is the most abundant miRNA within CNS and participates in diverse processes, such as neuronal identity acquisition and preservation (Conaco et al., 2006), synaptic plasticity, hematopoiesis, hippocampal axogenesis, regulation of neurite outgrowth and in astrocyte differentiation (Sun et al., 2015; Foggin et al., 2019). Moreover, miR-124 contribution to inflammatory status is tightly associated with an anti-inflammatory action (Ponomarev et al., 2011; Sun et al., 2013). Noteworthy, enhanced levels of miR-124 were found in SC and brainstem of mSOD1 mice, and associated with the neurodegenerative sites (Zhou et al., 2018). Finally, it was also reported as one of the most frequently dysregulated miRNAs in ALS, being closely related with later stages of disease (Foggin et al., 2019). In addition, miRNAs are one of the factors present in the secretome and particularly enriched in EVs (Brites, 2020), which make them good targets for therapeutic intervention since their modulation can simultaneously have benefits over the cells of origin but also the neighboring cells. Previous data from our group demonstrated NSC-34-MN-like cell line overexpressing the hSOD1^{G93A} mutation (mSOD1 MN) had increased levels of miR-124, that was also observed in their derived exosomes or secretome (Pinto et al, 2017; Colaço, Master Thesis 2020). It was then proposed that the transference of this miRNA have important paracrine signaling effects to the neighbor cells. In addition, recent data from the group showed that several mechanisms involved in mSOD1 MNs dysfunction, such as dysregulation of mitochondrial dynamics, axonal transport and synaptic signaling, were prevented upon transfection with anti-miR-124 (Vizinha, Master Thesis, 2018). In addition, microglia and astrocyte reactivity induced by mSOD1 MNs-derived secretome was abolished when each of these glial cells was incubated with secretome from mSOD1 MNs modulated with anti-miR-124, confirming the important role of miR-124 modulation to rescue cellular pathology in ALS.

It is widely accepted that complex interactions between multiple pathogenic mechanisms involving MN and the surrounding glial cells are the basis of MN degeneration and ALS progression (Parisi et al., 2016). Much effort has been done, by us and others, to understand such mechanisms. However, most of the studies are based on ALS monoculture models (cell lines/primary cultures). These systems do not allow the assessment of cell-to-cell dysregulated

communication. In this way, the combination of findings can easily lead us to construct a twisted big picture. To overcome such restriction here we used 3D ex-vivo SCOCs of the commonly TG mice carrying the $SOD1^{G93A}$ mutation (mSOD1) and aged-matched controls (WT animals). As so, we aimed to explore homeostatic imbalance in the early symptomatic stage of mSOD1 mice that results from anomalous interactions between the different cells that compose the tissue as well as the effect caused by different secretome in worsening/amelioration of cell's function. OC is a forward-looking 3D technique that preserves the tissue architecture, allowing the functional crosstalk between the different cells present in the tissue (Cavaliere et al., 2016). In this thesis, we used chronic OC by maintaining them 4 days in culture (DIV), that allowed the slices to recover from trauma cut injury in comparison with acute cultures (Lossi et al., 2009). Moreover, microglia return to its steady state after ~ 1 week *in vitro* following itself activation under the cut of the SC (Holopainen, 2005). As so the inflammatory response that may derive from microglia activation will be more related with exposure to additional stimuli than with the cut trauma. However, this model has also some limitations related with the need of process optimization and low yield, especially because we worked with tissue collected from adult mice and not pups as usual for these cultures (Guzmán-Lenis et al, 2009). Also, we did not succeed with MN evaluation for the choline O-acetyltransferase indicator, neither by PCR nor by immunohistochemistry. This is in line with other studies that point to MNs as the type of cells more affected in OC (Humpel, 2015). Nevertheless, synaptic-related genes were detected by RT-qPCR, meaning that some neuronal activity is occurring in TG OC during culture.

With this in mind, we started by characterizing the levels of necrotic death and the microglial/astroglial cell number in the TG SCOCs of early symptomatic mSOD1 mice and aged-matched controls (WT) after 4 DIV with culture medium. We first observed a basal cell demise of 20 %, in WT slices, which we believe to be related to the trauma caused by the cut of the SC. We also found ~ 30 % $GFAP^+$ and ~10 % Iba-1^+ cells, according to the described levels for, respectively, astrocytes and microglia in the CNS (Liddelow & Barres, 2017; Komine & Yamanaka, 2015; Butovsky & Weiner, 2018). One possibility is that this basal rate may be associated with the decease of neuronal cells since these cells are the ones considered to be mostly affected in this type of culture (Humpel, 2015). Regarding TG OC, additional cell demise and the impairment in the levels of synaptic markers also suggest MN decrease. However, it should be considered that MN loss has been identified as a feature in mSOD1 mice only at the symptomatic stage (Cunha et al., 2017). Additionally, enhanced levels of the pre-synaptic marker were already associated with an outgrowth of processes as an attempt to communicate with surrounding neurons (Antonova et al., 2009). The increase of synaptophysin along with the favoring of mitochondria fission (DRP1) observed by us suggests that in our model there are still some compensatory mechanisms triggered in the TG SCOCs, probably due to the fact that the mice are still in the early symptomatic stage (Turner and Talbot 2008) and the levels of MNs loss are not much elevated in comparison to later stages of disease progression. Dysfunctional MNs may also have more energy demands. Because of such demands, cells attempt to possess more available mitochondria and to reach the surrounding neurons, which are deprived in the post-

synaptic marker (Dlg4). On the other hand, lower levels of CX3CL1 in TG OCs may indicate a certain degree of neurodegeneration that derived from the inability of neurons to communicate with surrounding cells. Accordingly, Zhang and co-workers pointed out that reduced levels of fractalkine after disease onset may reflect an abnormal downregulation on MN and MN loss (Zhang et al., 2015).

Moreover, our results point to alterations in astrocytes in TG OCs, characterized by decreased levels of GFAP mRNA and upregulated ones of GLT-1, pointing to the existence of reactive astrocytes with still functional properties observed before disease onset (Cunha et al., 2017). In addition, dysregulation of both pro- (low iNOS/HMGB1 and high IL-1β) and anti- (low CX3CR1 and high IL-10) inflammatory associated genes (Cunha et al., 2017; Fernandes et al., 2018) along with dysregulation of both anti-inflammatory-associated miRNAs (high miR-21 and miR-146a) (Ponomarev et al., 2011; Sheedy, 2015; Brites, 2020) are consistent with a dysregulated inflammatory status. Microglia are considered the resident immune cells of the CNS. By increasing the levels of TREM2, a marker found elevated in the SC of mSOD1 mice (Cady et al., 2014) and referred as a regulator of microglia phenotype (Chiu et al., 2013), microglia change its phenotype as an attempt to solve the displaced environment. Yet, the mix of the pro-and anti-inflammatory phenotype observed may be a sign of the existence of compensatory mechanisms.

After the global characterization of WT and TG SCOCs, we investigated the influence of MN secretome in these cultures having the same markers (viability and the referred transcriptomic profile) into consideration. Thus, after 3 DIV with culture medium, WT and TG slices were firstly incubated with WT MN secretome for 24 h. Here the recovery of cell viability suggests a protective effect of the healthy MN secretome in TG SCOCs neurons. We also observed overexpression of miR-124 and miR-125b, which are commonly found upregulated in TG MN (Pinto et al., 2017; Colaço, Master Thesis, 2020). Additionally, the prolonged exposure of WT MN secretome in primary microglia has been shown by us to incite a calming in WT and $SOD1^{G93A}$ microglia (Colaço, Master Thesis, 2020) with an overall downregulation of inflammatory-associated genes. Perhaps by rescuing a proper inflammatory status (downregulation of genes related with a mix of a pro-and anti-inflammatory status) and maintaining increased levels of CX3CR1 WT MN secretome trigger a resolving phenotype in TG microglia since increased CX3CR1 are associated with surveilling/ anti-inflammatory microglia polarization (Cunha et al., 2016). Moreover, it is important to mention that CX3CR1 is only expressed by microglia in the CNS and that $CX3CR1^{-/-}$ knockout in $SOD1^{G93A}$ mice worsened disease outcome by displaying dysregulated microglia responses and extensive neuronal loss (Cardona et al., 2006). By that way, upregulation of CX3CR1, microglia probably protect neurons from demise. Therefore, the extent of cell demise is recovered. Moreover, the expression of synaptophysin marker change from 4 to 2-fold, may represent an attempt of recovery of synaptic dynamics toward the ones found in physiologic levels (in WT SCOCs). Regarding astrocytes, we did not detect mRNA fluctuations of GFAP (low) and GLT-1 (high) regarding TG OC treated with culture medium. Besides, a tendency in the recovery of $GFAP^{+}$ cells in diseased animals was observed. The contradictory results of GFAP suggest a mix of non-reactive/reactive astrocytes in SCOCs treated with WT MN secretome. However, the

same secretome seems to be also associated with negative components since it was responsible for overexpression of all the miRNAs evaluated in TG SCOCs, including miR-124 and miR-125b. The first, as mentioned in the course of the present work, is linked to detrimental outcomes in TG ALS models. As so, downregulation of such miRNA may encourage its regulation toward the levels found in physiologic circumstances as well as the expression of other miRNAs. In that way, we expect amelioration of disease traits found in early symptomatic mice SCOCs.

As already mentioned, miRNAs have been linked to neuroinflammation and imbalance in ALS. Beyond miR-124, miR-21, miR-146a and miR-155 play a role in disease pathology (Figueroa-Romero et al., 2016; Joilin et al., 2019). MiR-155 promotes pro-inflammatory signaling pathways claiming to be a virtuous therapeutic target since is one of the most affected in disease. Several ALS trials have been targeting this miRNA by inhibiting it (Koval et al., 2013; Butovsky et al., 2015), with that approach life extent of ALS mice model has been attained. However, in our ALS MN model, we did not notice detectable amounts of miR-155 but instead, we observed enriched levels of miR-124 in TG (mSOD1) NSC-34 cells MN (Pinto et al., 2017) as well as in their exosomes and secretome (Colaço Master Thesis 2020). For those reasons, we focused our experiments in the role of miR-124 and the effect of its modulation in other inflammatory associated miRNAs, namely miR-21, miR-125b and miR-146a in SCOCs.

A similar miRNA profile was observed in WT and TG OCs incubated with TG MN or WT pre-miR-124 MN secretome, except for miR-146a, suggesting a correlation of increased miR-124 expression with disease onset since the miRNA signature of WT mice moved towards the profile found in SCOCs from TG animals. Additional poor features were achieved in healthy animals including a decrease in cell viability, astrocyte reactivity, and dysregulation of synapses and mitochondria dynamics-related markers. Such features have been pointed over the present work as to be related to ALS. Moreover, the exacerbation of the extent of the miRNAs studied in TG OCs may be associated with disease progression. By acting on that way they possibly regulate soluble factors on surroundings cells. As a result, target cells become more dysfunctional, according to this is the restricted inflammatory response achieved in diseased SC.

With evidences of an activated, although dysregulated, microglia we questioned if the last had any influence in the phenotype of astrocytes. For that, we studied the expression of GFAP and GLT-1 in astrocytes, since when dysregulated the same markers are indicative of astroglia reactivity (Yoshii et al., 2011; Díaz-Amarilla et al., 2011; Verkhratsky & Nedergaard, 2018). Regarding TG MN secretome we detected upregulated levels of GLT-1 in both WT and TG slices, while a differential GFAP pattern of expression was detected on WT and TG OCs (decrease and increase, respectively). Regarding TG OCs, we may interpret the increase of GFAP as a result of astrogliosis since increased production of GFAP is considered as a hallmark the same process (Yoshii et al., 2011). Astrogliosis particularly takes place when nearby neurons are going through a process of destruction. In fact, the present secretome may trigger additional damages in TG OCs, as we notice an overall exacerbation of the dysfunctionalities under the exposure of mSOD1 MN secretome namely in terms of mitochondrial dynamics, synaptic function, and phagocytosis

dysregulation. As a result, astrocytes are requested to the injured areas as an attempt to resolve the problem. Additionally, the same authors associated the loss of GFAP in SOD1 mice, carrying another mutation (H46R), to the acceleration of ALS progression by enhancing the activation of glial cells. GFAP levels were frequently found decreased in mSOD1 mice in the present work as well. The last along with the approximation of TG OCs toward symptomatic phase can be linked to a speedup of the disease. Finally, data from the present work support the association between glial loss of function and the presence of neuronal cells undergoing cell death in mSOD1 mice.

Finally, with anti-miR-124 treatment, there was a general recovery of the above-mentioned parameters. The extent of related markers was counteracted toward physiologic levels and with that cells presented a transcriptomic profile and cellular viability comparable with the one observed in steady state (WT slices treated with WT MN secretome). In detail, with the same modulation, we achieved positive results in WT OCs when comparing with WT slices treated with (non-modulated) TG MN secretome. By downregulating miR-124 in mSOD1 MNs, we abrogated the pathological mechanisms induced by the diseased secretome. This includes a decrease of all miRNAs studied towards physiologic levels. By that way, we believe that cells receive fewer contradictory stimuli (pro- *vs*. anti- polarization signs). And so balanced expression of synaptic markers (SYP and Dlg4) and fractalkine-CX3CL1 axis are achieved. Moving to TG SCOCs, we also observed benefits in using secretome resulting from miR-124 modulation in mSDO1 MNs. Indeed, necrosis was prevented as observed by values of cell death similar to the ones found in WT OCs. Regarding miRNAs, by using secretome from mSOD1 MNs modulated with anti-miR-124, we successfully downregulated miR-124 and miR-21 was diminished as well. Moreover, miR-125b and miR-146a were slightly diminished when comparing to TG slices without secretome treatment. In addition, the overall transcriptomic profile was found repressed upon incubation with this secretome. Thus, we improved the inflammatory status of the slices, by downregulating IL-1β and IL-10 and by balancing mitochondrial fusion/fission dynamics. However, some compensatory mechanisms that may be present in this early symptomatic stage may be also lost, namely CX3CR1, SYP and GLT-1 upregulation. Although the last outcomes TG anti-miR-124 MN secretome may be applied in late stages of the disease where mice do not possess compensatory mechanisms.

Overall, with our studies in SCOCs of mSOD1 mice, we were able to determine that they differ from WT OCs by displaying features compatible with the ones found in the mSOD1 mice model (Cunha et al. 2017). In our case, such features include cell death by necrosis, synaptic dysregulation and microglia and astrocytes reactivity, together with the dysregulation of the inflamma-miRNA profile and of the inflammatory-associated genes, as schematically represented in **Figure V.1**. WT MN secretome did not promote significant alterations in WT SCOCs while in TG mice it displayed a soothing effect. Regarding incubation with TG MN secretome, we did observe significant alterations in OCs from both healthy and diseased animals. This secretome changes the transcriptomic profile and cell viability of WT slices towards a profile similar to the one found in TG OCs *per se*. Regarding TG mice, TG MN secretome promotes an overall exacerbation of the aforementioned parameters. The last findings suggest an important role of

TG MN secretome (characterized by miR-124 upregulation) in ALS onset. The anti-miR-124 treatment seems to fit as an effective therapy since TG MN secretome derived from neurons cells subjected to this modulation counteracted some of the dysfunctionalities found in OCs from diseased mice (**Figure V.1**). However, caution should be taken to avoid the loss of compensatory mechanisms that are needed for reparative actions. Knowing that therapeutics and modulating methodologies based in cell secretome have shown protective effects in other models we propose the present modulation to be performed in the mice model (intrathecal injection), at later stages of the disease progression, that may ultimately be translated to human models if promising results are achieved, at least in ALS patients that overexpress miR-124 in the SC.

CONCLUDING REMARKS

To conclude, the present thesis provides important knowledge on how MN-glial cells interconnectivity is disrupted in the SC of early symptomatic ALS mice. In line with that the deterioration in MN cells and the compromised glial cells response which in turn is reflected in the health of the first as well as in the inflammatory status of the present tissue. Thus, this work reflects the contribution of both cell and non-cell-autonomous disease in ALS and its contribution to disease onset and development. From there we point the dysregulation of inflammatory miRNAs, namely miR-124, as a process responsible, at least in part, for the irregularities observed. We may summarize the findings of the present thesis:

1. Transgenic (mSOD1) SCOCs display distinct features in comparison with their respective age-matched controls, presenting reduced cell viability, dysregulation of inflammatory miRNAs (high miRs-21/146a), dysregulation of the inflammatory status (high IL-1β/IL-10 and low iNOS/HMGB1), imbalance in synapses (high SYP and low Dlg4) and mitochondria dynamics (high DRP1), dissimilarity in neuron-microglia interconnectivity (disruption of CX3CL1-CX3CR1 axis), and reactive astrocytes (high GLT-1 and low GFAP);

2. WT MN secretome has a healing effect in TG slices by reducing the fraction of dead cells along with a calming effect in the immune response causing a reduction of the cytokines IL-1β and IL-10. However, the same secretome enhances the levels of miRNAs found enriched in neural cells (miRs-124/125b), that may compromise their putative benefits over TG OCs;

3. TG MN secretome induces deleterious outcomes in both WT and TG SC slices leading to a reduction in their cell viability. Moreover, WT OCs modifies its transcriptomic profile toward TG OCs (high miRs- 21/146a, IL-1β, CX3CR1, SYP, GLT-1, TREM2, DRP1, and low GFAP). Differently, increased miRs- 124/125b, intensified microglia phagocytic ability (increased MFGE-8/TREM-2), and a preferentially pro-inflammatory response (enhanced

iNOS/IL-1β) were detected in WT slices. No inflammatory response was noticed, in TG OCs, after 4h and 24h of secretome incubation which is consistent with the overall exacerbation of irregularities in this type of OC upon mSOD1 MN secretome;

4. The increase of miR-124 in WT MN is responsible for the damaging effects observed after TG MN secretome incubation by recapitulating the cell death rate and the levels of a considerable number of markers (miRs and genes);

5. Secretome resultant from the mSOD1 MN modulated with anti-miR-124 improves the inflammatory status by downregulating miR-21, miR-124 and IL-1β and IL-10 cytokines in TG slices when compared with TG OCs treated with culture medium. Moreover, a balanced mitochondrial fusion/fission (decrease of DRP1) and a reduction of necrotic cell death and of phagocytosis-related genes (low MFG-E8 and TREM2) was achieved. On the other hand, the expression of genes linked to reparatory mechanisms was lost under such modulation. With the last, CX3CR1, SYP, GFAP, and GLT-1 genes were found diminished.

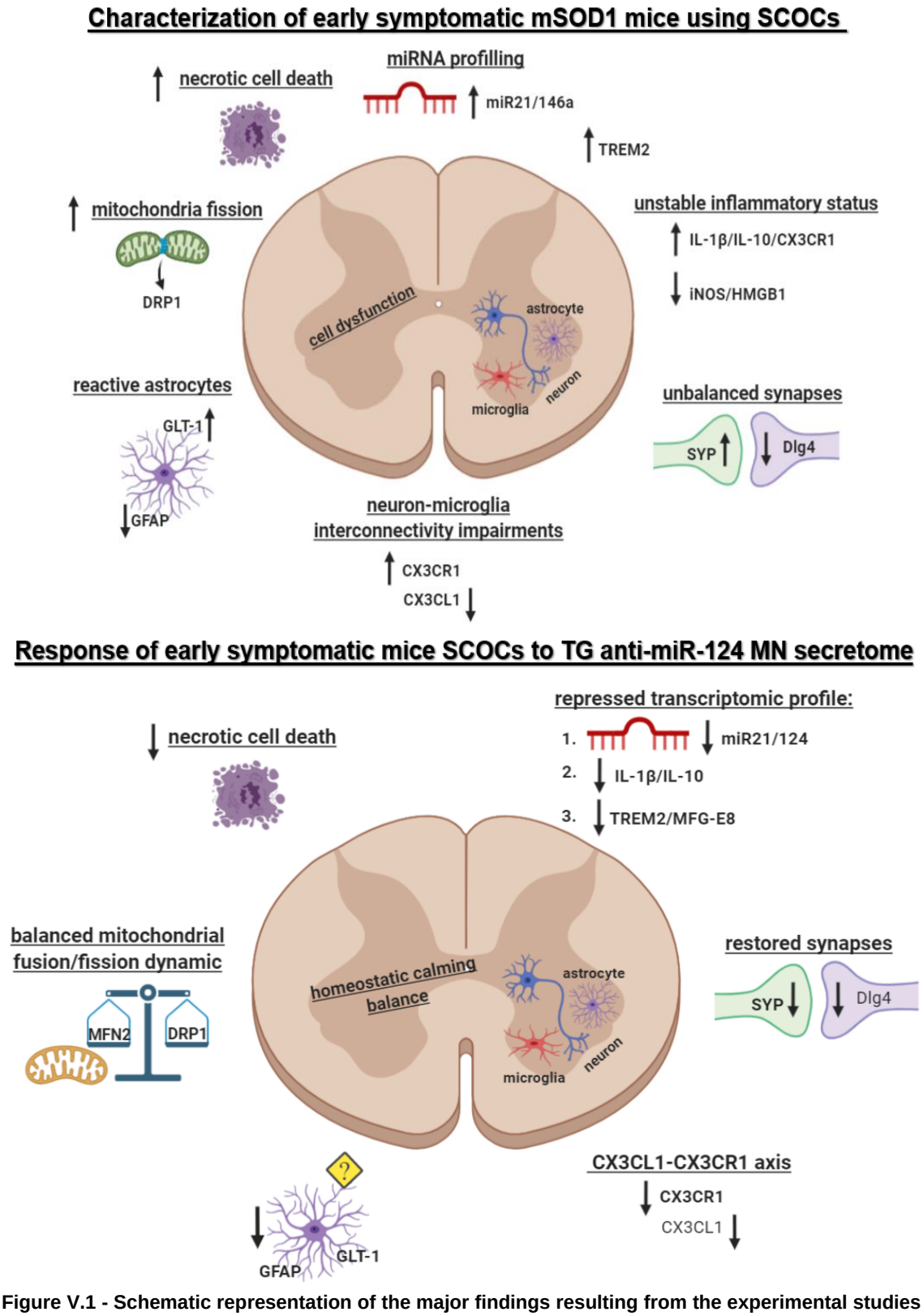

Figure V.1 - Schematic representation of the major findings resulting from the experimental studies developed in this thesis. We characterized early symptomatic mice (10-12 weeks old animals) carrying the human superoxide dismutase 1 (SOD1) with G93A mutation (mSOD1) by using spinal cord organotypic cultures (SCOCs). Slices were cultivated for 4 days. Transgenic (TG) SCOCs displayed distinct characteristics from WT ones, including: (i) higher necrotic cell death (assessed by propidium iodide (PI) staining), (ii) a miRNA profile distinguished by increased levels of miR-21 and miR-146a, (iii) upregulation of triggering receptor expressed on myeloid cells 2 (TREM2), (iv) an unstable inflammatory status, with upregulation of interleukin(IL)-1β, IL-10 and C-X3-C motif chemokine receptor 1(CX3CR1) and decrease of inducible nitric oxide synthase (iNOS) and high mobility group box 1 (HMBG1), (v) unbalanced synapses

with increased levels of synaptophysin (SYP) and downregulation of discs large MAGUK scaffold protein 4 (Dlg4), (vi) impairments in neuron-microglia interconnectivity with high CX3CR1 and depressed levels of C-X3-C motif chemokine ligand 1/fractalkine (CX3CL1), (vii) reactive astrocytes having, respectively, upregulated and downregulated levels of glutamate transporter-1 (GLT-1) and glial fibrillary acidic protein (GFAP) and, finally, (viii) favored fission mitochondrial dynamics with enhanced dynamin-related protein 1 (DRP1). A homeostatic calming balance was triggered following 24 h treatment with TG anti-miR-124 NSC-34 (MN-like) secretome. Decrease of necrotic cell death, balancing of mitochondrial fusion (mitofusin-2; MFN2) and fission (DRP1) dynamics and a repressed transcriptomic profile characterized by downregulated miR-21, miR-124, IL-1β, IL-10 and of phagocytosis-related genes TREM2 and milk fat globule-EGF factor 8 (MFG-E8) were observed in such condition. Adversely the expression of genes linked to compensatory mechanisms was lost as well. The pre-synaptic marker (SYP) became downregulated as the post-synaptic marker (Dlg4). Moreover, the CX3CL1-CX3CR1 axis and GFAP and GLT-1 mRNA content were found diminished in TG SCOCs.

FUTURE PERSPECTIVES

With the present study, we were able to characterize a neurogenic niche (SC) of early symptomatic mSOD1 mice by using an innovative technique, organotypic cultures. An abnormal cell as well as cell-to-cell communication processes were found dysregulated in TG SCOCs. Moreover, we reinforced that secretome function as a cell mirror being a vehicle of not only beneficial (e.g. TG anti-miR-124 MN secretome) but also detrimental soluble factors (e.g. TG non-modulated MN secretome). However, additional mechanisms can be explored.

As so, it would be interesting to investigate if the expression of some markers is reflected in protein levels. From those, we appoint SYP, DRP1, GLT-1 and TREM2 as possible targets since their expression is consistent in TG mice. It would be also interesting to better study the soluble form of neuronal CX3CL1 along with the membrane-bound form of CX3CR1 since the disruption of the present axis seem to be linked to many abnormalities such as microglia activation and astrocyte reactivity. Studies point that IL-1α, TNF and C1q cytokines released by microglia are necessary and sufficient to induce A1 astrocytes. Since microglia activation, even dysregulated, and astrocyte reactivity are some features observed in this work we propose the study of the expression of the above-mentioned cytokines in SCOCs to a better comprehension of communication of the above cells. Moreover, MN indicators should be more investigated in SCOCs since they play a central role in disease features. To complement the latter axonal retrograde (dynein) and anterograde (kinesin) transport indicators may be studied. Moreover, the study of the phagocytic ability along with morphologic oscillations in microglia and astrocytes in TG slices exposed to different secretome content (toxic *vs.* healing ones) come to as a relevant approach.

MiRNA-125b is another miRNA where future studies may be conducted. This miRNA displayed the same pattern as miRNA-124 in several conditions, as so it could be acting synergistically with the latter in processes that contribute to MN deterioration. To understand more its role in disease pathology modulation in MN, namely NSC-34 MN-like cell line, may be employed. In detail, its downregulation could be beneficial since it was found upregulated when TG OCs were treated with diseased MN secretome (characterized by increased levels of miR-124).

We also propose the study of the effect of miR-124 downregulation in older animals since at the early symptomatic stage some reparatory mechanisms seem to be lost under the last modulation. After performing some approaches to understand more some mechanism not explored in the present thesis injection of TG anti-miR-124 MN secretome in SC of Transgenic mice along with behavioral tests would be interesting to corroborate our results. If so translation of the anti-miR-124 treatment to ALS patients overexpressing miR-124 in the SC would be considered, even more, as a feasible and potential approach to counteract disease onset and progression.

VI. REFERENCES

Alexander, M., Hu, R., Runtsch, M. C., Kagele, D. A., Mosbruger, T. L., Tolmachova, T., Seabra, M. C., Round, J. L., Ward, D. M., & O'Connell, R. M. (2015). Exosome-delivered microRNAs modulate the inflammatory response to endotoxin. *Nature Communications*, 6, 7321. https://doi.org/10.1038/ncomms8321

Alexianu, M. E., Ho, B. K, Mohamed, A. H., La Bella, V., Smith, R. G., & Appel, S. H. (1994). The role of calcium-binding proteins in selective motoneuron vulnerability in amyotrophic lateral sclerosis. *Annals of Neurology*, 36(6), 846–858. https://doi.org/10.1002/ana.410360608

Alirezaei, M., Kiosses, W. B., Flynn, C. T., Brady, N. R., & Fox, H. S. (2008). Disruption of neuronal autophagy by infected microglia results in neurodegeneration. *PLoS ONE*, 3(8). https://doi.org/10.1371/journal.pone.0002906

Antonova, I., Lu, F. M., Zablow, L., Udo, H., & Hawkins, R. D. (2009). Rapid and long-lasting increase in sites for synapse assembly during late-phase potentiation in rat hippocampal neurons. *PLoS ONE*, 4(11), e7690. https://doi.org/10.1371/journal.pone.0007690

Attwell, D., Buchan, A. M., Charpak, S., Lauritzen, M., MacVicar, B. A., & Newman, E. A. (2010). Glial and neuronal control of brain blood flow. *Nature*, 468(7321), 232–243. https://doi.org/10.1038/nature09613

Bahrini, I., Song, J., Diez, D., & Hanayama, R. (2015). Neuronal exosomes facilitate synaptic pruning by up-regulating complement factors in microglia. *Scientific Reports,* 5, 1–8. https://doi.org/10.1038/srep07989

Barber, S. C., & Shaw, P. J. (2010). Oxidative stress in ALS: Key role in motor neuron injury and therapeutic target. *Free Radical Biology and Medicine*, 48(5), 629–641. https://doi.org/10.1016/j.freeradbiomed.2009.11.018

Basso, M., Pozzi, S., Tortarolo, M., Fiordaliso, F., Bisighini, C., Pasetto, L., Spaltro, G., Lidonnici, D., Gensano, F., Battaglia, E., Bendotti, C., & Bonetto, V. (2013). Mutant copper-zinc superoxide dismutase (SOD1) induces protein secretion pathway alterations and exosome release in astrocytes: Implications for disease spreading and motor neuron pathology in amyotrophic lateral sclerosis. *Journal of Biological Chemistry*, 288(22), 15699–15711. https://doi.org/10.1074/jbc.M112.425066

Batiuk, M. Y., Martirosyan, A., Wahis, J., de Vin, F., Marneffe, C., Kusserow, C., Koeppen, J., Viana, J. F., Oliveira, J. F., Voet, T., Ponting, C. P., Belgard, T. G., & Holt, M. G. (2020). Identification of region-specific astrocyte subtypes at single cell resolution. *Nature Communications*, 11(1), 1220. https://doi.org/10.1038/s41467-019-14198-8

Beaulieu, A. M., Bezman, N. A., Lee, J. E., Matloubian, M., Sun, J. C., & Lanier, L. L. (2013). MicroRNA function in NK-cell biology. *Immunological Reviews*, 253(1), 40–52. https://doi.org/10.1111/imr.12045

Berthod, F., & Gros-Louis, F. (2012). In Vivo and In Vitro Models to Study Amyotrophic Lateral Sclerosis. *Amyotrophic Lateral Sclerosis*, 3. https://doi.org/10.5772/39076

Bhalala, O. G., Pan, L., Sahni, V., Mcguire, T. L., Gruner, K., Tourtellotte, W. G., & Kessler, J. A. (2012). microRNA-21 Regulates Astrocytic Response Following Spinal Cord Injury. *Journal of Neuroscience*, 32(50), 17935–17947. https://doi.org/10.1523/JNEUROSCI.3860-12.2012

Bhaumik, D., Scott, K.G., Schokrpur, S., Patil, K.C., Orjalo, V.A., Rodier, F., Lithgow, J.G & Campisi, J. (2009). MicroRNAs miR - 146a / b negatively modulate the senescence - associated inflammatory mediators IL - 6 and IL - 8. *Aging*, 1(4), 402–411. https://doi.org/10.18632/aging.100042

Bonafede, R., Scambi, I., Peroni, D., Potrich, V., Boschi, F., Benati, D., Bonetti, B., & Mariotti, R. (2016). Exosome derived from murine adipose-derived stromal cells: Neuroprotective effect on in vitro model of amyotrophic lateral sclerosis. *Experimental Cell Research*, 340(1), 150–158. https://doi.org/10.1016/j.yexcr.2015.12.009

Bozzoni, V., Pansarasa, O., Diamanti, L., Nosari, G., Cereda, C., & Ceroni, M. (2016). Amyotrophic lateral sclerosis and environmental factors. *Functional Neurology*, 31(1), 7–19. https://doi.org/10.11138/FNeur/2016.31.1.007

Bristol, L. A., & Rothstein, J. D. (1996). Glutamate transporter gene expression in amyotrophic lateral sclerosis motor cortex. *Annals of Neurology*, 39(5), 676–679. https://doi.org/10.1002/ana.410390519

Brites, D. (2020). Regulatory function of microRNAs in microglia. *Glia*, 68(8), 1631–1642. https://doi.org/10.1002/glia.23846

Brites, D., & Vaz, A. R. (2014). Microglia centered pathogenesis in ALS: Insights in cell interconnectivity. *Frontiers in Cellular Neuroscience*, 8, 1–24. https://doi.org/10.3389/fncel.2014.00117

Brooks, B. R. (1991). The Role of Axonal Transport in Neurodegenerative Disease Spread: A Meta-Analysis of Experimental and Clinical Poliomyelitis Compares with Amyotrophic Lateral Sclerosis. *Canadian Journal of Neurological Sciences / Journal Canadien Des Sciences Neurologiques*, 18(S3), 435–438. https://doi.org/10.1017/S0317167100032625

Brown, R. H., & Al-Chalabi, A. (2017). Amyotrophic lateral sclerosis. *New England Journal of Medicine*, 377(2), 162–172. https://doi.org/10.1056/NEJMra1603471.

Bruijn, L. I., Becher, M. W., Lee, M. K., Anderson, K. L., Jenkins, N. A., Copeland, N. G., Sisodia, S. S., Rothstein, J. D., Borchelt, D. R., Price, D. L., & Cleveland, D. W. (1997). ALS-linked SOD1 mutant G85R mediates damage to astrocytes and promotes rapidly progressive disease with SOD1-containing inclusions. *Neuron*, 18(2), 327–338. https://doi.org/10.1016/S0896-6273(00)80272-X

Bucchia, M., Merwin, S. J., Re, D. B., & Shingo, K. (2018). Limitations and Challenges in Modeling Diseases Involving Spinal Motor Neuron Degeneration in Vitro. *Frontiers in Cellular Neuroscience*, 12, 6.1 https://doi.org/10.3389/fncel.2018.00061

Busatto, S., Zendrini, A., Radeghieri, A., Paolini, L., Romano, M., Presta, M., & Bergese, P. (2020). The nanostructured secretome. *Biomaterials Science*, 8(1), 39–63. https://doi.org/10.1039/c9bm01007f

Butovsky, O., & Weiner, H. L. (2018). Microglial signatures and their role in health and disease. *Nature Reviews Neuroscience*, 19(10), 622–635. https://doi.org/10.1038/s41583-018-0057-5

Butovsky, O., Jedrychowski, M. P., Cialic, R., Krasemann, S., Murugaiyan, G., Fanek, Z., Greco, D. J., Wu, P. M., Doykan, C. E., Kiner, O., Lawson, R. J., Frosch, M. P., Pochet, N., El Fatimy, R., Krichevsky, A. M., Gygi, S. P., Lassmann, H., Berry, J., Cudkowicz, M. E., & Weiner, H. L. (2015). Targeting miR-155 restores abnormal microglia and attenuates disease in SOD1 mice. *Annals of Neurology*, 77(1), 75–99. https://doi.org/10.1002/ana.24304

Butovsky, O., Siddiqui, S., Gabriely, G., Lanser, A. J., Dake, B., Murugaiyan, G., Doykan, C. E., Wu, P. M., Gali, R. R., Iyer, L. K., Lawson, R., Berry, J., Krichevsky, A. M., Cudkowicz, M. E., & Weiner, H. L. (2012). Modulating inflammatory monocytes with a unique microRNA gene signature ameliorates murine ALS, *Journal of Clinical Investigation*, 122(9), 3063–3087. https://doi.org/10.1172/JCI62636DS1

Cady, J., Koval, E. D., Benitez, B. A., Zaidman, C., Jockel-Balsarotti, J., Allred, P., Baloh, R. H., Ravits, J., Simpson, E., Appel, S. H., Pestronk, A., Goate, A. M., Miller, T. M., Cruchaga, C., & Harms, M. B. (2014). TREM2 variant p.R47H as a risk factor for sporadic amyotrophic lateral sclerosis. *JAMA Neurology*, 71(4), 449–453. https://doi.org/10.1001/jamaneurol.2013.6237

Caescu, C. I., Guo, X., Tesfa, L., Bhagat, T. D., Verma, A., Zheng, D., & Stanley, E. R. (2016). Colony stimulating factor-1 receptor signaling networks inhibit mouse macrophage in fl ammatory responses by induction of microRNA-21. *Blood*, 125(8), 1–14. https://doi.org/10.1182/blood-2014-10-608000

Cardona, A. E., Pioro, E. P., Sasse, M. E., Kostenko, V., Cardona, S. M., Dijkstra, I. M., Huang, D., Kidd, G., Dombrowski, S., Dutta, R., Lee, J.-C., Cook, D. N., Jung, S., Lira, S. A., Littman, D. R., & Ransohoff, R. M. (2006). Control of microglial neurotoxicity by the fractalkine receptor. *Nature Neuroscience*, 9(7), 917–924. https://doi.org/10.1038/nn1715

Cashman, N. R., Durham, H. D., Blusztajn, J. K., Oda, K., Tabira, T., Shaw, I. T., Dahrouge, S., & Antel, J. P. (1992). Neuroblastoma x spinal cord (NSC) hybrid cell lines resemble developing motor neurons. *Developmental dynamics*, 194(3), 209–221. https://doi.org/10.1002/aja.100194030

Cavaliere, F., Benito-Muñoz, M., & Matute, C. (2016). Organotypic Cultures as a Model to Study Adult Neurogenesis in CNS Disorders. *Stem Cells International*, 2016, 1-6. https://doi.org/10.1155/2016/3540568

Chaboub, L. S., & Deneen, B. (2013). Developmental origins of astrocyte heterogeneity: The final frontier of CNS development. *Developmental Neuroscience*, 34(5), 379–388. https://doi.org/10.1159/000343723

Chia, R., Tattum, M. H., Jones, S., Collinge, J., Fisher, E. M. C., & Jackson, G. S. (2010). Superoxide dismutase 1 and tgSOD1G93A mouse spinal cord seed fibrils, suggesting a propagative cell death mechanism in amyotrophic lateral sclerosis. *PLoS ONE*, 5(5). https://doi.org/10.1371/journal.pone.0010627

Chiu, I. M., Morimoto, E. T. A., Goodarzi, H., Liao, J. T., O'Keeffe, S., Phatnani, H. P., Muratet, M., Carroll, M. C., Levy, S., Tavazoie, S., Myers, R. M., & Maniatis, T. (2013). A neurodegeneration-specific gene-expression signature of acutely isolated microglia from an amyotrophic lateral sclerosis mouse model. *Cell Reports*, 4(2), 385–401. https://doi.org/10.1016/j.celrep.2013.06.018

Cho, G. W., Kim, G. Y., Baek, S., Kim, H., Kim, T., Kim, H. J., & Kim, S. H. (2011). Recombinant human erythropoietin reduces aggregation of mutant Cu/Zn-binding superoxide dismutase (SOD1) in NSC-34 cells. *Neuroscience Letters*, 504(2), 107–111. https://doi.org/10.1016/j.neulet.2011.09.008

Christoforidou, E., Joilin, G., & Hafezparast, M. (2020). Potential of activated microglia as a source of dysregulated extracellular microRNAs contributing to neurodegeneration in amyotrophic lateral sclerosis. *Journal of Neuroinflammation*, 17(1), 1–15. https://doi.org/10.1186/s12974-020-01822-4

Clement, A. M., Nguyen, M. D., Roberts, E. A., Garcia, M. L., Boillée, S., Rule, M., McMahon, A. P., Doucette, W., Siwek, D., Ferrante, R. J., Brown, R. H., Julien, J. P., Goldstein, L. S. B., & Cleveland, D. W. (2003). Wild-type nonneuronal cells extend survival of SOD1 mutant motor neurons in ALS mice. *Science*, 302(5642), 113–117. https://doi.org/10.1126/science.1086071

Colaço, A. R. 2020, *Dissecting neuronal miRNA-124 modulation: effects on secretome-mediated microglia deregulation in mSOD1-associated Amyotrophic Lateral Sclerosis*. Master Thesis, Faculdade de Medicina da Universidade de Lisboa.

Conaco, C., Otto, S., Han, J. J., & Mandel, G. (2006). Reciprocal actions of REST and a microRNA promote neuronal identity. *Proceedings of the National Academy of Sciences of the United States of America*, 103(7), 2422–2427. https://doi.org/10.1073/pnas.0511041103

Conde, B., Winck, J. C., & Azevedo, L. F. (2019). Estimating Amyotrophic Lateral Sclerosis and Motor Neuron Disease Prevalence in Portugal Using a Pharmaco-Epidemiological Approach and a Bayesian Multiparameter Evidence Synthesis Model. *Neuroepidemiology*, 53(1–2), 73–83. https://doi.org/10.1159/000499485

Cunha, C., Gomes, C., Vaz, A. R., & Brites, D. (2016). Exploring New Inflammatory Biomarkers and Pathways during LPS-Induced M1 Polarization. *Mediators of Inflammation*, 2016, 1-17. https://doi.org/10.1155/2016/6986175

Cunha, C., Santos, C., Gomes, C., Fernandes, A., Correia, A. M., Sebastião, A. M., Vaz, A. R., & Brites, D. (2017). Downregulated Glia Interplay and Increased miRNA-155 as Promising

Markers to Track ALS at an Early Stage. *Molecular Neurobiology*, 55(5), 4207-4224 https://doi.org/10.1007/s12035-017-0631-2

David, S., & Kroner, A. (2011). Repertoire of microglial and macrophage responses after spinal cord injury. *Nature Reviews Neuroscience*, 12(7), 388–399. https://doi.org/10.1038/nrn3053

Deo, M., Yu, J. Y., Chung, K. H., Tippens, M., & Turner, D. L. (2006). Detection of mammalian microRNA expression by in situ hybridization with RNA oligonucleotides. *Developmental Dynamics*, 235(9), 2538–2548. https://doi.org/10.1002/dvdy.20847

Devaux, Y., Dankiewicz, J., Salgado-Somoza, A., Stammet, P., Collignon, O., Gilje, P., Gidlöf, O., Zhang, L., Vausort, M., Hassager, C., Wise, M. P., Kuiper, M., Friberg, H., Cronberg, T., Erlinge, D., & Nielsen, N. (2016). Association of circulating MicroRNA-124-3p levels with outcomes after out-of-hospital cardiac arrest: A substudy of a randomized clinical trial. *JAMA Cardiology*, 1(3), 305–313. https://doi.org/10.1001/jamacardio.2016.0480

Di Carlo, V. Di, Grossi, E., & Laneve, P. (2013). TDP-43 Regulates the Microprocessor Complex Activity During In Vitro Neuronal Differentiation. *Molecular Neurobiology*, 48(3), 952–963. https://doi.org/10.1007/s12035-013-8564-x

Di Giorgio, F. P., Carrasco, M. A., Siao, M. C., Maniatis, T., & Eggan, K. (2007). Non-cell autonomous effect of glia on motor neurons in an embryonic stem cell-based ALS model. *Nature Neuroscience*, 10(5), 608–614. https://doi.org/10.1038/nn1885

Díaz-Amarilla, P., Olivera-Bravo, S., Trias, E., Cragnolini, A., Martínez-Palma, L., Cassina, P., Beckman, J., & Barbeito, L. (2011). Phenotypically aberrant astrocytes that promote motoneuron damage in a model of inherited amyotrophic lateral sclerosis. *Proceedings of the National Academy of Sciences of the United States of America*, 108(44), 18126–18131. https://doi.org/10.1073/pnas.1110689108

Duroux-Richard, I., Roubert, C., Ammari, M., Présumey, J., Grün, J. R., Häupl, T., Grützkau, A., Lecellier, C., Codogno, P., Escoubet, J., Pers, Y., & Jorgensen, C. (2016). miR-125b controls monocyte adaptation to inflammation through mitochondrial metabolism and dynamics. *Blood*, 128(26), 3125–3136. https://doi.org/10.1182/blood-2016-02-697003

Ebert, M. S., & Sharp, P. A. (2010). MicroRNA sponges: Progress and possibilities. *Rna*, 16(11), 2043–2050. https://doi.org/10.1261/rna.2414110

Endo, F., Komine, O., & Yamanaka, K. (2016). Neuroinflammation in motor neuron disease. *Clinical and Experimental Neuroimmunology*, 7(2), 126–138. https://doi.org/10.1111/cen3.12309

Feng, J., Li, A., Deng, J., Yang, Y., Dang, L., Ye, Y., Li, Y., & Zhang, W. (2014). miR-21 attenuates lipopolysaccharide-induced lipid accumulation and inflammatory response: potential role in cerebrovascular disease. *Lipids in health and disease*, 13, 27. https://doi:10.1186/1476-511x-13-27.

Fernandes, A., Ribeiro, A. R., Monteiro, M., Garcia, G., Vaz, A. R., & Brites, D. (2018). Secretome from SH-SY5Y APPSwe cells trigger time-dependent CHME3 microglia activation phenotypes, ultimately leading to miR-21 exosome shuttling. *Biochimie*, 155, 67–82. https://doi.org/10.1016/j.biochi.2018.05.015

Figueroa-Romero, C., Hur, J., Lunn, J. S., Paez-Colasante, X., Bender, D. E., Yung, R., Sakowski, S. A., & Feldman, E. L. (2016). Expression of microRNAs in human post-mortem amyotrophic lateral sclerosis spinal cords provides insight into disease mechanisms. *Molecular and Cellular Neuroscience*, 71, 34–45. https://doi.org/10.1016/j.mcn.2015.12.008

Foggin, S., Mesquita-Ribeiro, R., Dajas-Bailador, F., & Layfield, R. (2019). Biological significance of microRNA biomarkers in ALS-innocent bystanders or disease culprits? *Frontiers in Neurology*, 10, 578. https://doi.org/10.3389/fneur.2019.00578

Forsberg, K., Andersen, P. M., Marklund, S. L., & Brännström, T. (2011). Glial nuclear aggregates of superoxide dismutase-1 are regularly present in patients with amyotrophic lateral sclerosis. *Acta Neuropathologica*, 121(5), 623–634. https://doi.org/10.1007/s00401-011-0805-3

Gaudet, A. D., Fonken, L. K., Watkins, L. R., Nelson, R. J., & Popovich, P. G. (2017). MicroRNAs : Roles in Regulating Neuroinflammation. *Neuroscientist*, 24(3), 221-245. https://doi.org/10.1177/1073858417721150

Ge, X., Lei, P., Wang, H., Zhang, A., Han, Z., Chen, X., Li, S., Jiang, R., Kang, C., & Zhang, J. (2014). miR-21 improves the neurological outcome after traumatic brain injury in rats. *Scientific reports*, 4, 6718. https://doi.org/10.1038/srep06718

Ghasemi, M., & Brown, R. H. (2018). Genetics of amyotrophic lateral sclerosis. *Cold Spring Harbor Perspectives in Medicine*, 8(5), 1–38. https://doi.org/10.1101/cshperspect.a024125.

Givan, A. L. (1992). *Flow Cytometry: First Principles*, 2nd Edition. London: Wiley and Sons. Retrieved November 8, 2020, from https://www.wiley.com/en-us/Flow+Cytometry%3A+First+Principles%2C+2nd+Edition-p-9780471382249

Gomes, C., Cunha, C., Nascimento, F., Ribeiro, J. A., Vaz, A. R., & Brites, D. (2019). Cortical Neurotoxic Astrocytes with Early ALS Pathology and miR-146a Deficit Replicate Gliosis Markers of Symptomatic SOD1G93A Mouse Model. *Molecular Neurobiology*, 56(3), 2137–2158. https://doi.org/10.1007/s12035-018-1220-8.

Gomes, C., Palma, A. S., Almeida, R., Regalla, M., McCluskey, L. F., Trojanowski, J. Q., & Costa, J. (2008). Establishment of a cell model of ALS disease: Golgi apparatus disruption occurs independently from apoptosis. *Biotechnology Letters*, 30(4), 603–610. https://doi.org/10.1007/s10529-007-9595-z

Gomes, C., Sequeira, C., Barbosa, M., Cunha, C., Vaz, A. R., & Brites, D. (2020). Astrocyte regional diversity in ALS includes distinct aberrant phenotypes with common and causal pathological processes. *Experimental Cell Research*, 395(2). https://doi.org/10.1016/j.yexcr.2020.112209

Gooch, C. L., & Shefner, J. M. (2004). ALS surrogate markers. Mune. *Amyotrophic Lateral Sclerosis and Other Motor Neuron Disorders*, 5(1), 104–107. https://doi.org/10.1080/17434470410019889

Grad, L. I., Pokrishevsky, E., Silverman, J. M., & Cashman, N. R. (2014). Exosome-dependent and independent mechanisms are involved in prion-like transmission of propagated Cu/Zn superoxide dismutase misfolding. *Prion*, 8(5), 331–335. https://doi.org/10.4161/19336896.2014.983398

Grad, L. I., Rouleau, G. A., Ravits, J., & Cashman, N. R. (2017). Clinical Spectrum of Amyotrophic Lateral. *Cold Spring Harbor Perspectives in Medicine*, 7(8), a024117. https://doi.org/10.1101/cshperspect.a024117

Guo, H., Lai, L., Butchbach E.R., M. E. R., Stockinger, M. P., Shan, X., Bishop, G. A., & Lin, C. L. G. (2003). Increased expression of the glial glutamate transporter EAAT2 modulates excitotoxicity and delays the onset but not the outcome of ALS in mice. *Human Molecular Genetics*, 12(19), 2519–2532. https://doi.org/10.1093/hmg/ddg267

Gurney, M. E., Pu, H., Chiu, A. Y., Dal Canto, M. C., Polchow, C. Y., Alexander, D. D., Caliendo, J., Hentati, A., Kwon, Y. W., Deng, H. X., Chen, W., Zhai, P., Sufit, R. L., & Siddique, T. (1994). Motor neuron degeneration in mice that express a human Cu,Zn superoxide dismutase mutation. *Science*, 264(5166), 1772–1775. https://doi.org/10.1126/science.8209258

Guzmán-Lenis, M. S., Navarro, X., & Casas, C. (2009). Drug screening of neuroprotective agents on an organotypic-based model of spinal cord excitotoxic damage. *Restorative Neurology and Neuroscience*, 27(4), 335–349. https://doi.org/10.3233/RNN-2009-0482

Guzmán-Lenis, M.-S., Navarro, X., Casas, C. (2009). Selective sigma receptor agonist 2-(4-morpholinethyl)1 phenylcyclohexanecarboxylate (PRE084) promotes neuroprotection and neurite elongation through protein kinase C (PKC) signaling on motoneurons. *Neurosci*, 162(1), 31–38. https://doi.org/10.1016/j.neuroscience.2009.03.067

Ha, M., & Kim, V. N. (2014). Regulation of microRNA biogenesis. *Nature Reviews Molecular Cell Biology*, 15(8), 509–524. https://doi.org/10.1038/nrm3838

Han, D., Dong, X., Zheng, D., & Nao, J. (2020). MiR-124 and the underlying therapeutic promise of neurodegenerative disorders. *Frontiers in Pharmacology*, 10, 1–9. https://doi.org/10.3389/fphar.2019.01555

Hardiman, O., Al-Chalabi, A., Chio, A., Corr, E. M., Logroscino, G., Robberecht, W., Shaw, P. J., Simmons, Z., & Van Den Berg, L. H. (2017). Amyotrophic lateral sclerosis. *Nature Reviews Disease Primers*, 3. https://doi.org/10.1038/nrdp.2017.71

He, X. W., Shi, Y. H., Liu, Y. S., Li, G. F., Zhao, R., Hu, Y., Lin, C. C., Zhuang, M. T., Su, J. J., & Liu, J. R. (2019). Increased plasma levels of miR-124-3p, miR-125b-5p and miR-192-5p are associated with outcomes in acute ischaemic stroke patients receiving thrombolysis. *Atherosclerosis*, 289, 36–43. https://doi.org/10.1016/j.atherosclerosis.2019.08.002

Helmut, K., Hanisch, U. K., Noda, M., & Verkhratsky, A. (2011). Physiology of microglia. *Physiological Reviews*, 91(2), 461–553. https://doi.org/10.1152/physrev.00011.2010

Henkel, J. S., Engelhardt, J. I., Siklós, L., Simpson, E. P., Kim, S. H., Pan, T., Goodman, J. C., Siddique, T., Beers, D. R., & Appel, S. H. (2004). Presence of Dendritic Cells, MCP-1, and Activated Microglia/Macrophages in Amyotrophic Lateral Sclerosis Spinal Cord Tissue. *Annals of Neurology*, 55(2), 221–235. https://doi.org/10.1002/ana.10805

Ho, R., Sances, S., Gowing, G., Amoroso, M. W., O'Rourke, J. G., Sahabian, A., Wichterle, H., Baloh, R. H., Sareen, D., & Svendsen, C. N. (2016). ALS disrupts spinal motor neuron maturation and aging pathways within gene co-expression networks. *Nature Neuroscience*, 19(9), 1256–1267. https://doi.org/10.1038/nn.4345

Hogden, A., Foley, G., Henderson, R. D., James, N., & Aoun, S. M. (2017). Amyotrophic lateral sclerosis: Improving care with a multidisciplinary approach. *Journal of Multidisciplinary Healthcare*, 10, 205–215. https://doi.org/10.2147/JMDH.S134992

Hoitzing, H., Johnston, I. G., & Jones, N. S. (2015). What is the function of mitochondrial networks? A theoretical assessment of hypotheses and proposal for future research. *BioEssays*, 37(6), 687–700. https://doi.org/10.1002/bies.201400188

Hou, Q., Ruan, H., Gilbert, J., Wang, G., Ma, Q., Yao, W. D., & Man, H. Y. (2015). MicroRNA miR124 is required for the expression of homeostatic synaptic plasticity. *Nature Communications*, 6(1), 1–12. https://doi.org/10.1038/ncomms10045

Hounoum, B. M., Vourc'h, P., Felix, R., Corcia, P., Patin, F., Guéguinou, M., Potier-Cartereau, M., Vandier, C., Raoul, C., Andres, C. R., Mavel, S., & Blasco, H. (2016). NSC-34 motor neuron-like cells are unsuitable as experimental model for glutamate-mediated excitotoxicity. *Frontiers in Cellular Neuroscience*, 10. https://doi.org/10.3389/fncel.2016.00118

Howland, D. S., Liu, J., She, Y., Goad, B., Maragakis, N. J., Kim, B., Erickson, J., Kulik, J., DeVito, L., Psaltis, G., DeGennaro, L. J., Cleveland, D. W., & Rothstein, J. D. (2002). Focal loss of the glutamate transporter EAAT2 in a transgenic rat model of SOD1 mutant-mediated amyotrophic lateral sclerosis (ALS). *Proceedings of the National Academy of Sciences of the United States of America*, 99(3), 1604–1609. https://doi.org/10.1073/pnas.032539299

Hu, Z., & Li, Z. (2017). miRNAs in synapse development and synaptic plasticity. *Current Opinion in Neurobiology* 45, 24–31. https://doi.org/10.1016/j.conb.2017.02.014

Huang, S., Ge, X., Yu, J., Han, Z., Yin, Z., Li, Y., Chen, F., Wang, H., Zhang, J., & Lei, P. (2017). Increased miR-124-3p in microglial exosomes following traumatic brain injury inhibits neuronal inflammation and contributes to neurite outgrowth via their transfer into neurons. *FASEB Journal*, 32(1), 512-528. https://doi.org/10.1096/fj.201700673R

Humpel, C. (2015). Neuroscience forefront review organotypic brain slice cultures: A review. *Neuroscience*, 305, 86–98. https://doi.org/10.1016/j.neuroscience.2015.07.086

Huynh, W., Dharmadasa, T., Vucic, S., & Kiernan, M. C. (2019). Functional biomarkers for amyotrophic lateral sclerosis. *Frontiers in Neurology*, 10, 1–10. https://doi.org/10.3389/fneur.2018.01141

Isgaard, J., Aberg, D. & Nilsson, M. (2007). Protective and regenerative effects of the GH/IGF-I axis on the brain. *Minerva Endocrinologica*, 32(2), 103-113.

Jaarsma, D., Haasdijk, E. D., Grashorn, J. A. C., Hawkins, R., Van Duijn, W., Verspaget, H. W., London, J., & Holstege, J. C. (2000). Human Cu/Zn superoxide dismutase (SOD1) overexpression in mice causes mitochondrial vacuolization, axonal degeneration, and premature motoneuron death and accelerates motoneuron disease in mice expressing a familial amyotrophic lateral sclerosis mutant SOD1. *Neurobiology of Disease*, 7(6), 623–643. https://doi.org/10.1006/nbdi.2000.0299

Jackson, M., Ganel, R., & Rothstein, J. D. (2002). Models of Amyotrophic Lateral Sclerosis. *Current Protocols in Neuroscience*. 9. https://doi:10.1002/0471142301.ns0913s20

Jacobsen, A. B., Bostock, H., & Tankisi, H. (2019). Following disease progression in motor neuron disorders with 3 motor unit number estimation methods. *Muscle and Nerve*, 59(1), 82–87. https://doi.org/10.1002/mus.26304

Joilin, G., Leigh, P. N., Newbury, S. F., & Hafezparast, M. (2019). An Overview of MicroRNAs as Biomarkers of ALS. *Frontiers in Neurology*, 10. https://doi.org/10.3389/fneur.2019.00186

Kakarla, R., Hur, J., Kim, Y. J., Kim, J., & Chwae, Y. J. (2020). Apoptotic cell-derived exosomes: messages from dying cells. *Experimental and Molecular Medicine*, 52(1). https://doi.org/10.1038/s12276-019-0362-8

Kanouchi, T., Ohkubo, T., & Yokota, T. (2012). Can regional spreading of amyotrophic lateral sclerosis motor symptoms be explained by prion-like propagation? *Journal of Neurology, Neurosurgery and Psychiatry*, 83(7), 739–745. https://doi.org/10.1136/jnnp-2011-301826

Khakh, B. S., & Deneen, B. (2019). The Emerging Nature of Astrocyte Diversity. *Annual Review of Neuroscience*, 42(1), 187–207. https://doi.org/10.1146/annurev-neuro-070918-050443

Kirk, S. E., Tracey, T. J., Steyn, F. J., & Ngo, S. T. (2019). Biomarkers of metabolism in amyotrophic lateral sclerosis. *Frontiers in Neurology*, 10. https://doi.org/10.3389/fneur.2019.00191

Kiryu-Seo, S., Tamada, H., Kato, Y., Yasuda, K., Ishihara, N., Nomura, M., Mihara, K., & Kiyama, H. (2016). Mitochondrial fission is an acute and adaptive response in injured motor neurons. *Scientific Reports*, 6(1), 1–14. https://doi.org/10.1038/srep28331

Koval, E. D., Shaner, C., Zhang, P., Du Maine, X., Fischer, K., Tay, J., Nelson Chau, B., Wu, G. F., & Miller, T. M. (2013). Method for widespread microRNA-155 inhibition prolongs survival in ALS-model mice. *Human Molecular Genetics*, 22(20), 4127–4135. https://doi.org/10.1093/hmg/ddt261

Kumar, A., Stoica, B. A., Loane, D. J., Yang, M., Abulwerdi, G., Khan, N., Kumar, A., Thom, S. R., & Faden, A. I. (2017). Microglial-derived microparticles mediate neuroinflammation after traumatic brain injury. Journal of neuroinflammation, 14(1), 47. https://doi.org/10.1186/s12974-017-0819-4

Le, M. T. N., Teh., C., Shyh-Chang, N., Xie, H., Zhou, B., Korzh, V., Lodish, H. F., & Lim, B. (2009). MicroRNA-125b is a novel negative regulator of p53. *Genes and Development*, 23(7), 862–876. https://doi.org/10.1101/gad.1767609

Le, M. T. N., Xie, H., Zhou, B., Chia, P. H., Rizk, P., Um, M., Udolph, G., Yang, H., Lim, B., & Lodish, H. F. (2009). *Molecular and cellular biology*, *29*(19), 5290–5305. https://doi.org/10.1128/MCB.01694-08

Lee, M., Lee, Y., Song, J., Lee, J., & Chang, S. Y. (2018). Tissue-specific role of CX3CR1 expressing immune cells and their relationships with human disease. *Immune Network. Korean Association of Immunologists*, 18(1),e5. https://doi.org/10.4110/in.2018.18.e5

Li, B., Liu, X.-Y., Li, Z., Bu, H., Sun, M.-M., Guo, Y.-S., & Li, C.-Y. (2008). *J. Neurol. Sci*, 35, 220–225. https://doi.org/10.1017/S0317167100008672

Li, J. J., Wang, B., Kodali, M. C., Chen, C., Kim, E., Patters, B. J., Lan, L., Kumar, S., Wang, X., Yue, J., & Liao, F. (2018). In vivo evidence for the contribution of peripheral circulating inflammatory exosomes to neuroinflammation. *Journal of Neuroinflammation*, 15(1), 8. https://doi.org/10.1186/s12974-017-1038-8

Liddelow, S. A., & Barres, B. A. (2017). Reactive Astrocytes: Production, Function, and Therapeutic Potential. *Immunity*, 46(6), 957–967. https://doi.org/10.1016/j.immuni.2017.06.006

Liddelow, S. A., Guttenplan, K. A., Clarke, L. E., Bennett, F. C., Bohlen, C. J., Schirmer, L., Bennett, M. L., Münch, A. E., Chung, W. S., Peterson, T. C., Wilton, D. K., Frouin, A., Napier, B. A., Panicker, N., Kumar, M., Buckwalter, M. S., Rowitch, D. H., Dawson, V. L., Dawson, T. M., & Barres, B. A. (2017). Neurotoxic reactive astrocytes are induced by activated microglia. *Nature*, 541(7638), 481–487. https://doi.org/10.1038/nature21029

Lim, L. P., Lau, N. C., Garrett-Engele, P., Grimson, A., Schelter, J. M., Castle, J., Bartel, D. P., Linsley, P. S., & Johnson, J. M. (2005). Microarray analysis shows that some microRNAs downregulate large numbers of-target mRNAs. *Nature*, 433(7027), 769–773. https://doi.org/10.1038/nature03315

Lindsay, M. A. (2008). microRNAs and the immune response. *Trends in Immunology*, 29(7), 343–351. https://doi.org/10.1016/j.it.2008.04.004

Liu, W., Yamashita, T., Tian, F., Morimoto, N., Ikeda, Y., Deguchi, K., & Abe, K. (2013). Mitochondrial Fusion and Fission Proteins Expression Dynamically Change in a Murine Model of Amyotrophic Lateral Sclerosis. *Current Neurovascular Research*, 10(3), 222–230. https://doi.org/10.2174/15672026113109990060

Liu, Y., Yang, X., Guo, C., Nie, P., Liu, Y., & Ma, J. (2013). Essential Role of MFG-E8 for Phagocytic Properties of Microglial Cells. *PLoS ONE*, 8(2), e55754. https://doi.org/10.1371/journal.pone.0055754

Lossi, L., Alasia, S., Salio, C., & Merighi, A. (2009). Cell death and proliferation in acute slices and organotypic cultures of mammalian CNS. *Progress in Neurobiology*, 88(4), 221–245. https://doi.org/10.1016/j.pneurobio.2009.01.002

Lue, L. F., Schmitz, C. T., Serrano, G., Sue, L. I., Beach, T. G., & Walker, D. G. (2015). TREM2 Protein Expression Changes Correlate with Alzheimer's Disease Neurodegenerative Pathologies in Post-Mortem Temporal Cortices. *Brain Pathology*, 25(4), 469–480. https://doi.org/10.1111/bpa.12190

Lukiw, W. J., Andreeva, T. V., Grigorenko, A. P., & Rogaev, E. I. (2013). Studying micro RNA function and dysfunction in Alzheimer's disease. *Frontiers in Genetics*, 3, 1–13. https://doi.org/10.3389/fgene.2012.00327

Luo, X. G., & Chen, S. Di. (2012). The changing phenotype of microglia from homeostasis to disease. *Translational Neurodegeneration*, 1, 1–13. https://doi.org/10.1186/2047-9158-1-9

Maguire, G., Paler, L., Green, L., Mella, R., Valcarcel, M., & Villace, P. (2019). Rescue of degenerating neurons and cells by stem cell released molecules: using a physiological renormalization strategy. *Physiological Reports*, 7(9), 1–17. https://doi.org/10.14814/phy2.14072

Maier, O., Böhm, J., Dahm, M., Brück, S., Beyer, C., & Johann, S. (2013). Differentiated NSC-34 motoneuron-like cells as experimental model for cholinergic neurodegeneration. *Neurochemistry International*, 62(8), 1029–1038. https://doi.org/10.1016/j.neuint.2013.03.008

Mancuso, R., & Navarro, X. (2015). Amyotrophic lateral sclerosis: Current perspectives from basic research to the clinic. *Progress in Neurobiology*, 133, 1–26. https://doi.org/10.1016/j.pneurobio.2015.07.004

Marcuzzo, S., Kapetis, D., Mantegazza, R., Baggi, F., Bonanno, S., Barzago, C., Cavalcante, P., Kerlero de Rosbo, N., & Bernasconi, P. (2014). Altered miRNA expression is associated with

neuronal fate in G93A-SOD1 ependymal stem progenitor cells. *Experimental Neurology*, 253, 91–101. https://doi.org/10.1016/j.expneurol.2013.12.007

Mathis, S., Goizet, C., Soulages, A., Vallat, J. M., & Masson, G. Le. (2019). Genetics of amyotrophic lateral sclerosis: A review. *Journal of the Neurological Sciences*, 399, 217–226. https://doi.org/10.1016/j.jns.2019.02.030

Medelin, M., Rancic, V., Cellot, G., Laishram, J., Veeraraghavan, P., Rossi, C., Muzio, L., Sivilotti, L., & Ballerini, L. (2016). Altered development in GABA co-release shapes glycinergic synaptic currents in cultured spinal slices of the SOD1G93A mouse model of amyotrophic lateral sclerosis. *Journal of Physiology*, 594(13), 3827–3840. https://doi.org/10.1113/JP272382

Mendes-Pinheiro, B., Marote, A., Marques, C. R., Teixeira, F. G., Ribeiro, J. C., & Salgado, A. J. (2020). Applications of the stem cell secretome in regenerative medicine. *Mesenchymal Stem Cells in Human Health and Diseases*, 5,79-114. Academic Press. https://doi.org/10.1016/b978-0-12-819713-4.00005-0

Menzies, F. M. (2002). Mitochondrial dysfunction in a cell culture model of familial amyotrophic lateral sclerosis. *Brain*, 125(7), 1522–1533. https://doi.org/10.1093/brain/awf167

Mishima, T., Mizuguchi, Y., Kawahigashi, Y., Takizawa, T., & Takizawa, T. (2007). RT-PCR-based analysis of microRNA (miR-1 and -124) expression in mouse CNS. *Brain Research*, 1131(1), 37–43. https://doi.org/10.1016/j.brainres.2006.11.035

Morel, L., Regan, M., Higashimori, H., Ng, S. K., Esau, C., Vidensky, S., Rothstein, J., & Yang, Y. (2013). Neuronal exosomal mirna-dependent translational regulation of astroglial glutamate transporter glt1. *Journal of Biological Chemistry*, 288(10), 7105–7116. https://doi.org/10.1074/jbc.M112.410944

Morlando, M., Dini, S., Torrelli, G., Rosa, A., Carlo, V. Di, Caffarelli, E., & Bozzoni, I. (2012). FUS stimulates microRNA biogenesis by facilitating co-transcriptional Drosha recruitment. *The EMBO Journal*, 31(24), 4502–4510. https://doi.org/10.1038/emboj.2012.319

Münch, C., O'Brien, J., & Bertolotti, A. (2011). Prion-like propagation of mutant superoxide dismutase-1 misfolding in neuronal cells. *Proceedings of the National Academy of Sciences of the United States of America*, 108(9), 3548–3553. https://doi.org/10.1073/pnas.1017275108

Nagai, M., Re, D. B., Nagata, T., Chalazonitis, A., Jessell, T. M., Wichterle, H., & Przedborski, S. (2007). Astrocytes expressing ALS-linked mutated SOD1 release factors selectively toxic to motor neurons. *Nature Neuroscience*, 10(5), 615–622. https://doi.org/10.1038/nn1876

Nascimento, F., Pousinha, P. A., Correia, A. M., Gomes, R., Sebastião, A. M., & Ribeiro, J. A. (2014). Adenosine A2A receptors activation facilitates neuromuscular transmission in the pre-symptomatic phase of the SOD1(G93A) ALS mice, but not in the symptomatic phase. *PLoS ONE*, 9(8), 1–10. https://doi.org/10.1371/journal.pone.0104081

Neuwirth, C., Barkhaus, P. E., Burkhardt, C., Castro, J., Czell, D., de Carvalho, M., Nandedkar, S., Stålberg, E., & Weber, M. (2017). Motor Unit Number Index (MUNIX) detects motor neuron loss in pre-symptomatic muscles in Amyotrophic Lateral Sclerosis. *Clinical Neurophysiology*, 128(3), 495–500. https://doi.org/10.1016/j.clinph.2016.11.026

O'Connell, R. M., Taganov, K. D., Boldin, M. P., Cheng, G., & Baltimore, D. (2007). MicroRNA-155 is induced during the macrophage inflammatory response. *Proceedings of the National Academy of Sciences of the United States of America*, 104(5), 1604–1609. https://doi.org/10.1073/pnas.0610731104

Özdinler, P. H., Benn, S., Yamamoto, T. H., Güzel, M., Brown, R. H., & Macklis, J. D. (2011). Corticospinal Motor Neurons and Related Subcerebral Projection Neurons Undergo Early and Specific Neurodegeneration in hSOD1G93A Transgenic ALS Mice. *The Journal of Neuroscience*, 31(11), 4166–4177. https://doi.org/10.1523/JNEUROSCI.4184-10.2011

Palareti, G., Legnani, C., Cosmi, B., Antonucci, E., Erba, N., Poli, D., Testa, S., & Tosetto, A. (2016). Comparison between different D-Dimer cutoff values to assess the individual risk of

recurrent venous thromboembolism: Analysis of results obtained in the DULCIS study. *International Journal of Laboratory Hematology*, 38(1), 42–49. https://doi.org/10.1111/ijlh.12426

Pansarasa, O., Bordoni, M., Diamanti, L., Sproviero, D., Gagliardi, S., & Cereda, C. (2018). Sod1 in amyotrophic lateral sclerosis: "ambivalent" behavior connected to the disease. *International Journal of Molecular Sciences*, 19(5), 1–13. https://doi.org/10.3390/ijms19051345

Papadeas, S. T., Kraig, S. E., O'Banion, C., Lepore, A. C., & Maragakis, N. J. (2011). Astrocytes carrying the superoxide dismutase 1 (SOD1 G93A) mutation induce wild-type motor neuron degeneration in vivo. *Proceedings of the National Academy of Sciences of the United States of America*, 108(43), 17803–17808. https://doi.org/10.1073/pnas.1103141108

Parakh, S., Spencer, D. M., Halloran, M. A., Soo, K. Y., & Atkin, J. D. (2013). Redox regulation in amyotrophic lateral sclerosis. *Oxidative Medicine and Cellular Longevity*, 2013, 408681. https://doi.org/10.1155/2013/408681

Parisi, C., Napoli, G., Amadio, S., Spalloni, A., Apolloni, S., Longone, P., & Volonte, C. (2016). MicroRNA-125b regulates microglia activation and motor neuron death in ALS. *Cell Death Differ*, 23(3), 531–541. https://doi.org/10.1038/cdd.2015.153

Philips, T., & Rothstein, J. D. (2014). Glial cells in amyotrophic lateral sclerosis. *Experimental Neurology*, 262(Part B), 111–120. https://doi.org/10.1016/j.expneurol.2014.05.015

Pinto, S., Cunha, C., Barbosa, M., Vaz, A. R., & Brites, D. (2017). Exosomes from NSC-34 cells transfected with hSOD1-G93A are enriched in mir-124 and drive alterations in microglia phenotype. *Frontiers in Neuroscience*, 11, 273. https://doi.org/10.3389/fnins.2017.00273

Ponomarev, E. D., Veremeyko, T., Barteneva, N., Krichevsky, A. M., & Weiner, H. L. (2011). MicroRNA-124 promotes microglia quiescence and suppresses EAE by deactivating macrophages via the C/EBP-α-PU.1 pathway. *Nature Medicine*, 17(1), 64–70. https://doi.org/10.1038/nm.2266

Purves D, Augustine GJ, Fitzpatrick D, et al. (2001). *Neuroscience*. 2nd edition. Sunderland (MA): Sinauer Associates. Available from: https://www.ncbi.nlm.nih.gov/books/NBK10869/

Qin, Z., Wang, P. Y., Su, D. F., & Liu, X. (2016). miRNA-124 in immune system and immune disorders. *Frontiers in Immunology,* 7, 406. https://doi.org/10.3389/fimmu.2016.00406

Quiroz, J., Tsai, E., Coyle, M., Sehm, T., & Echeverri, K. (2014). Precise control of miR-125b levels is required to create a regeneration-permissive environment after spinal cord injury : a cross-species comparison between salamander and rat. *Disease models & mechanisms*, 7(6), 601–611. https://doi.org/10.1242/dmm.014837

Rajasethupathy, P., Fiumara, F., Sheridan, R., Betel, D., Puthanveettil, S. V., Russo, J. J., Sander, C., Tuschl, T., & Kandel, E. (2009). Characterization of Small RNAs in Aplysia Reveals a Role for miR-124 in Constraining Synaptic Plasticity through CREB. *Neuron*, 63(6), 803–817. https://doi.org/10.1016/j.neuron.2009.05.029

Rajgor, D. (2018). Macro roles for microRNAs in neurodegenerative diseases. *Non-coding RNA Research*, 3(3), 154–159. https://doi.org/10.1016/j.ncrna.2018.07.001

Ravits, J. M., & La Spada, A. R. (2009). ALS motor phenotype heterogeneity, focality, and spread: Deconstructing motor neuron degeneration. *Neurology*, 73(10), 805. https://doi.org/10.1212/WNL.0b013e3181b6bbbd

Renton, A. E., Chiò, A., & Traynor, B. J. (2014). State of play in amyotrophic lateral sclerosis genetics. *Nature Neuroscience,* 17(1), 17–23. https://doi.org/10.1038/nn.3584

Rocha, M. C., Pousinha, P. A., Correia, A. M., Sebastião, A. M., & Ribeiro, J. A. (2013). Early Changes of Neuromuscular Transmission in the SOD1(G93A) Mice Model of ALS Start Long before Motor Symptoms Onset. *PLoS ONE*, 8(9). https://doi.org/10.1371/journal.pone.0073846

Rong, Y., Liu, W., Wang, J., Fan, J., Luo, Y., Li, L., Kong, F., Chen, J., Tang, P., & Cai, W. (2019). Neural stem cell-derived small extracellular vesicles attenuate apoptosis and neuroinflammation after traumatic spinal cord injury by activating autophagy. *Cell Death Dis*, 10(5). https://doi.org/10.1038/s41419-019-1571-8

Rosen, D. R., Siddique, T., Patterson, D., Figlewicz, D. A., Sapp, P., Hentati, A., Donaldson, D., Goto, J., O'Regan, J. P., Deng, H. X., Rahmani, Z., Krizus, A., McKenna-Yasek, D., Cayabyab, A., Gaston, S. M., Berger, R., Tanzi, R. E., Halperin, J. J., Herzfeldt, B., … Brown, R. H. (1993). Mutations in Cu/Zn superoxide dismutase gene are associated with familial amyotrophic lateral sclerosis. *Nature*, 362(6415), 59–62. https://doi.org/10.1038/362059a0

Rothstein, J. D., Martin, L. J., & Kuncl, R. W. (1992). Decreased Glutamate Transport by the Brain and Spinal Cord in Amyotrophic Lateral Sclerosis. *New England Journal of Medicine*, 326(22), 1464–1468. https://doi:10.1056/nejm199205283262204

Rupaimoole, R., & Slack, F. J. (2017). MicroRNA therapeutics: Towards a new era for the management of cancer and other diseases. *Nature Reviews Drug Discovery*, 16(3), 203–221. https://doi.org/10.1038/nrd.2016.246

Scott, S., Kranz, J. E., Cole, J., Lincecum, J. M., Thompson, K., Kelly, N., Bostrom, A., Theodoss, J., Al-Nakhala, B. M., Vieira, F. G., Ramasubbu, J., & Heywood, J. A. (2008). Design, power, and interpretation of studies in the standard murine model of ALS. *Amyotrophic Lateral Sclerosis*, 9(1), 4–15. https://doi.org/10.1080/17482960701856300

Seeley, W. W., Crawford, R. K., Zhou, J., Miller, B. L., & Greicius, M. D. (2009). Neurodegenerative Diseases Target Large-Scale Human Brain Networks. *Neuron*, 62(1), 42–52. https://doi.org/10.1016/j.neuron.2009.03.024

Shamir, E. R., & Ewald, A. J. (2014). Three-dimensional organotypic culture: Experimental models of mammalian biology and disease. *Nature Reviews Molecular Cell Biology*, 15(10), 647–664. https://doi.org/10.1038/nrm3873

Shigetomi, E., Tong, X., Kwan, K. Y., Corey, D. P., & Khakh, B. S. (2012). TRPA1 channels regulate astrocyte resting calcium and inhibitory synapse efficacy through GAT-3. *Nature Neuroscience*, 15(1), 70–80. https://doi.org/10.1038/nn.3000

Singh, V. K., Kalsan, M., Kumar, N., Saini, A., & Chandra, R. (2015). Induced pluripotent stem cells: Applications in regenerative medicine, disease modeling, and drug discovery. *Frontiers in Cell and Developmental Biology*, 3, 1–18. https://doi.org/10.3389/fcell.2015.00002

Sison, S. L., Patitucci, T. N., Seminary, E. R., Villalon, E., Lorson, C. L., & Ebert, A. D. (2017). Astrocyte-produced miR-146a as a mediator of motor neuron loss in spinal muscular atrophy. *Hum Mol Genet*, 26(17), 3409–3420. https://doi.org/10.1093/hmg/ddx230

Smirnova, E., Griparic, L., Shurland, D. L., & Van der Bliek, A. M. (2001). Dynamin-related protein Drp1 is required for mitochondrial division in mammalian cells. *Molecular Biology of the Cell*, 12(8), 2245–2256. https://doi.org/10.1091/mbc.12.8.2245

Smirnova, L., Gräfe, A., Seiler, A., Schumacher, S., Nitsch, R., & Wulczyn, F. G. (2005). Regulation of miRNA expression during neural cell specification. *Eur J Neurosc*, 21(6), 1469–1477. https://doi.org/10.1111/j.1460-9568.2005.03978.x

Smyth, L. A., Boardman, D. A., Tung, S. L., Lechler, R., & Lombardi, G. (2015). MicroRNAs affect dendritic cell function and phenotype. *Immunology*, 144(2), 197–205. https://doi.org/10.1111/imm.12390

Sofroniew M. V. (2014). Astrogliosis. Cold Spring Harbor perspectives in biology, 7(2), a020420. https://doi.org/10.1101/cshperspect.a020420

Sofroniew, M. V., & Vinters, H. V. (2010). Astrocytes: Biology and pathology. *Acta Neuropathologica*, 119(1), 7–35. https://doi.org/10.1007/s00401-009-0619-8

Song, P., Kwon, Y., Joo, J. Y., Kim, D. G., & Yoon, J. H. (2019). Secretomics to discover regulators in diseases. *International Journal of Molecular Sciences*, 20(16), 1–20. https://doi.org/10.3390/ijms20163893

Stefano, L., Racchetti, G., Bianco, F., Passini, N., Gupta, R. S., Bordignon, P. P., & Meldolesi, J. (2009). The surface-exposed chaperone, Hsp60, is an agonist of the microglial TREM2 receptor. *Journal of Neurochemistry*, 110(1), 284–294. https://doi.org/10.1111/j.1471-4159.2009.06130.x

Stifani, N., & Mobility, A. (2014). Motor neurons and the generation of spinal motor neuron diversity. *Frontiers in Cellular Neuroscience*, 8, 293. https://doi.org/10.3389/fncel.2014.00293

Stogsdill, J. A., Ramirez, J., Liu, D., Kim, Y. H., Baldwin, K. T., Enustun, E., Ejikeme, T., Ji, R. R., & Eroglu, C. (2017). Astrocytic neuroligins control astrocyte morphogenesis and synaptogenesis. *Nature*, 551(7679), 192–197. https://doi.org/10.1038/nature24638

Stoppini, L., Buchs, P. A., & Muller, D. (1991). A simple method for organotypic cultures of nervous tissue. *Journal of Neuroscience Methods*, 37(2), 173–182. https://doi.org/10.1016/0165-0270(91)90128-M

Su, W., Aloi, M. S., & Garden, G. A. (2016). MicroRNAs mediating CNS inflammation: Small regulators with powerful potential. *Brain, Behavior, and Immunity*, 52, 1–8. https://doi.org/10.1016/j.bbi.2015.07.003

Sun, D., & Jakobs, T. C. (2012). Structural remodeling of astrocytes in the injured CNS. *Neuroscientist*, 18(6), 567–588. https://doi.org/10.1177/1073858411423441

Sun, P., Liu, D. Z., Jickling, G. C., Sharp, F. R., & Yin, K. J. (2018). MicroRNA-based therapeutics in central nervous system injuries. *Journal of Cerebral Blood Flow and Metabolism*, 38(7), 1125–1148. https://doi.org/10.1177/0271678X18773871

Sun, Y., Li, Q., Gui, H., Xu, D. P., Yang, Y. L., Su, D. F., & Liu, X. (2013). MicroRNA-124 mediates the cholinergic anti-inflammatory action through inhibiting the production of pro-inflammatory cytokines. *Cell Research*, 23(11), 1270–1283. https://doi.org/10.1038/cr.2013.116

Sun, Y., Luo, Z. M., Guo, X. M., Su, D. F., & Liu, X. (2015). An updated role of microRNA-124 in central nervous system disorders: A review. *Frontiers in Cellular Neuroscience*, 9, 1–8. https://doi.org/10.3389/fncel.2015.00193

Tahamtan, A., Teymoori-Rad, M., Nakstad, B., & Salimi, V. (2018). Anti-inflammatory MicroRNAs and their potential for inflammatory diseases treatment. *Frontiers in Immunology*, 9, 1–14. https://doi.org/10.3389/fimmu.2018.01377

Treiber, T., Treiber, N., & Meister, G. (2019). Regulation of microRNA biogenesis and its crosstalk with other cellular pathways. *Nature Reviews Molecular Cell Biology*, 20(1), 5–20. https://doi.org/10.1038/s41580-018-0059-1

Trias, E., Ibarburu, S., Barreto-Núñez, R., & Barbeito, L. (2017). Significance of aberrant glial cell phenotypes in pathophysiology of amyotrophic lateral sclerosis. *Neuroscience Letters,* 636, 27–31.https://doi.org/10.1016/j.neulet.2016.07.052

Turner, B. J., & Talbot, K. (2008). Transgenics, toxicity and therapeutics in rodent models of mutant SOD1-mediated familial ALS 85(1), 94–134. *Progress in Neurobiology*. https://doi.org/10.1016/j.pneurobio.2008.01.001

Turner, M. R., Cagnin, A., Turkheimer, F. E., Miller, C. C. J., Shaw, C. E., Brooks, D. J., Leigh, P. N., & Banati, R. B. (2004). Evidence of widespread cerebral microglial activation in amyotrophic lateral sclerosis: An [11C](R)-PK11195 positron emission tomography study. *Neurobiol. Dis*, 15(3), 601–609. https://doi.org/10.1016/j.nbd.2003.12.012

Valentine, J. S., & Hart, P. J. (2003). Misfolded CuZnSOD and amyotrophic lateral sclerosis. *Proc Natl Acad Sci U S A*, 100(7), 3617–3622. https://doi.org/10.1073/pnas.0730423100

Van Damme, P., Robberecht, W., & Van Den Bosch, L. (2017). Modelling amyotrophic lateral sclerosis: Progress and possibilities. *DMM Disease Models and Mechanisms*, 10(5), 537–549. https://doi.org/10.1242/dmm.029058

Vaz, A. R., Cunha, C., Gomes, C., Schmucki, N., Barbosa, M., & Brites, D. (2015). Glycoursodeoxycholic Acid Reduces Matrix Metalloproteinase-9 and Caspase-9 Activation in a Cellular Model of Superoxide Dismutase-1 Neurodegeneration. *Molecular Neurobiology*, 51(3), 864–877. https://doi.org/10.1007/s12035-014-8731-8

Vaz, A. R., Pinto, S., Ezequiel, C., Cunha, C., Carvalho, L. A., Moreira, R., & Brites, D. (2019). Phenotypic effects of wild-type and mutant SOD1 expression in n9 murine microglia at steady state, inflammatory and immunomodulatory conditions. *Front Cell Neurosci*, 13, 1–15. https://doi.org/10.3389/fncel.2019.00109

Veremeyko, T., Kuznetsova, I. S., Dukhinova, M., Yung, A. W. Y., Kopeikina, E., Barteneva, N. S., & Ponomarev, E. D. (2018). Neuronal extracellular microRNAs miR - 124 and miR - 9 mediate cell-cell communication between neurons and microglia. *Journal of neuroscience research*, 97(2), 162–184. https://doi.org/10.1002/jnr.24344

Verkhratsky, A., & Nedergaard, M. (2018). Physiology of astroglia. *Physiological Reviews*, 98(1), 239–389. https://doi.org/10.1152/physrev.00042.2016

Vizinha, D. 2018. *Targeting miR-124 in motor neurons as a therapeutic strategy to prevent neurodegeneration and glial activation in ALS*. Master Thesis, Faculdade de Farmácia da Universidade de Lisboa.

Waller, R., Wyles, M., Heath, P. R., Kazoka, M., Wollff, H., Shaw, P. J., & Kirby, J. (2018). Small RNA sequencing of sporadic amyotrophic lateral sclerosis cerebrospinal fluid reveals differentially expressed miRNAs related to neural and glial activity. *Frontiers in Neuroscience*, 11, 1–13. https://doi.org/10.3389/fnins.2017.00731

Wang, L., Gutmann, D. H., & Roos, R. P. (2011). Astrocyte loss of mutant SOD1 delays ALS disease onset and progression in G85R transgenic mice. *Human Molecular Genetics*, 20(2), 286–293. https://doi.org/10.1093/hmg/ddq463

Wang, M., Mungur, R., Lan, P., Wang, P., & Wan, S. (2018). MicroRNA-21 and microRNA-146a negatively regulate the secondary inflammatory response of microglia after intracerebral hemorrhage. *Int J Clin Exp Pathol*, 11(7), 3348–3356.

Wang, W., Zhang, F., Li, L., Tang, F., Siedlak, S. L., Fujioka, H., Liu, Y., Su, B., Pi, Y., & Wang, X. (2015). MFN2 couples glutamate excitotoxicity and mitochondrial dysfunction in motor neurons. *Journal of Biological Chemistry*, 290(1), 168–182. https://doi.org/10.1074/jbc.M114.617167

Wang, X. H., & Wang, T. L. (2018). MicroRNAs of microglia: Wrestling with central nervous system disease. *Neural regeneration research*, 13(12), 2067–2072. https://doi.org/10.4103/1673-5374.241444

Wolf, S. A., Boddeke, H. W. G. M., & Kettenmann, H. (2017). Microglia in Physiology and Disease. *Annual Review of Physiology*, 79(1), 619–643. https://doi.org/10.1146/annurev-physiol-022516-034406

Yamanaka, K., & Komine, O. (2018). The multi-dimensional roles of astrocytes in ALS. *Neuroscience Research*, 126, 31–38. https://doi.org/10.1016/j.neures.2017.09.011

Yang, L., Niu, F., Yao, H., Liao, K., Chen, X., Kook, Y., Ma, R., Hu, G., & Buch, S. (2018). Exosomal miR-9 Released from HIV Tat Stimulated Astrocytes Mediates Microglial Migration. *J Neuroimmune Pharm*, 13(3), 330–344. https://doi.org/10.1007/s11481-018-9779-4

Yoshii, Y., Otomo, A., Pan, L., Ohtsuka, M., & Hadano, S. (2011). Loss of glial fibrillary acidic protein marginally accelerates disease progression in a SOD1 H46R transgenic mouse model of ALS. *Neuroscience Research*, 70(3), 321–329. https://doi.org/10.1016/j.neures.2011.03.006

Zamanian, J. L., Xu, L., Foo, L. C., Nouri, N., Zhou, L., Giffard, R. G., & Barres, B. A. (2012). Genomic analysis of reactive astrogliosis. *Journal of Neuroscience*, 32(18), 6391–6410. https://doi.org/10.1523/JNEUROSCI.6221-11.2012

Zhang, B., Tu, P. H., Abtahian, F., Trojanowski, J. Q., & Lee, V. M. Y. (1997). Neurofilaments and orthograde transport are reduced in ventral root axons of transgenic mice that express human SOD1 with a G93A mutation. *Journal of Cell Biology*, 139(5), 1307–1315. https://doi.org/10.1083/jcb.139.5.1307

Zhang, J., Liu, Y., Liu, X., Li, S., Cheng, C., Chen, S., & Le, W. (2018). Dynamic changes of CX3CL1/CX3CR1 axis during microglial activation and motor neuron loss in the spinal cord of ALS mouse model. *Translational Neurodegeneration*, 7(1), 1–14. https://doi.org/10.1186/s40035-018-0138-4

Zhang, L., Dong, L. Y., Li, Y. J., Hong, Z., & Wei, W. S. (2012). miR-21 represses FasL in microglia and protects against microglia-mediated neuronal cell death following hypoxia/ischemia. *Glia*, 60(12), 1888–1895. https://doi.org/10.1002/glia.22404

Zhao, W., Xie, W., Xiao, Q., Beers, D. R., & Appel, S. H. (2006). Protective effects of an anti-inflammatory cytokine, interleukin-4, on motoneuron toxicity induced by activated microglia. *Journal of Neurochemistry*, 99(4), 1176–1187. https://doi.org/10.1111/j.1471-4159.2006.04172.x

Zhou, F., Zhang, C., Guan, Y., Chen, Y., Lu, Q., Jie, L., Gao, H., Du, H., Zhang, H., Liu, Y., & Wang, X. (2018). Screening the expression characteristics of several miRNAs in G93A-SOD1 transgenic mouse: Altered expression of miRNA-124 is associated with astrocyte differentiation by targeting Sox2 and Sox9. *J Neurochem*, 145, 51-67. https://doi: 10.1111/jnc.14229

Zhou, L., Xu, Z., Ren, X., Chen, K., & Xin, S. (2016). MicroRNA-124 (MiR-124) Inhibits Cell Proliferation, Metastasis and Invasion in Colorectal Cancer by Downregulating Rho-Associated Protein Kinase 1(ROCK1). *Cellular Physiology and Biochemistry*, 38(5), 1785–1795. https://doi.org/10.1159/000443117

VII. SUPPLEMENTARY DATA

Supplementary table VII.1 - WT slices treated with WT MN secretome are characterized by a stable inflammatory status nonetheless with the dysregulation of fractalkine and post-synaptic marker.

Gene	**Fold change** (WTOC + WTMNSec *vs.* Non-treated WTOC) **Mean ± SEM**	***p* values**
iNOS	1.17 ± 0.87	0.91
IL-1β	1.80 ± 0.36	0.11
IL-10	1.67 ± 0.31	0.32
HMGB1	1.19 ± 0.21	0.99
CX3CR1	2.42 ± 0.75	> 0.99
CX3CL1	0.70 ± 0.12	**0.02**
S100B	0.92 ± 0.14	0.49
GFAP	0.97 ± 0.28	0.79
Dlg4	2.66 ± 0.38	**0.02**
SYP	1.95 ± 0.52	0.15
MFG-E8	0.58 ± 0.26	0.14
TREM2	1.02 ± 0.45	0.34
GLT-1	0.96 ± 0.14	0.63
MFN2	1.27 ± 0.31	0.79
DRP1	0.87 ± 0.11	0.25

Results are shown in mean ± SEM fold change *vs.* non-treated WTOC of, at least, 4 independent experiments. mRNA levels of a selected set of markers were evaluated by RT-qPCR. *p* values were calculated by using the Student's *t*-test and in bold are the ones statistically significant. **WTOC**, wild type organotypic culture; **WTMNSec**, wild type motor neuron secretome; **RT-qPCR**, reverse transcription-quantitative polymerase chain reaction; **iNOS,** inducible nitric oxide synthase; **IL-1β**, interleukin 1-beta; **IL-10**, interleukin-10: **HMGB1**, high mobility group box 1; **CX3CR1**, C-X3-C motif chemokine receptor 1; **CX3CL1**, C-X3-C motif chemokine ligand 1/fractalkine; **S100B**, S100 calcium-binding protein B; **GFAP**, glial fibrillary acidic protein; **Dlg4**, discs large MAGUK scaffold protein 4 (that encodes for postsynaptic density protein 95, PSD-95); **SYP**, synaptophysin; **MFG-E8**, milk fat globule-EGF factor 8; **GLT-1**, glutamate transporter-1, **TREM2**, triggering receptor expressed on myeloid cells 2; **MFN2**, mitofusin-2; **DRP1**, dynamin-related protein 1; **β-actin**, beta-actin.

Supplementary table VII.2 - WT organotypic cultures treated with WT MN secretome and non-treated WT slices display an identical miRNAs signature.

miRNAs	**Fold change** (WTOC + WTMNSec *vs.* Non-treated WTOC) **Mean ± SEM**	***p* values**
miR-21	0.89 ± 0.29	0.54
miR-124	0.71 ± 0.22	0.19
miR-125b	0.82 ± 0.15	0.29
miR-146a	1.00 ± 0.20	0.81

Results are shown in mean ± SEM fold change *vs.* non-treated WTOC of, at least, 4 independent experiments. Levels of selected inflammatory-associated miRNAs were evaluated by RT-qPCR. *p* values were calculated by using the Student's *t*-test. **RT-qPCR**, reverse transcription-quantitative polymerase chain reaction; **miR**, miRNA.

Supplementary table VII.3 - TG organotypic cultures treated with WT MN secretome are characterized by a repressed inflammatory status, repression of CX3CL1-CX3CR1 axis, and downregulation of phagocytosis and synaptic genes.

Gene	**Fold change** (TGOC + WTMNSec *vs.* Non-treated TGOC) **Mean ± SEM**	***p* values**
iNOS	0.15 ± 0.008	**<0.0001**
IL-1β	0.36 ± 0.13	**0.03**
IL-10	0.24 ± 0.07	**0.001**
HMGB1	1.02 ± 0.24	0.98
CX3CR1	0.28 ± 0.08	**0.001**
CX3CL1	0.12 ± 0.06	**<0.0001**
S100B	0.80 ± 0.12	0.26
GFAP	0.28 ± 0.07	**0.008**
Dlg4	0.43 ± 0.17	**0.04**
SYP	0.21 ± 0.09	**0.002**
MFG-E8	0.08 ± 0.03	**0.002**
TREM2	0.30 ± 0.12	**0.04**
GLT-1	0.88 ± 0.38	0.74
MFN2	1.95 ± 1.15	0.51
DRP1	2.50 ± 1.37	0.36

Results are shown in mean ± SEM fold change *vs.* non-treated TGOC of, at least, 4 independent experiments. mRNA levels of a selected set of markers were evaluated by RT-qPCR. *p* values were calculated by using the Student's *t*-test and in bold are the ones statistically significant. **RT-qPCR**, reverse transcription-quantitative polymerase chain reaction; **iNOS,** inducible nitric oxide synthase; **IL-1β**, interleukin-1 beta; **IL-10**, interleukin-10: **HMGB1**, high mobility group box 1; **CX3CR1**, C-X3-C motif chemokine receptor 1; **CX3CL1**, C-X3-C motif chemokine ligand 1/fractalkine; **S100B**, S100 calcium-binding protein B; **GFAP**, glial fibrillary acidic protein; **Dlg4**, discs large MAGUK scaffold protein 4 (that encodes for postsynaptic density protein 95, PSD-95); **SYP**, synaptophysin; **MFG-E8**, milk fat globule-EGF factor 8; **GLT-1**, glutamate transporter-1, **TREM2**, triggering receptor expressed on myeloid cells 2; **MFN2**, mitofusin-2; **DRP1**, dynamin-related protein 1; **β-actin**, beta-actin.

Supplementary table VII.4 - WT MN secretome enhances the levels of miRNA-124 while decreases the extent of miR-146a in TG organotypic cultures.

miRNAs	**Fold change** (TGOC + WTMNSec *vs.* Non-treated TGOC) **Mean ± SEM**	***p* values**
miR-21	1.27 ± 0.47	0.69
miR-124	1.63 ± 0.14	**0.004**
miR-125b	1.30 ± 0.29	0.44
miR-146a	0.65 ± 0.10	**0.05**

Results are shown in mean ± SEM fold change *vs.* non-treated TGOC of, at least, 4 independent experiments. Levels of selected inflammatory-associated miRNAs were evaluated by RT-qPCR. *p* values were calculated by using the Student's *t*-test and in bold are the ones statistically significant. **RT-qPCR**, reverse transcription-quantitative polymerase chain reaction; **miR**, miRNA.